Targeting DNA Damage Response *via* miRNAs to enhance Radiosensitivity

Dissertation

with the aim of achieving a doctoral degree

at the Faculty of Mathematics, Informatics and Natural Sciences

Department of Biology

of Universität Hamburg

Submitted by

Hamed Helal

September, 2016 Hamburg

The present work was accomplished in the laboratory of radiobiology and experimental radiooncology – University medical center – Eppendorf (UKE).

Day of oral defense: 03.03.2017

Evaluators:

Prof. Dr. Wilhelm Schäfer
Department of Biology
Faculty of Mathematics, Informatics and Natural Sciences
University of Hamburg (Supervisor)

Prof. Dr. Kirsten Lauber
Molecular Oncology
Department of Radiation Oncology
Ludwig Maximilians University Munich

Dedication

To my father’s soul. His words of inspiration and encouragement in pursuit of excellence, still linger on.

TABLE OF CONTENTS

LIST OF ABBREVIATIONS

amiRNA	Artificial miRNA
AT	Ataxia-telangiectasia
ATM	Ataxia-telangiectasia mutated
ATR	ATM and Rad3-related protein
ATP	Adenosine triphosphate
ATF2	activating transcription factor 2
BRCA1	breast cancer type 1 susceptibility protein
BRCA2	breast cancer type 2 susceptibility protein
BSA	Bovine serum albumin
BCA	bicinchoninic acid
BER	base excision repair
Chk1	Checkpoint kinase 1
Chk2	Checkpoint kinase 2
Cdk1	Cyclin-dependent kinase 1
Cdk2	Cyclin-dependent kinase 2
DNA-PK	DNA-dependent protein kinase
DNA-PKcs	DNA- protein kinase catalytic subunit
DMSO	Dimethyl sulfoxide

DTT	Ditheotheratol
DMEM	Dulbecco's Modified Eagle Medium
DAPI	4',6-diamidino-2-phenylindole
DDR	DNA damage response
DNA	Deoxyribonucleic acid
DSBs	Double-strand breaks
EDTA	Ethylene diamine tetra acetic acid
EV	Empty vector
emiRNA	Endogenous miRNA
FCS	Fetal calf serum
GBM	glioblastoma multiforme
HR	homologous recombination
HNPCC	hereditary nonpolyposis colon cancer
H2AX	Histone H2A
H3K9me3	histone H3 lysine 9 tri-methylation
HP1b	heterochromatin protein 1b
IR	Ionizing Radiation
IdUrd	5-Iodo-20-deoxyuridine
ICLs	intra- and inter-strand crosslinks

kb	Kilo-base
KDa	Kilo-dalton
MMR	mismatch repair
miRNAs	micro RNAs
mTOR	Mechanistic Target Of Rapamycin
MDM2	Mouse double minute 2 homolog
MDC1	mediator of damage checkpoint 1
mRNA	messenger RNA
miRISC	miRNA-containing RNA-induced silencing complex
NER	nucleotide excision repair
NHEJ	non-homologous end joining
ncRNAs	Non-coding RNAs
ORF	open reading frame
PARP	Poly-ADP-ribose polymerase
PI3K	phospho-inositide 3-kinase
PIKK	phospho-inositide 3-kinase (PI3K)- related protein kinase
PP2	protein phosphatase 2A
PP5	protein phosphatase 5
pri-miRNAs	primary miRNAs

pre-miRNAs	Precursor miRNAs
PBS	phosphate buffered saline
pLV-	Plasmid lentiviral
PcDNA-	Plasmid circular DNA
PE	plating efficiency
RT	Radiotherapy
ROS	reactive oxygen species
RPA	Replication protein A
RNA	Ribonucleic acid
RNAi	RNA interference
SBRT	stereotactic body radiotherapy
scRNA	Scrambled RNA
shRNA	Short hairpin RNA
siRNA	Small interference RNA
SDS-PAGE	sodium dodecyl sulphate
Ser-	Serionine
SSB	single-strand break
SNPs	single-nucleotide polymorphisms
ssRNAs	single-stranded RNAs

TBS	Tris-buffered saline
TBS-T	Tris-buffered saline Tween 20
UV	Ultra violet
XP	Xeroderma pigmentosum
ZFR	zinc finger recombinase
ɣH2AX	phospho-H2AX
3'UTR	3-untranslated region
8-OxoG	8-oxo-7,8-dihydroguanine
53BP1	53 binding protein 1
5'UTR	5'- Untranslated region

LIST OF FIGURES

LIST OF TABLES

ACKNOWLEDGMENT

I'm thankful to the German Academic Exchange service for their great support during the German Egyptian Research Long-term Scholarship (GERLS) program for four years. I’d like also to thank the Egyptian ministry of higher education and scientific research for their unlimited help.

My deep gratefulness and special thanks to *Prof. Dr. Ekkehard Dikomey*, for giving me the opportunity to pursue a PhD degree in his lab, supervision, his fruitful reading and reviewing the manuscript. I am grateful to *Prof. W. Schäfer,* for his supervision, reviewing and constructive criticizing of the manuscript.

Also, many thanks to all members of lab of radiobiology and experimental radiooncology for helping in practical work.

Finally, my appreciation and gratitude are extended to all members of my dear family especially my wife for her loving support, continuous backing, prayers, and understanding during the period in which this work was accomplished. Also, I would like to thank Maria Arruda for her great help in proofreading of the thesis.

SUMMARY

Radiotherapy (RT) is considered the cornerstone for the treatment of solid tumors. However, collateral damage to the surrounding tissues by ionizing radiation (IR) may cause severe side effects of RT, which leads to a limitation in the total IR dose employed. Therefore, specific targeting of tumor cells is required to enhance tumor radiosensitivity. To achieve this goal, the development of efficient radiosensitizing strategies is of great importance. Given that IR exerts its killing activity by damaging the DNA, one promising target for augmenting radiosensitivity would be through the DNA damage response (DDR). *Ataxia-telangiectasia mutated* (ATM) kinase is the main orchestrator of the DDR after IR. Consequently, the genetic knockdown of ATM may confer an extraordinary radiosensitization effect. In the current study, we aim to investigate the effect of targeting ATM via miRNAs on IR sensitivity. ATM inhibition in prostate cancer cell line (PC3) was studied *in vitro* using both endogenous (miR-18a, miR-100-5p, miR-101-3p and miR-421 either individually or in combination) and artificially pre-designed micro-RNAs (miRNAs) to target ATM. In breast cancer cell lines (MCF-7 and MDA-MB-468 cells) ATM was inhibited *in vitro* using only the artificial miRNAs.

Targeting ATM with an ATM inhibitor, KU55933, leads to an ATM-deficient phenotype evidenced by (i) reduced ATM protein expression, (ii) impaired pATM and pCHK2, (iii) deficient double-stranded break (DSB) repair indicated by an increased number of γH2AX foci at 24h time point after 2Gy, and more importantly (iv) an enhanced radiosensitivity phenotype measured by a colony forming assay. Transient transfection with a pool of siRNAs or shRNAs targeting ATM resulted in ATM translational inhibition as indicated by reduced ATM protein expression and enhanced radiosensitivity measured through the colony forming assay. Moreover, targeting ATM translation using the siRNAs pool lead to impaired DSB repair as indicated by a higher number of γH2AX foci after 24 hours. In addition, miRNAs targeting ATM affected ATM expression in the PC3 prostate cancer cell line. A vector expressing a combination of four endogenous miRNAs (pmiRNAs-4X) was stably integrated into the PC3 cell line resulting in moderate IR sensitivity, which positively correlated with the level of ATM knockdown. Cells harboring the three artificial miRNAs (pmiRNAs-3X) showed an efficient downregulation in the expression of ATM and the enhanced radiosensitive phenotype strongly correlated with the level of ATM downregulation.

In conclusion, although it has been previously demonstrated that individual miRNAs can downregulate ATM expression, a combined miRNA approach lead to efficient ATM knockdown and further enhanced radiosensitivity of several cancer cell

lines. These findings have significant implications for future treatment strategies of cancer.

1 INTRODUCTION

The treatment of tumors using radiotherapy (RT) is considered the cornerstone of cancer treatment. The concept of such treatment is based on tumors being destroyed by targeted irradiation, or ionizing radiation (IR) exposure, while the surrounding, normal tissue remains unaffected. However, the current outcomes of radiotherapy are relatively poor with respect to therapy efficacy and quality of life in cancer patients (Wang and Lang 2012). The failure to control a tumor with a given dose of radiotherapy tends to suggest that the tumor is 'radio-resistant'. Radio-resistance may arise from several mechanisms including hypoxia, DNA damage response (DDR) activity, and a deregulated survival pathway (e.g., through ERK or AKT signaling) (Begg et al. 2011).

The DDR comprises the genome maintenance machinery, which consists of multiple integrated cellular events that detect DNA damage, signal its presence and promotion of its repair (Jackson 2009). Importantly, micro RNAs (miRNAs) regulate gene expression at the post-transcriptional level. They play crucial role in tuning of DDR protein expression, which is involved in double-strand break (DSB) repair (Zhao et al. 2012). The overexpression of certain miRNAs leads to a reduction in key regulatory factors during the DDR, such as ataxia-telangiectasia mutated (ATM), ataxia telangiectasia and Rad3-related protein (ATR) and the histone variant H2AX (Lal et al. 2009; Hu et al. 2010; Wang et al. 2013). ATM underlies ataxia-telangiectasia (AT), an autosomal recessive disease. Since ATM is the central regulator of DDR (Shiloh 2006), modulation of ATM function has become an area of interest for the treatment of cancer. AT patients who carry a mutation in the ATM gene exhibit severe radiosensitivity and susceptibility to cancer (Chun and Gatti 2004). Experimental validations were used to confirm a direct interaction between the miRNAs and ATM. This was performed using a luciferase reporter vector containing the 3-untranslated region (3'UTR) of the ATM gene (Mansour et al. 2013). In this study, we investigated the functional interaction between miRNAs/ATM under physiological conditions i.e., during the response to ionizing radiation (IR), and evaluated the effect of these miRNAs on ATM expression and radiosensitivity.

1.1 The DNA damage response (DDR)

Exposure of cancer cells to agents that cause DNA damage such as ionizing radiation (IR), results in plenty of lesions that arise from single-strand breaks (SSBs) to double-strand breaks (DSBs) events (Lord and Ashworth 2012). Notably, IR induces DSBs both directly and indirectly whereas many chemotherapeutic drugs form DSBs

indirectly (Bishop et al. 1998). In addition, DSBs can be induced during normal cellular processes e.g., in the event of oxidative respiration that generates toxic reactive oxygen species (ROS). Other processes include germ cell meiotic recombination and the immune system's antigen receptor gene rearrangement events (i.e. V (D)J and class switch recombination) (Bassing and Alt 2004; Richardson et al. 2004; Valko et al. 2006; Shiloh and Ziv 2012). The function of the DNA damage response (DDR) is to detect and initiate the repair of such lesions (Jackson 2009; Bensimon et al. 2011).

In order to repair these lesions DDR employs different repair mechanisms (see **Figure 1**) to ensure proficient resolution. These mechanisms include mismatch repair, which is responsible for the removal of base mismatches resulting from replication error or by other endogenous modifications such as methylation and oxidation. The second mechanism is the base

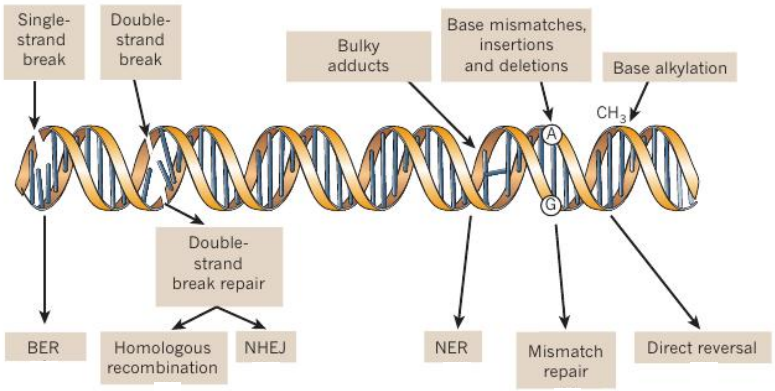

From Lord and Ashworth 2012

Figure 1. DNA damage lesions and repair mechanisms.

excision repair (BER) mechanism, which removes the damaged bases such as 8-oxo-7,8-dihydroguanine (8-OxoG). The third repair mechanism is nucleotide excision repair (NER), which deletes the bulky repair adducts and the intra-strand cross links (Lord and Ashworth 2012). DSBs are considered the most toxic of DNA lesions (Richardson and Jasin 2000). Cells have two mechanisms to circumvent these breaks; the first is non-homologous end joining (NHEJ), which is an error-prone pathway and mainly found in the cell cycle phase G1, and the second is homologous recombination (HR).

HR is an error-free mechanism that requires an undamaged DNA template and mainly works by repair of the DSBs generated during the replication process in S and G2 phases of the cell cycle (Lord and Ashworth 2012).

When DNA damage is irreparable, it often leads to cell death through apoptosis (Khalil et al. 2012). DNA lesion is recognized by various sensor proteins. These sensors initiate signaling pathways and amplify the signal by transducers, which affects many cellular processes. As illustrated in **Figure 2**, there are three steps in the DDR to repair DNA damage; these consist of sensors, mediators and effectors (Jackson 2009). Sensors are responsible for detecting lesions and changes in chromatin structure after DNA damage has occurred. Mediators are proteins that initiate a host of signaling events that reverse the DNA damage. Lastly, the effectors are considered to complete the DDR, as they are responsible for carrying out the final response relayed by the sensors to the transducers.

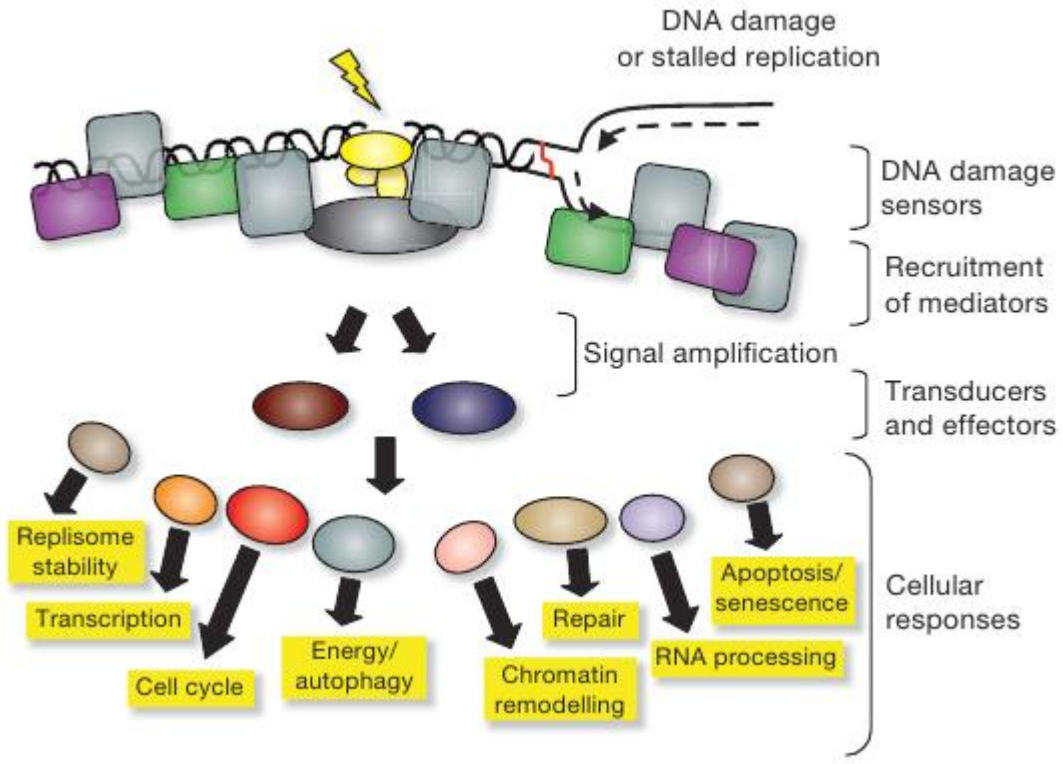

From Jackson S. & Bartek J, 2009

Figure 2. Steps of the DNA damage response (DDR).

1.2 Proteins involved in the DDR

There are a number of proteins that participate in the DDR. Some of these proteins include The MRE11–RAD50–NBS1 (MRN) complex, RAD9–RAD1–HUS1 (9-1-1) complex, ATM protein, ATR protein and checkpoint kinase 1 (Chk1) and checkpoint kinase 2 (Chk2). Other proteins taking part in the DDR include DNA-dependent protein kinase (DNA-PK) and Ku protein. Each protein in the MRN complex has a specific role to play. MRE11 has both endonuclease (for both single and double stranded DNA) and exonuclease activity. The RAD50 protein is considered to function as a dimerization domain (de Jager et al. 2001).

As illustrated in **figure 3**, The MRN complex and the 9-1-1 complex are the two main DNA damage sensors. Replication protein A (RPA) also detect single-stranded DNA (Sulli et al. 2012). The ATM and ATR are recruited by these sensors. The histone variant H2AX is phosphorylated on residue Ser-139 by ATM and recruit mediator of DNA damage checkpoint 1 (MDC1) that amplify the DDR signal. This phosphorylated H2AX, also termed as γH2AX. Once DNA damage occurs, aggregates of γ-H2AX assemble at the locations where there is DNA damage, at which point the damaged DNA recruits the MRN complex thereby activating the DDR (Shiloh 2003). The H2AX histone protein is an indicator of DNA damage as it is rapidly phosphorylated after cell exposure to ionizing radiation (Bakkenist and Kastan 2003).

Consequently, the ATM protein phosphorylates downstream proteins involved in the cell cycle. The first of these proteins to be phosphorylated are Chk1 (activated by ATR) and Chk2 (Downstream kinases). According to (Shiloh 2003) both Chk1 and Chk2 phosphorylate CDC25A, a phosphatase protein. CDC25A is responsible for the dephosphorylation of the cyclin dependent kinases (Cdk) and maintains activity of Cdk1 and Cdk2. The dephosphorylation of Cdk2 activity results in a halt in the cell cycle at the G1-S phase, which will provide enough time for damaged DNA to be repaired before DNA replication occurs and mitosis is complete (Shiloh 2003; Jackson 2009; Bensimon et al. 2011). The tumor suppressor, p53 (Effector), is known to play an integral role in arresting the cell cycle at the G1/S phase (Bakkenist and Kastan 2003). Both ATM and Chk2 proteins are known to activate p53 by phosphorylating it at residue Ser-15 and Ser-20 respectively (Shiloh 2003). Other function of ATM is to phosphorylate proteins involved in DNA repair processes such as the breast cancer susceptibility gene (BRCA1). BRCA1 can be also phosphorylated by ATR (Sulli et al. 2012).

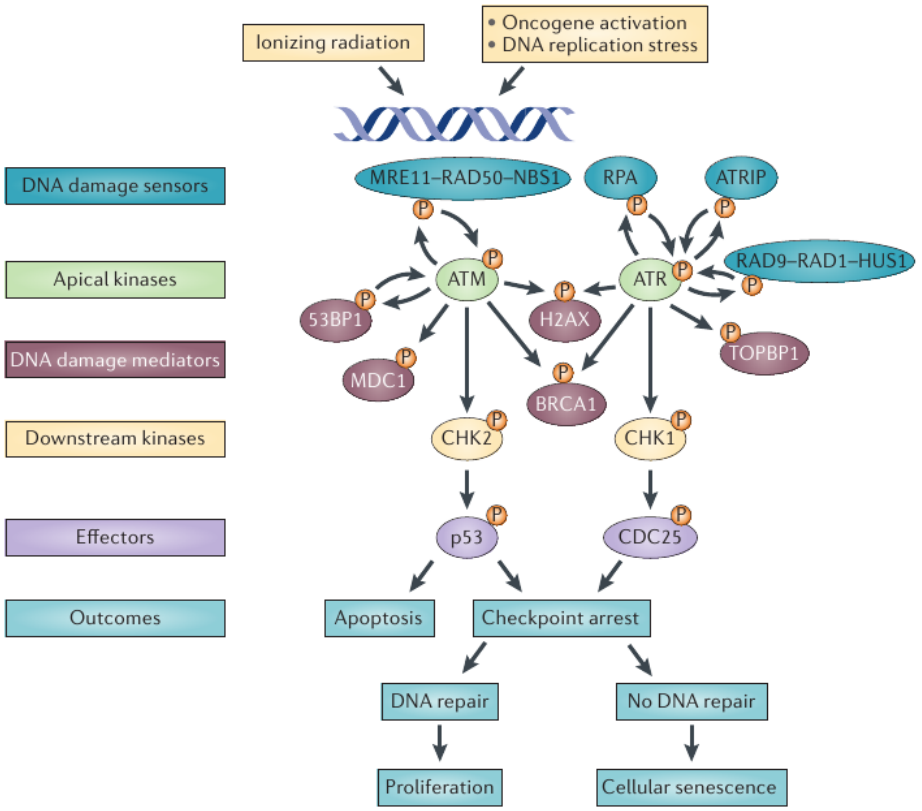

From Sulli G. et al., 2012

Figure 3. The DNA damage response proteins.

1.3 The DNA damage response and cancer

Cells have to regularly respond to DNA damage lesions such as SSBs and DSBs which arises from replication stress, telomere shortening, and several exogenous and endogenous DNA targeting materials. Of the various types of DNA damage that cells can incur, DSB remains the greatest threat. In mammalian cells, unrepaired or incorrectly repaired DSBs are a frequent source of chromosomal rearrangements with carcinogenic potential and a triggering of cellular apoptosis (Richardson and Jasin 2000; Khanna and Jackson 2001; Lips and Kaina 2001). The DDR aims to repair these lesions by correcting SSBs and DSBs and maintaining control of the cell cycle checkpoints (Bensimon et al. 2011). The DDR has been shown to utilize different and distinct repair mechanisms in order to avoid genomic instability, which is a hallmark of cancer (O'Connor 2015). Most of the information pertaining to the DNA damage response stems from hereditary disease caused by defects in DNA damage signaling such as xeroderma pigmentosum (XP). XP occurs because of a mutation in the XP family of genes which is characterized by a predisposition to skin

cancer due to an innate inability to repair UV-light-induced DNA lesions by nucleotide excision repair (NER). Furthermore, the genetic conditions ataxia telangiectasia and Nijmegen breakage syndrome (NBS) have mutations in the ataxia-telangiectasia mutated (ATM) and NBS1 genes, respectively which are characterized by a predisposition to lymphoid malignancies (Shiloh 1997). Ovarian and breast cancer predisposition are concomitant with mutations in the BRCA1 and BRCA2 genes which play very important roles in DSBs repair especially by homologous recombination (Huen et al. 2010). The expressed proteins from these two genes are involved in DSBs signaling. Furthermore, Colon cancer and uterine tumors have a dysfunction in the hereditary nonpolyposis colon cancer (HNPCC) genes that are involved in DNA mismatch repair (MMR). All of the aforementioned mutations lead to cancer susceptibility. In contrast, they can also lead to increased radiosensitivity in the case of ATM-deficient tumors. The molecular investigation of these types of cancer has established a very important link between DDR and tumor development, as well as DNA damaging agents and DDR defects (Luch 2005).

1.4 The DNA damage response (DDR) in tumor radiotherapy

Radiotherapy (RT) is considered as one of the key treatments for the treatment of tumors, especially solid tumors. RT generates different DNA lesions by inducing release of reactive oxygen species. Irradiation induces base modification lesions as 8-OxoG. In addition, ionizing radiation induced DNA breaks e.g., 1 Gy induces approximately 1,000 SSBs and 35 DSBs/cell (Nikjoo H 1998; Rothkamm and Löbrich 2003). Irreparable DSBs play a central role in irradiation-induced cytotoxicity. Therefore, pathways involved in sensing and repairing of these DSBs are critical for successful outcomes of radiotherapy.

Changes in the DSBs repair processes in tumors because of genetic and epigenetic factors affects cancer cells sensitivity to radiotherapy. Willems et al. detected many single-nucleotide polymorphisms (SNPs) in the Ku70 and Ku80 genes that are correlated with enhanced sensitivity of tumors to radiation (Willems et al. 2008). Moreover, the non-functional BRCA1 has been reported to induce radiosensitization (Fourquet et al. 2009; Ernestos et al. 2010). Furthermore, the reduction of BRCA1 expression due to hyper-methylation is a major event in multiple non-hereditary cancer types (Esteller et al. 2000; Lee et al. 2007), suggesting that radiation sensitivity can be predicted using BRCA1 promoter methylation acts as a marker of radiosensitivity.

ATM plays a main role in DSBs repair through sensing the damage, promotion of end-processing and BRCA1 recruitment to initiate repair homologous recombination (Jazayeri et al. 2006; Huen et al. 2010). Ataxia-telangiectasia patients exhibit severe

radiosensitivity, which suggests a major function of the ATM gene in protection against ionizing radiation (Shiloh 1997). By inference, this suggests that ATM is a relevant target for radiosensitization. Consequently, many small-molecule inhibitors of ATM have been used in pre-clinical models to radiosensitize cancer cells (Hickson et al. 2004; Rainey et al. 2008). This profound radiosensitivity is independent of p53 status (Westphal et al. 1998) and molecular inhibitors of ATM effectively enhance radiosensitivity in p53-mutant glioblastoma cells (Biddlestone-Thorpe et al. 2013). The ability of ATM inhibitors to sensitize p53-deficient cancer cells to ionizing radiation is very important in the context of resistant tumors to radiotherapy since there is a high frequency of p53 mutations in malignant tumors.

Another important pathway in DSBs repair in cancer cells is the non-homologous end-joining pathway, where inhibition of this has a central role in radiosensitization. In fact, DNA-PK inhibitors reveal a pronounced radiosensitization in tumor cells (Veuger et al. 2003). After ionizing radiation, DSBs can be repaired by either NHEJ and also by HR and both mechanisms cooperate in the repair of these breaks (Takata et al. 1998). Therefore, the inhibition of DNA-PK and ATM appears to be a potential strategy that can be used to enhance radiosensitivity. The small molecule NVP-BEZ235, was first used as a mTOR inhibitor and was found to also inhibit ATM and DNA-PK enhancing radiosensitivity in pre-clinical models (Konstantinidou et al. 2009; Mukherjee et al. 2012). However, this inhibitor was also found to inhibit ATR, which is a very important protein in the stalling of replication forks (Toledo et al. 2011). Furthermore, ATR is required for survival where an absence of ATR results in lack of cell viability even without exposure to genotoxic stressors (Brown and Baltimore 2000, 2003). There is an urgent need to develop radiosensitizing molecules which inhibit both ATM and DNA-PK and augment the anti-cancer effects of radiotherapy.

1.5 ATM Gene and protein structure

ATM is a one of the phosphoinositide 3-kinase (PI3K)-related protein kinase (PIKK) family. Members of this family are very large proteins (300–500 KDa) which in addition to ATM also include ataxia telangiectasia and Rad3-related protein (ATR), and the DNA-dependent protein kinase (DNA-PKcs) (Shiloh 2003).

ATM is a large molecular weight protein with distinct domains (Shiloh and Kastan 2001). The protein product of this transcript is approximately 350 kilo-dalton (KDa) and contains 3056 amino acids (Savitsky et al. 1995; Uziel et al. 1996). However, the only domain with a defined regulatory function is its kinase domain that is found on the carboxyl terminal region of ATM. The non-kinase portions of ATM are dominated by N-terminal HEAT (Huntingtin, Elongation factor 3, alpha subunit of PP2A

and TOR1) repeat units. A unit of HEAT repeat consists of paired interacting anti-parallel helices joined by a flexible intra-unit loop (Perry and Kleckner 2003). The N-terminus also serves as an important surface for interaction between ATM and other proteins such as p53 (Chen et al. 2003).

ATM gene in AT patients is localized to chromosome 11q22-23 and cloned by positional cloning (Gatti et al. 1988; Savitsky et al. 1995; Uziel et al. 1996). The ATM gene is extended over 160 kb of genomic DNA, contains 66 exons, and encodes a 13 kb transcript. As illustrated in **figure 4**, ATM contains a FAT domain, a protein kinase domain and a FATC domain. In addition to three autophosphorylation sites include Ser-367, Ser-1893 and Ser-1981. Many other Ser and Thr phosphorylation sites (P) are also found on activated ATM. Three phosphatases, protein phosphatase-2A (PP2A), PP5 and wild type p53- induced phosphatase 1 (WIP1) control ATM activation. Various ATM substrates bind also to N terminus region (called substrate binding site, SBS) beside the binding to the kinase domain (Lavin 2008).

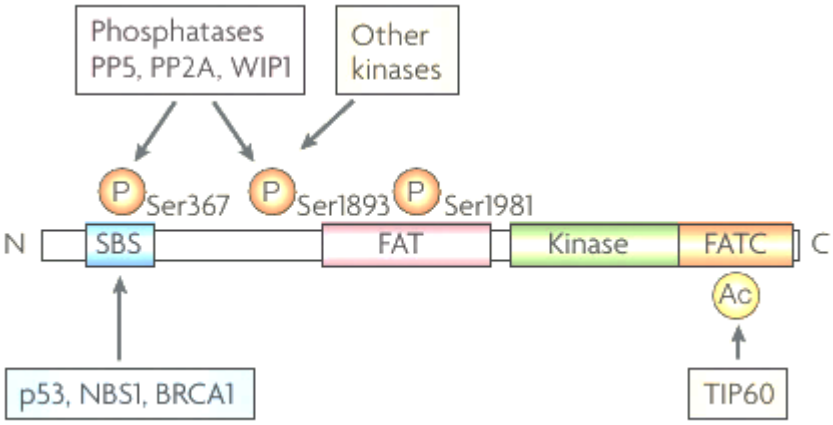

From Martin F. Lavin 2008

Figure 4. Schematic representation of ATM gene.

1.6 The activation of ATM

In normal cells, ATM exists as either a dimeric or multimeric form (Bakkenist and Kastan 2003). After DSBs occurs, ATM autophosphorylated in at least four sites (S367, S1893, S1981, and S2996) thus promoting monomerization and kinase activity (Bakkenist and Kastan 2003; Kozlov et al. 2011). Autophosphorylation is governed by the interaction of several phosphatases, including protein phosphatase 2A (PP2A), protein phosphatase 5 (PP5), and wild WIP1 (Ali et al. 2004; Goodarzi et al. 2004; Shreeram et al. 2006). As shown in **Figure 5**, after DNA damage MRN complex and NBS1 are responsible of the activation of ATM. It is converted to active monomer which is phosphorylated and acetylated. On the other hand, ROS can directly activate ATM which oxidize cysteine residues to promote disulfide bridge-mediated dimerization (Stracker et al. 2013). ATM defective cells complemented with S1981A, S367A, or S2996A mutants exhibit defective ATM-dependent responses to DNA damage (Kozlov et al. 2011).

In addition, chromatin status plays a major role in ATM activation and the regulation of its activity at break sites (Bakkenist and Kastan 2003; Murga et al. 2007). ATM interactions with chromatin before DNA damage happened regulate its activation (Kim and Wong 2009).

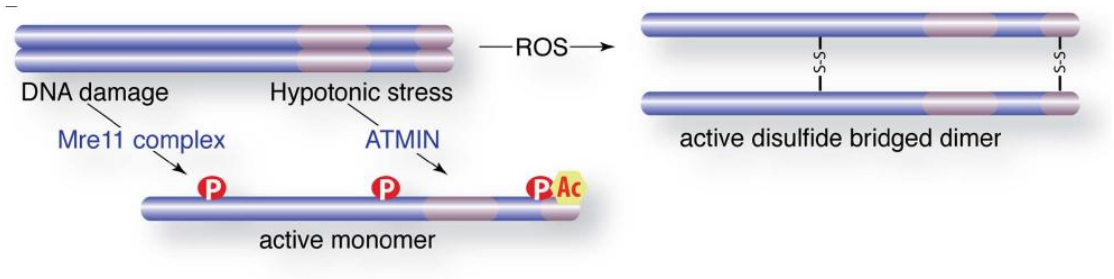

From Stracker T. et al. 2013

Figure 5. ATM protein activation.

1.7 Involvement of ATM in the DNA damage response

Different DDR mechanisms are formed depending on the type of DNA damage; ATM-dependent signaling is the main response to DSBs (Harper and Elledge 2007). Posttranslational modifications of ATM such as phosphorylation (including autophosphorylation) and acetylation are essential for optimal kinase activity. The ATM autophosphorylation mechanism activates ATM and phosphorylated–S1981 (p-S1981) is often used as a marker of the active protein.

In **Figure 6**, the DNA-damage response is preliminary started by monomerization of ATM and phosphorylation of histone H2AX. The ATM substrate; mediator of DNA-damage checkpoint protein-1 (MDC1) then binds to γH2AX. The MRN complex conjugate with MDC1 by NBS1 protein. Thereafter, BRCA1 and p53 binding protein-1 (53BP1) are recruited at the DSB site. 53BP1, is another important mediator protein, which also attracts the MRN complex to the DSB site. This results in further amplification of ATM-dependent DNA damage signaling (Lee et al. 2010). This orchestrated assembly of damage response proteins including MDC1, 53BP1 and p-S1981 ATM extends several kilo-bases from the break site and is thought to concentrate repair factors at DSB, thus expediting the DNA repair process (Löbrich et al. 2010). Notably, ATM is dispensable in initiating the assembly process of damage response proteins at the DSB site since DNA-PKcs can phosphorylate histone H2AX in a redundant but early process (Rogakou et al. 1998; Stiff et al. 2004).

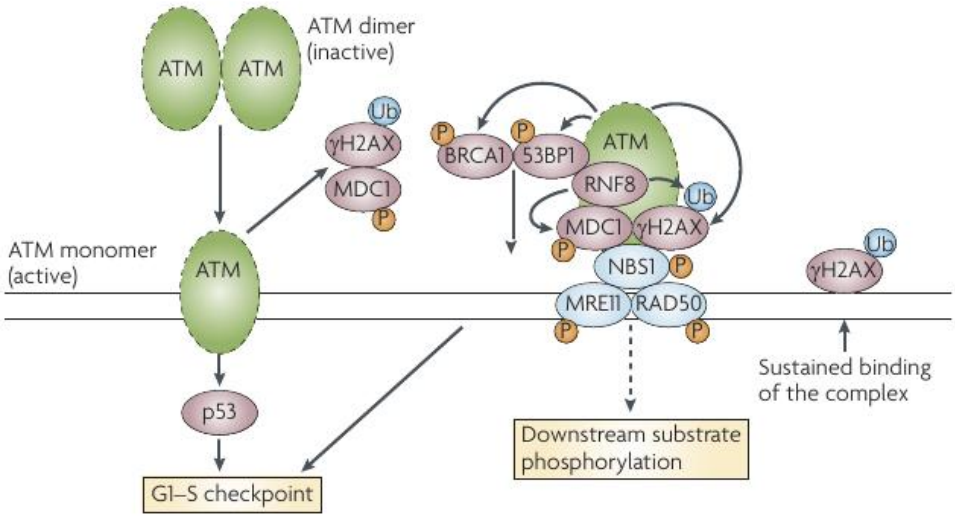

From Lavin M. 2008

Figure 6. ATM-dependent DNA damage response (DDR).

1.8 RNA interference (RNAi)

RNA interference (RNAi), known as dsRNA-mediated gene silencing, is a naturally occurring phenomenon in eukaryotes in which a double-stranded RNA knocks down or suppresses the expression of a target gene. Three major RNAi pathways found have been characterized for small non-coding RNAs. The major RNAi pathways are microRNA (miRNA), piwiRNA (piRNA) and small interfering RNA (siRNA). SiRNAs are 21-23 base pair (bp) derived from dsRNA (Aravin et al. 2007).

The siRNA pathway is activated by exogenous dsRNA, and this pathway serves to defend the genome against invading nucleic acids. RNAi experiments exploit the siRNA pathway by delivering dsRNA to induce knockdown of the target gene (Perwitasari et al. 2013).

As illustrated in **figure 7**, when a dsRNA is introduced into a cell, either by using chemically modified siRNAs or by short hairpin RNA (shRNA); it is processed into ~21bp small interfering RNAs (siRNAs) by an enzyme called Dicer (not shown). The siRNAs are incorporated into an RNA- Induced Silencing Complex (RISC). The double-stranded siRNA is unwound, the passenger strand is degraded and the RISC complex uses the guide strand to guide the complex to the homologous mRNA. The RISC complex has endonuclease activity and cleaves the mRNA. The mRNA is destroyed, and the protein for which the mRNA is coding is not expressed (Mohr et al. 2014).

siRNA and microRNA (miRNA) have some similarities because both use RISC pathway components but differ in their mode of gene silencing and outcome. siRNAs show full length complementarity to target mRNAs causing specific knockdown of gene via target mRNA cleavage while miRNAs show a partial complementarity with target gene.

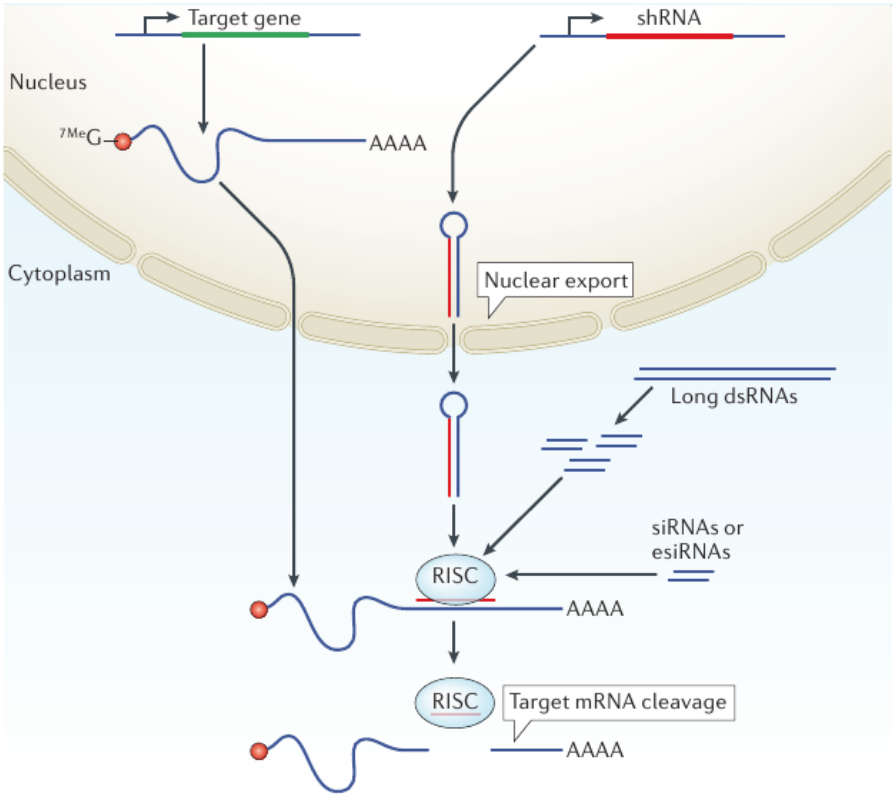

From Mohr et al. 2014

Figure 7. RNAi mechanism to silence gene expression.

1.9 Micro RNAs (miRNAs)

Currently over 1,223 human miRNAs mature sequences have been reported in the mirbase online resource (Mestdagh et al. 2012). The miRNAs are expressed from independent transcription units, because they do not contain an open reading frame (ORF) and are expressed separately from the nearby genes (Lau et al. 2001). miRNAs are gene expression regulators which work in post-transcriptional level. They destabilize or inhibit the translation of messenger RNA (mRNA). Furthermore, miRNAs are small (~ 22 nucleotide) non-coding RNAs which inhibit protein synthesis (Östling et al. 2011). Specifically, the 5' end of a miRNA (positions 2–8 nt) binds to a targeting sequence, located at the 3' end of the mRNA- 3' UTR region, depending on the level of complementarity between the two sequences (Betel et al. 2008; Catto et al. 2011).

Remarkably, each miRNA might control hundreds of target genes and may modulate up to 60% of all transcripts (Östling et al. 2011), accounting for ~1% of the

genome (Kim 2005). Nevertheless, most miRNAs induce a modest reduction (less than two-fold) in their target molecule concentration (Bartel 2009).

1.9.1 The Biogenesis of miRNAs

miRNAs are transcribed in the nucleus by a polymerase II into a long primary transcript (pri-miRNAs), which contains both a 5'-cap structure (7MGpppG), as well as a 3'-end poly(A) tail, and is approximately 70 nucleotides in length (Iorio and Croce 2012; Takada and Asahara 2012; MISSING: 2016). miRNAs fold back on themselves to form hairpin-shaped precursor miRNAs (pre-miRNAs) by the action of nuclear RNAase III Drosha (Kim 2005), and are associated with a double stranded RNA-binding protein DGCR8, known as the microprocessor complex (Carthew and Sontheimer 2009; Iorio and Croce 2012). Alternatively, miRNA processing might occur through splicing of pri-miRNA transcripts to release introns, which are structurally identical to pre-miRNAs (Carthew and Sontheimer 2009).

Following nuclear processing, pre-miRNAs are transported to the cytoplasm, where maturation and action will take place. This transport occurs via one of the nuclear Ran-GTP-dependent transport receptors, exportin-5 (Kim 2005; Iorio and Croce 2012). A RNAase III enzyme, Dicer, processes pre-miRNAs into ~22-nucleotide miRNA duplexes (Kim 2005). The maturation process is finalized by the cleavage of a precursor miRNA hairpin into mature miRNA (Griffiths-Jones 2004; Bhayani et al. 2012; Iorio and Croce 2012). These mature miRNAs are primed to regulate a variety of pathways, by interfering with the translation process of certain mRNAs. This process requires an incorporation of the miRNA mature sequence into a miRNA-containing ribonucleoprotein complex, termed miRISC (miRNA-containing RNA-induced silencing complex) (Kim 2005). The resulted miRNA can either mRNA degradation or translational repression.

In addition, it has been shown miRNAs also bind to the open reading frame (ORF) sequences and the 5′ UTR. This interaction resulted in gene expression activation rather than repression (Orom et al. 2008). It is possible also that miRNAs bind directly to RNA- binding proteins and stop them from binding to their targets. The whole biogenesis and function process of miRNAs is illustrated in **figure 8**.

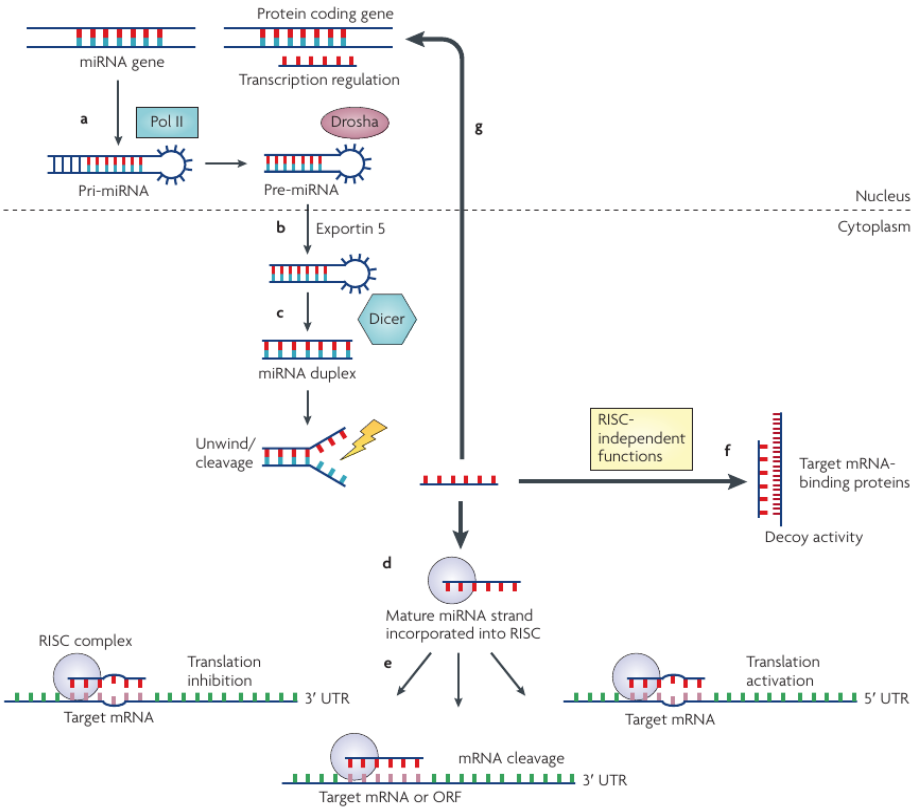

From Garzon R. et al. 2010

Figure 8. MicroRNA biogenesis and mechanism of action.

Target binding is made by complementarity into the 3' untranslated regions (UTR) of the target transcript (Östling et al. 2011; Iorio and Croce 2012). miRNAs can also regulate gene expression of mRNAs that contain miRNA target sites in their 5'UTR (Lytle et al. 2007). However, there is currently only one known example of a miRNA targeting the 5'UTR of naturally occurring mRNA. This miRNA which binds to 5'UTR is associated with gene activation rather than gene repression (Orom et al. 2008).

1.9.2 Role of miRNAs in the DNA damage response

Recently, it was shown that non-coding ribonucleic acids (ncRNAs) add an additional layer of complexity to the DDR by controlling DDR proteins (Francia et al. 2012). As illustrated in **figure 9**, Ionizing radiation-induced DNA damage in tumors triggers the DNA damage response (DDR) and activates multiple intracellular substrate proteins involved in post-transcriptional regulation (Zhao et al. 2012). MiRNAs can play

a role in fine tuning of proteins involved in the DDR, which are participating in DSBs repair pathways (Chowdhury et al. 2013).

After DSBs occur, the DDR apparatus start to sense and detect the position of damage by different proteins such as the MRN complex, ATM and KU heterodimers. These proteins are the products of transcripts that have long 3' untranslated regions (UTR), which contain many miRNA-binding sites (Savitsky et al. 1997; Miranda et al. 2006). These long transcripts infer that these genes are post-transcriptionally regulated by miRNAs.

In fact, overexpression of miRNAs such as miR-421 and miR-101, which target ATM and DNA-PK respectively, lead to reduction of their expression and is correlated with enhanced radiosensitivity (Hu et al. 2010; Yan et al. 2010). Yan and his colleagues reported that miR-101 suppresses the activity of DNA-PKcs in various cancers (Yan et al. 2010). Another mediator is ATR, which is very important for survival and its loss cannot be tolerated by the cell (Fang et al. 2004). MiR-185 represses ATR expression and enhances radiation-induced apoptosis (Wang et al. 2013).

Furthermore, overexpression of miRNA-24 reduces histone H2AX expression and impairs DNA damage repair efficiency, while enhancing radiosensitivity (Lal et al. 2009). The downregulation of miR-24 expression in differentially terminated cancer cells promotes DNA DSB repair and reduces cellular sensitivity to DDR (Lal et al. 2009; Srivastava et al. 2011). Consequently, miRNAs play a regulatory role in the DDR process, which will facilitate tumor radiosensitivity.

Although various researchers have suggested a negative correlation between single miRNA expression and target gene expression/function, Recent studies of miRNAs detection in tumors were not able to demonstrate such correlation between single miRNA expression and the target gene (Hanna et al. 2012).

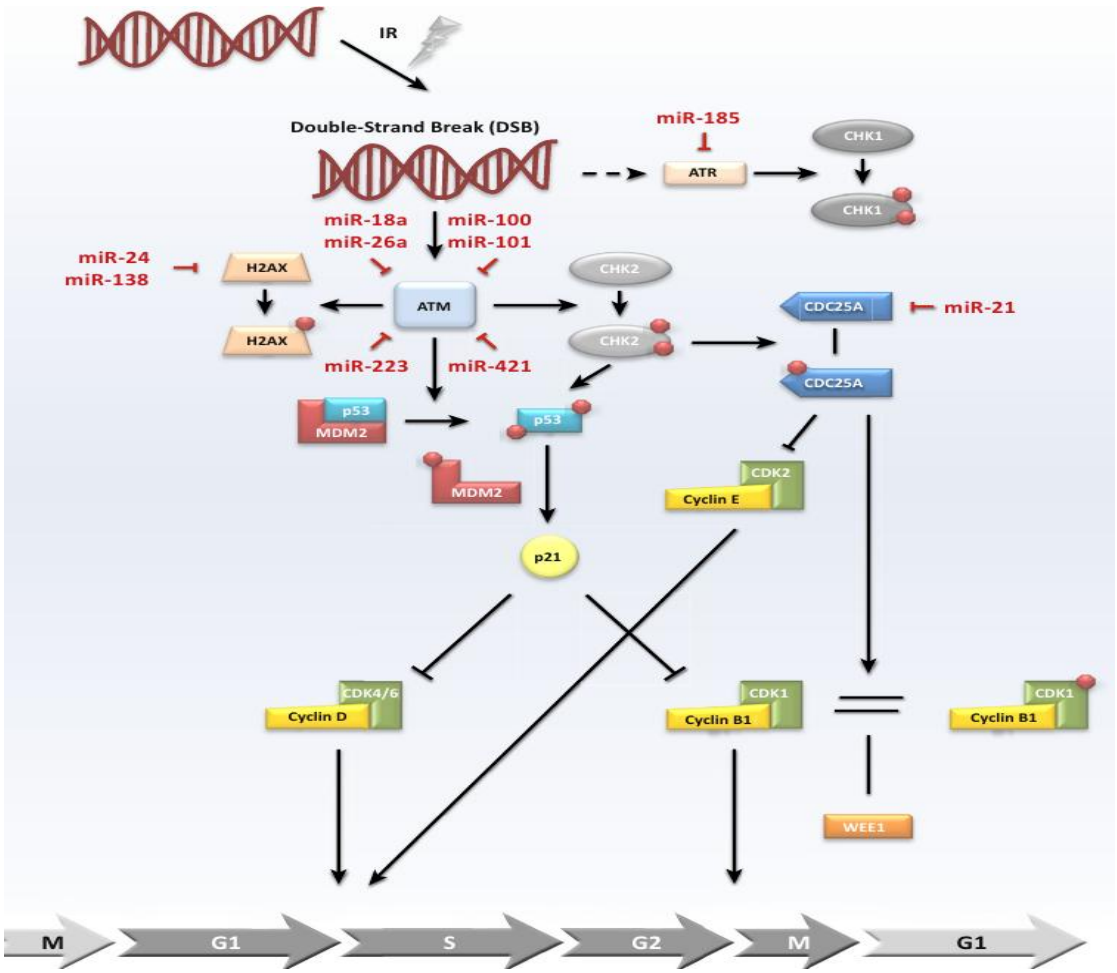

From Gandellini et al. 2014

Figure 9. miRNAs involved in the DNA damage response.

In conclusion, numerous studies have shown that overexpression or deregulation of DNA damage response components can be the reason to develop therapy resistance in different types of tumors. Therefore, designing effective modifiers to target key players in DDR pathway and improve radiotherapy efficiency is of high importance. ATM is one of the central kinases involved in the cellular response to DSBs which activated after cell exposure to ionizing radiation (IR). Despite great advancement in our understanding of ATM signaling and function in recent years, the protein expression of ATM at the post-transcriptional level is subjected to very complex mechanisms that are not yet fully resolved. In this context, non-coding RNAs, such as

microRNAs (miRNAs), have emerged as important regulators of gene expression of key components of DDR pathway. Regulation of DDR proteins using endogenous miRNAs attract the eyes of many researchers and the researches revealed a negative correlation between miRNAs expression level and DDR proteins level in *vitro*. However, recent study by Hanna et al cannot prove this correlation in *vivo*.

In this thesis, we aimed to test the hypothesis of whether co-expression of different miRNAs have a synergistic effect on ATM expression and cellular radiosensitivity in comparison to single miRNA expression.

2 MATERIALS AND METHODS

2.1 Materials

2.1.1 Laboratory equipment

- **General:**

Refrigerated microcentrifuge R	Beckmann Instruments GmbH, Munich, Germany
Refrigerated centrifuge, Megafuge 1.0 R	Heraeus, Hanau, Germany
Refrigerated centrifuge 5804R	Eppendorf, Hamburg, Germany
Centrifuge function line	Heraeus, Hanau, Germany
Bio-photometer	Eppendorf, Hamburg, Germany
Freezer -20°C	Kryotech, Hamburg, Germany
Freezer -80 °C	Fryka, Esslingen, Germany
Bio-photometer	Eppendorf, Hamburg, Germany
Hot-plate thermostat 5320	Eppendorf, Hamburg, Germany
Magnetic stirrer, RH Basis	IKA Labortechnik, Staufen, Germany
Minispin plus centrifuge	Eppendorf, Hamburg, Germany
Pair of scales AE160 / P1200	Mettler, Giessen, Germany
pH meter 300	Beckmann Instruments GmbH, Munich, Germany
Pipetboy	Eppendorf, Hamburg, Germany
Pipettes	Eppendorf, Hamburg, Germany
Refrigerator	Bosch, Stuttgart, Germany
Water bath	Lauda, Lauda-Königshofen, Germany

- **Cell culture:**

Sterile work benches, Herasafe	Kendro, Hanau, Germany
Olympus CK2	Olympus Optical Co., LTD, Japan
Coulter Counter model Z1	Beckman Coulter, Krefeld, Germany
Cell incubator inCu safe	Sanyo, Leicestershire, UK
Cell incubator Hera cell 240	Kendro, Hanau, Germany
Axiovert 40CFL	Carl Zeiss, Göttingen, Germany
Mr. Frosty	Nalgene, NY, USA

- **Western blot:**

Criterion Precast Gel System (Criterion electrophoresis cell and Criterion Blotter)	Bio-Rad Laboratories, Hercules, CA, USA
Power Supply Consort E455 / E802	Labortechnik Fröbel GmbH, Lindau/Bodensee Germany
Western blot development cassette	Amersham Pharmacia, Buckinghamshire, UK
Tilting table / shaker platform	neoLab, Heidelberg, Germany
Light sensitive CCD camera system (NightOWL)	Berthold Technologies GmbH&Co. KG Bad Wildbad, Germany
Developer, curix 60	agfa, Mortsel, Belgium
Bag sealer	Severin, Sundern, Germany

- **Others:**

Fluorescence microscope, Axioplan 2 System for confocal pictures: Apotome, AxioCam MRn	Carls Zeiss, Göttingen, Germany
Primus Thermal cycler	MWG Biotech, Ebersberg, Germany
X-ray generator type RS225 research	Gulmay Medical LTD, Oxford, UK

2.1.2 Plasmids

hsa-amiR-ATM-10355	GAAAGAAGAAGCCCAATGGAT
hsa-amiR-ATM-10844	ATAAAGGTGGGACACATGGAA
hsa-amiR-ATM-12745	TTAATCTGGACACAACTGTTC
PcDNA-emiR-4X (miR-421, miR-100, miR-101, miR-18a)	The four sequences are shown below in section 2.1.14
pLV-ATMi	CTGAGTAATACGCAAATCC (Addgene plasmid # 14542)

2.1.3 Software

- Prism 4.03 for Windows, Graphpad software, Inc
- Image J for Windows

2.1.4 Laboratory Materials

- **General:**

Pasteur pipettes, plastic	Falkon, NJ, USA
Pipette tips	Eppendorf, Hamburg, Germany
Pipette tips, stuffed	Eppendorf, Hamburg, Germany
Pipettes, plastic (1-50ml)	Falkon, NJ, USA
Tubes 1.5ml, 2ml	Eppendorf, Hamburg, Germany
Tubes 15ml, 50ml	Falkon, NJ, USA
Wipes	Wepa, Arnsberg, Germany
Gloves, latex	Hartmann, Heidenheim, Germany
Gloves, nitrile	Ansell, Staffordshire, UK
Parafilm	Pechiney Plastic, Chicago, USA

- **Cell culture:**

6-well plates	Falkon, NJ, USA
Cell culture flasks T25, T75	Sarstedt, Nümbrecht, Germany
Cryo-tubes	Sarstedt, Nümbrecht, Germany
Pasteur pipettes, glass	Carl Roth GmbH, Karlsruhe, Germany
Sterile filter (Rotilabo 0,22 µm)	Millipore, MA, USA
12-well plates	Falkon, NJ, USA
24-well plates	Falkon, NJ, USA

- **Western blot:**

Filter paper, Whatman	Bio-Rad Laboratories, Hercules, CA, USA
Nitrocellulose membrane	Trans Blot supported, BioRad
Criterion-Gels	Bio-Rad Laboratories, Hercules, CA, USA

- **Others:**

Cover slips	Karl Hecht, Sondheim, Germany
MicroAmp® Fast Optical 96-well Reaction Plate (0.1ml)	Applied Biosystems, CA, USA
Microscope slides	Karl Hecht, Sondheim, Germany
Optical Adhesive Covers	Applied Biosystems, CA, USA
Round-bottom tube	Sarstedt, Nümbrecht, Germany

2.1.5 Chemicals, reagents and kits

- **Reagents:**

Bovine serum albumin (BSA)	PAA, Pasching, Austria
Bromophenol blue	Sigma-Aldrich, Deisenhofen, Germany
Crystal violet stain	Sigma-Aldrich, Deisenhofen, Germany
Dimethyl sulfoxide (DMSO)	Sigma-Aldrich, Deisenhofen, Germany
Disodium hydrogen phosphate (Na_2HPO_4)	Merck, Bad Soden, Germany
Dithiothreitol (DTT)	Sigma-Aldrich, Deisenhofen, Germany
Ethanol	Th. Geyer, Hamburg, Germany
Formaldehyde 37%	Merck, Bad Soden, Germany
Glucose	Sigma-Aldrich, Deisenhofen, Germany
Glycerin	Sigma-Aldrich, Deisenhofen, Germany
Hydrochloric acid (HCl)	Merck, Bad Soden, Germany
Magnesium chloride ($MgCl_2$)	Sigma-Aldrich, Deisenhofen, Germany
Methanol	J.T. Baker, NJ, USA
Potassium chloride (KCl)	Merck, Bad Soden, Germany
Potassium dihydrogen phosphate (KH_2PO_4)	Merck, Bad Soden, Germany
RNAase	Serva, Heidelberg, Germany
Sodium chloride (NaCl)	J.T. Baker, NJ, USA
Sodium dodecyl sulfate (SDS)	Sigma-Aldrich, Deisenhofen, Germany
Sodium hydrogen phosphate (NaH_2PO_4)	Merck, Bad Soden, Germany
Sucrose	Merck, Bad Soden, Germany
Tris-HCl	Sigma-Aldrich, Deisenhofen, Germany
Triton X	Serva, Heidelberg, Germany
Trizma base	Sigma-Aldrich, Deisenhofen, Germany
Tween 20 (polyoxyethylene (20) sorbitan monolaurate)	Sigma-Aldrich, Deisenhofen, Germany
ß-mercaptoethanol	Sigma-Aldrich, Deisenhofen, Germany
2-propanol	Merck, Bad Soden, Germany
Antifade mounting medium, Vectashield	Vector Laboratories, Ca, USA
ATM inhibitor KU55933	Tocris Bioscience, Missouri, USA

Protease inhibitor cocktail	Cell signaling, USA
RIPA buffer	Roche,Swizerland

- **Kits:**

BCA Protein Assay	Pierce Biotechnology, IL, USA
Nucleobond AX plasmid purification kit	MACHEREY-NAGEL, Germany
Mycoplasma PCR Elisa Kit	Roche Diagnoistics, Mannheim, Germany

2.1.6 Cell lines and media for cell culture

All cell lines used in this study were regularly tested for mycoplasma infection.

MCF7 Human breast adenocarcinoma cell line; this was first isolated in 1970 from the breast tissue of a 69-year old Caucasian woman **origin**: mammary gland, breast; derived from metastatic site: pleural effusion; **cultivation:** in DMEM supplemented with 10% fetal calf serum, w/o 100 U/ml penicillin or 100 µg/ml streptomycin.

PC3 Human prostate adenocarcinoma cell line; PC-3 was initiated from a bone metastasis of a grade IV prostatic adenocarcinoma from a 62-year-old male Caucasian; **cultivation:** in DMEM supplemented with 10% fetal calf serum, w/o 100 U/ml penicillin or 100 µg/ml streptomycin.

MDA-MB231 Human breast adenocarcinoma cell line; MDA-MB-231 was isolated from pleural effusions of a Caucasian breast cancer patient; **cultivation:** in DMEM supplemented with 10% fetal calf serum, w/o 100 U/ml penicillin or 100 µg/ml streptomycin.

MDA-MB468 Human triple negative breast cancer cell line; MDA-MB-468 was isolated in 1977 by Cailleau, et al., from a pleural effusion of a 51-year-old Afro-Caribbean female patient with metastatic adenocarcinoma of the breast; **cultivation:** in DMEM supplemented with 10% fetal calf serum, w/o 100 U/ml penicillin or 100 µg/ml streptomycin.

Breast cancer cell lines were used as representative of the most frequent cancer in women and prostate cell line were chosen as representative of the most frequent cancer type in men.

All media and reagents for cell culture were obtained from Invitrogen GmbH Karlsruhe, Germany.

• DMEM	Dulbecco's Modified Eagle Medium
• Opti-MEM	Reduced Serum Media is a modification of Eagle's Minimum Essential Media, buffered with HEPES and sodium bicarbonate, and supplemented with hypoxanthine, thymidine, sodium pyruvate, L-glutamine, trace elements, and growth factors.
• Trypsin-EDTA	used widely for dissociation of tissues and cell monolayers
• Fetal calf serum (FCS)	the most widely used growth supplement for cell culture media
• Cryopreservation solution	10% DMSO in FCS

2.1.7 Antibiotics

• Penicillin	10,000 U/ml Penicillin
• Streptomycin	10,000 µg/ml Streptomycin
• Puromycin	3µg/ml and 1µg/ml
• Blasticidin	15µg/ml and 5µg/ml

2.1.8 Antibodies

- **Primary antibodies**
  - Polyclonal

Rabbit anti-ATM	Epitomics, CA, USA
Rabbit anti-pChk2 Thr68	Cell Signaling, MA, USA
Rabbit anti-phospho 53BP1 Ser25	Novos, USA

  - Monoclonal

Mouse anti-β–actin	Sigma-Aldrich, Deisenhofen, Germany
Mouse anti-ɣH2AX Ser139	Cell Signaling, MA, USA
Mouse anti-phospho ATM Ser1981	Rockland, USA

- **Secondary antibodies**
  - Western blot analysis

horseradish peroxidase-linked anti-rabbit IgG	Amersham Pharmacia Biotech, Freiburg, Germany
horseradish peroxidase-linked anti-mouse IgG	Amersham Pharmacia Biotech, Freiburg, Germany

  - Immunofluorescent microscopy

anti-mouse Alexafluor594 IgG	Invitrogen, Karlsruhe, Germany
anti-rabbit fluorescein IgG	Amersham Pharmacia Biotech, Freiburg, Germany

2.1.9 Buffers and solutions

Deionized water was used for all buffer preparations. Ultrapure RNAase-free water (Invitrogen, Karlsruhe, Germany) was used for RNA-interference experiments.

PBS (phosphate buffered saline)

140 mM	NaCl
3 mM	KCl
8 mM	Na_2HPO_4

Crystal violet staining solution

0.1 % (w/v)	Crystal violet/double-distilled H_2O

- **Solutions for Western blot:**

Protein extraction buffer (5x)

Tablet	Protease inhibitor cocktail
ml	in RIPA buffer,
50µl	Phenylmethylsulfonyl fluoride (PMSF) 200mM
9ml	ddH2O

10x Tris-glycine buffer

1.92 M	Glycine

0.25 M	Trizma base

Electrophoresis buffer (1x)

100 ml/l	10x TG buffer
10 ml/l	10% SDS

Transfer buffer

200 ml	10x TG buffer
400 ml	Methanol
1.4 l	cold ddH2O

TBS, pH 7.5 (10x)

100 mM	Tris-HCl
1 M	NaCl

TBST (0.2% Tween 20)

2 ml	Tween 20
998 ml	TBS

Blocking Solution (10% BSA)

10 % (w/v)	BSA / PBS

Protein loading buffer, pH 6.8 (5x)

50 mM	Tris-HCl
100 mM	DTT
2% (w/v)	SDS
0.1% (w/v)	Bromophenol blue
10%	Glycerol

- **Solutions for Immunofluorescence:**

Fixing solution

2%	Formaldehyde 37% / PBS

Permeabilization solution

0.2%	Triton-X
1%	BSA / PBS

Blocking solution

3%	BSA / PBS

PBST (0.5% Tween 20)

0.5 ml	Tween 20
995 ml	PBS

2.1.10 DNA staining solutions

DAPI (4',6-Diamidino-2-phenylindole dihydrochloride)	1mg/ml

2.1.11 Molecular weight markers

Protein markers: Bench Mark pre-stained protein ladder (Invitrogen, Karlsruhe, Germany)
Magic Mark Western standard (Invitrogen, Karlsruhe, Germany)
SeeBlue Plus2 pre-stained standard (Invitrogen, Karlsruhe, Germany)

2.1.12 Oligonucleotides (sense and antisense siRNAs)

siRNA sequences:

All siGENOME ON-TARGET plus SMART pool duplexes were obtained from Dharmacon, CO, USA.

hATM:

1) sense sequence		GCAAAGCCCUAGUAACAUA
antisense sequence	5'-P	UAUGUUACUAGGGCUUUGCUU
2) sense sequence		GGUGUGAUCUUCAGUAUAU
antisense sequence	5'-P	AUAUACUGAAGAUCACACCUU
3) sense sequence		GAGAGGAGACAGCUUGUUA
antisense sequence	5'-P	UAACAAGCUGUCUCCUCUCUU
4) sense sequence		GAUGGGAGGCCUAGGAUUU
antisense sequence	5'-P	AAAUCCUAGGCCUCCCAUCUU

Controls:
ON-TARGET plus Non-targeting Pool #1 - D-001210-01-05

2.1.13 Transfection

Two different chemical transfection methods were used:

1) Lipofectamine RNAiMax transfection reagent for siRNA and miRNA mimics — Invitrogen, USA
2) Fugene HD transfection agent for plasmid DNA — Promega, USA

2.1.14 miRNAs mimics

Four different miRNA mimics (Invitrogen, USA) were used:

1) hsa-miR-421 — AUCAACAGACAUUAAUUGGGCGC
2) hsa-miR-100-5p — AACCCGUAGAUCCGAACUUGUG
3) hsa-miR-18a-5p — UAAGGUGCAUCUAGUGCAGAUAG
4) hsa-miR-101-3p — UACAGUACUGUGAUAACUGAA

2.2 Methods

2.2.1 Cell manipulation

All cell culture work was conducted in a sterile laminar flow hood. Cell growth was examined regularly using an inverted-phase microscope. For cell sub-passaging, the medium was removed from the flasks, leaving the adherent cells to the growth surface of the flask. The cells were washed with 5-10 ml pre-warmed sterile PBS. After removing the PBS, pre-warmed trypsin EDTA was added (1 ml per T25 flask, 2 ml per T75 flask) and the cells were subsequently incubated at 37°C until they detached from the flask surface. To help dislodge the remaining adherent cells, the bottom of the flask was tapped sharply with the palm of the hand. After all cells had detached, medium containing serum was added to inactivate the trypsin. For resuspension, the cells were gently pipetted up and down. The cells were then counted using the cell counter and the appropriate number of cells was distributed to fresh flasks for sub-culturing.

For cell preparation, resuspended cells were collected by centrifugation at 1,200 rpm for 5 min. The cell pellet was washed by adding 5 ml pre-warmed sterile PBS. The cell suspension was centrifuged at 1,200 rpm for 5 min. After centrifugation,

the supernatant was removed and the cell pellet was used for experiments. Sub-confluent cells were used for preservation. Trypsinized and resuspended cells were centrifuged at 1,200 rpm for 5 min. Thereafter, the supernatant was removed and the cell pellet was gently suspended in cell preservation solution, before aliquoting into cryo-tubes (3-5x10 cells/tube) and incubated at -80°C overnight using a Mr. Frosty before finally being stored in liquid nitrogen (-196°C). For reculturing of the stored cells, the cells were quickly thawed at 37°C and gently pipetted into a T75 cell culture flask containing 15 ml pre-warmed medium/10% FCS. Shortly after the cells had attached to the growth surface of the flask, the medium containing the cell preservation solution was removed and 15 ml fresh pre-warmed medium/10% FCS was added.

2.2.2 Mycoplasma test:

To check for the potential infection of cells with Mycoplasma bacteria, a subset of cells was cultivated separately for several days without the presence of any antibiotics, and the medium was examined for Mycoplasma-specific DNA sequences using a Mycoplasma PCR Elisa Kit (Roche, Germany) according to the supplier's descriptions.

2.2.3 Toxicity test

In order to select clones that had stably integrated the plasmids expressing shATM (puromycin resistance gene), artificial miRNAs and endogenous miRNAs (blasticidin resistance gene), puromycin and blasticidin antibiotics were used. For the first step, the toxicity of puromycin and blasticidin for non-transfected cells was determined by growing $5x10^4$ cells in T25 flasks in concentrations ranging between 1 – 15 µg/ml of the medium. In the case of the shATM lentiviral vector, flasks were examined for colony growth after one week. At a concentration of 1 and 3 µg/ml puromycin, neither PC3 nor MCF7 cells, respectively, showed any viable colonies. Meanwhile, for the artificial and endogenous miRNAs plasmid, neither PC3 nor MDA-MB-468 showed any viable clones after blasticidin concentrations of 15 µg/ml and 5 µg/ml, respectively.

2.2.4 Colony formation assay

Colony formation assays were developed (Puck et al., 1956) to study the effect of specific treatments (i.e. ionizing radiation) on the cells' ability to form colonies (i.e. to

continuously produce offspring). Cells were seeded with an appropriate number of cells and allowed to adhere at 37°C (for 3-4 h) prior to drug treatment or irradiation. After X-ray irradiation, cells were incubated for a period between one to two weeks to allow for colony formation. The cells were then washed with PBS, fixed with 70% ethanol, and stained with crystal violet. Colonies were subsequently counted by eye. Colonies containing fifty or more cells (> 5 cell divisions) were considered to be “survivors”. The plating efficiency (PE) was calculated by dividing the number of colonies formed by the number of seeded cells. Survival curves were derived from duplicate of at least two independent experiments. For controls, DMSO was used instead of the inhibitor at the same concentration and scrambled RNAs were used instead of siRNAs against ATM.

2.2.5 Immunofluorescence

Immunofluorescence is a technique that allows for the visualization of a specific protein or antigen in cells or tissues through the binding of a specific secondary antibody, which is chemically conjugated to a fluorescent dye responsible for emitting the signal. Stained samples are examined using a fluorescence microscope providing monochromatic light at the desired wavelength. We applied this technique to visualize the local enrichment of proteins involved in DDR or DSB repair at the sites of DNA damage, forming so-called “foci”. A limited dose range between (0.001 and 2 Gy) has been suggested to establish a linear relationship between radiation dose and the number of foci (Rothkamm and Löbrich 2003). All experiments for immunofluorescent microscopy were performed using cover slips. To this end, cells were grown in 6-well plates containing 1-3 cover slips each, followed by drug treatment and irradiation. After certain time points, the cells were fixed in 2% formaldehyde in PBS for 10 minutes and washed (3x) with PBS. The fixed cells were then permeabilized for 5 min. on ice. The permeabilization step is needed to ensure free access of the antibody to its antigen. Afterwards, blocking solution was added to the cover slips (the side containing the fixed cells) for at least 1 h in order to block nonspecific sites where the antibody might bind. Cells were subsequently incubated with primary antibody in washing solution containing 1% BSA for 1 h. After washing with PBS three times for 10 min to remove excess unbound antibody, cells were incubated with either anti-mouse conjugated with Alexafluor594 or anti-rabbit conjugated with fluorescein antibodies (in washing solution/1% BSA). Finally, the DNA was stained using DAPI (1:1000). This step and the following must be performed in the dark. After washing the cells again three times for 10 min each, the cells were mounted using anti-fade mounting medium. The cover slips - with the cells facing down – were placed on microscope slides with some mounting medium. The cover slips were pressed gently on to the microscope slide and sealed

with nail polish to preserve the samples. The slides were then examined and photographed under the Zeiss Axioplan 2 (fluorescent microscope, by which the fluorescent tags are excited with the respective wavelength, resulting in emission of a fluorescent signal).

2.2.6 Western blot

The expression levels of proteins of interest were examined by Western blot analysis. Total proteins were extracted from the whole cells. The same amount of protein was electrophorezed on a 4-15% gradient SDS-PAGE gel and then transferred onto a Nitrocellulose membrane. Protein expression was detected using an antibody. To determine the protein at phosphorylated form, exponentially growing cells were exposed to 10 Gy of IR. At this dose, the phosphorylation reaches a maximum after 30 minutes. Then, Cells were fixed for protein extraction.

- **Protein extraction and quantification**

The extraction of total proteins was achieved using radio-immunoprecipitation assay buffer. Cells were collected by trypsinization and the cell suspension centrifuged at 1,200 rpm for 5 min. The pellet was resuspended in the same volume of protein extraction buffer. Thirty minutes later, samples were sonicated for 10 seconds to break the cells. The samples were kept on ice during sonication. The lysed mixture was centrifuged at 12,000 rpm at 4°C for 15 min. The supernatant containing the total soluble protein was then transferred to a new tube and optionally stored at -80°C.

The BCA method was used to determine total protein concentration (Smith, Krohn et al. 1985) which was originally based upon the Biuret reaction. The BCA Protein Assay reagent was prepared by mixing reagent A and reagent B in a ratio of 50:1. Two µl of protein extracts were added to 48 µl ddH2O. 50 µl of ddH2O was used as a blank. One ml of the color reagent was added to the diluted samples as well as the blank and after vortexing, they were incubated at 37°C for 30 minutes. The color intensity was determined using a spectrophotometer at a wavelength of 562 nm.

- **Polyacrylamide gel electrophoresis (PAGE) and blotting on to Nitrocellulose membrane**

For the electrophoresis, the same concentration of total protein and 5x loading buffer was added to ddH2O up to a final volume of 20 µl. The samples were vortexed and denatured at 100°C for 5 min., centrifuged, placed on ice or optionally stored at

4°C. The samples were then loaded on to pre-cast gels (4–15% Criterion™ Tris-HCl polyacrylamide gel with an 18-well comb). For molecular weight determination, Magic Mark, Bench Mark, or See Blue Plus2 Protein Standards were run in parallel lanes on the gel. The electrophoresis was performed at 100 V for 10 min to collect the proteins through the stacking gel and at 200 V for 80 min for separation. The electrophorezed proteins were transferred on to Nitrocellulose membranes with 0.2 µm pores. The membranes were activated by submersion in transfer buffer for 15 min. Both gel and membrane were equilibrated in transfer buffer for 5 min. Transfer was performed by electroblotting for 4 h at 50 V and 4°C.

- **Detection of proteins**

After blotting, the membrane was blocked for 1 h in blocking solution (10% BSA) at RT to prevent any nonspecific protein binding to the nitrocellulose material that could lead to a strong background and prevent band visualization. All of the following incubations were performed on a shaker platform to achieve optimal contact between solutions and membrane. The membrane was incubated overnight at 4°C with the primary antibody in 5% BSA and TBST. The membrane was then washed three times for 10 min in TBST solution at RT. Thereafter, the secondary antibody (ECL anti-rabbit/anti-mouse IgG) was added in 5% BSA (1:3000/1:1000 respectively) and incubated for 1 hour at RT. The membrane was washed again three times with TBST solution in order to remove unbound secondary antibodies from the membrane. The chemo-luminescence signal was detected using the imaging system. After detection of the respective protein signal on the membrane, the signal due to the housekeeping protein β-actin was analogously measured as a control to verify equal loading of the samples.

$$\text{Relative protein signal} = \frac{(\text{protein1 signal-Background signal}) \,/\, (\text{ß-actin signal - Background signal})_{\text{treated}}}{(\text{protein signal-Background signal}) \,/\, (\text{ß-actin signal - Background signal})_{\text{control}}} \times 100$$

2.2.7 Transfection Techniques

- **siRNA transfection (RNAiMax transfection agent)**

RNA interference (RNAi) is a mechanism that inhibits gene expression at the level of translation. The RNAi pathway is initiated by the enzyme Dicer, which cleaves long double-stranded RNA molecules into short fragments of approximately 20 base pairs. These fragments are called small interfering RNA (siRNA). The siRNA is

recognized by a multiprotein complex called the RNA-induced silencing complex (RISC), which incorporates one strand of the siRNA and uses it to target complementary mRNA molecules for degradation. The RNAi pathway is found in many eukaryotes and participates in control of gene activity. In cell culture, synthetic siRNA introduced into the cells can similarly be used to drastically decrease the expression of a gene of interest through the degradation of its mRNA. The RNAi technique may not totally abolish the expression of the protein and is therefore referred to as “knockdown” to distinguish it from “knockout” procedures.

To prevent the destruction of siRNA molecules added to regular medium by traces of RNAase, experiments using siRNA were performed in RNAase-free medium. In this study, ATM and control (scrambled) siRNA oligonucleotides were obtained from Dharmacon. We used smart pool siRNA, which is composed of four different oligonucleotides targeting the same mRNA, to enhance the knockdown effect. We transiently transfected siRNAs using RNAiMax transfection reagent (Invitrogen) according to the manufacturer’s instructions. For the transfection of 6-well plates, 50nM siRNA and 6 µl RNAiMax transfection reagent were added to 500 µl OptiMEM. This mixture was incubated for 15-20 minutes in dark. Finally, $2.5x10^5$ cells (MCF7) were seeded into 6-well plates in 2.5 ml medium/10% FCS (without antibiotics). This solution was distributed on to the plates before the cells had attached (“reverse protocol”).

- **MiRNAs mimics transfection (RNAiMax transfection agent)**

The MiRNA duplex approach or miRNA mimic is a method to overexpress miRNA in tumor cells. The guide strand of a synthetic miRNA duplex must contain an identical sequence to the miRNA of interest, whereas the passenger strand is designed to be partially complementary to the guide strand. These features allow for proper miRNA mimic incorporation into RISC complexes and ensures biological function.

Experiments using miRNA mimics were performed in RNAase-free medium. In this study, miRNAs mimics for control, miR-421, miR-100, miR-101 and miR-18a were obtained from Invitrogen. We used different miRNAs to target ATM either individually or in combination to enhance the knockdown effect. We transiently transfected mRNAs using RNAiMax transfection reagent (Invitrogen) according to the manufacturer’s instructions. For the transfection of 6-well plates, 25nM miRNAs and 6 µl RNAiMax transfection reagent were added to 500 µl OptiMEM. This mixture was incubated for 15-20 minutes in the dark. Then, $2.5x10^5$ cells (PC3) were seeded in 6-well plates in 1.5 ml medium/10% FCS (without antibiotics). This solution was distributed onto the plates before the cells had attached (“reverse protocol”).

- **Plasmid transfection (Fugene HD transfection agent)**

In order to test the functionality of plasmids and if they efficiently express either short RNAs or micro RNAs, we transiently transfected these plasmids in MCF7, PC3, and MDA-MB-468 cell lines using Fugene HD transfecting agent. Cells were seeded 24 hours before the start of the experiment; this was the “Forward method”. For the transfection, 6-well plates, 1µg plasmid DNA and 3µl Fugene HD transfection reagent (3:1) were added to 100 µl OptiMEM. This mixture was incubated for 15-20 minutes in the dark. The old medium was removed and medium without antibiotics was added to cells. 100 µl of the transfection mixture was added to each well. The cell pellet was collected after 24, 48 and 72 hours to progress further experiments.

2.2.8 Stable integration

Stable integration is a long-term transfection technique used to isolate and propagate single clones containing transfected DNA. Therefore, it is important to determine which cells have taken up the exogenous DNA. This screening can be achieved by genes that encode resistance to a lethal drug when an appropriate drug resistance marker is enclosed in the transfected DNA. Only the individual cells that survive under the drug treatment have assimilated the transfected DNA.

In order to achieve chromosomal integration, one million (1×10^6) cells were seeded in T25 flasks in normal DMEM medium. After 24 hours, cells were transfected with plasmids (in a 3:1 ratio) using Fugene HD transfecting agent in DMEM without antibiotics. Next, the medium was changed and cells were split by different densities (10.000, 20.000, 40.000, 50.000 and 100.000) in normal DMEM medium. Cells kept in incubators (10% CO_2 and 37°C) for 24 hours. For lentiviral vector expressing shATM (pLV-ATMi) integration, puromycin was used at concentrations of 3 µg/ml and 1 µg/ml in MCF7 and PC3 cell lines, respectively. For plasmids expressing artificial or endogenous micro-RNAs (pa/emiRNAs), blasticidin was used at a concentration of 15 µg/ml and 5 µg/ml in PC3 and MDA-MB-468 cell lines, respectively. After 2-3 weeks, all cells without integrated plasmids died and distinct clones of “survivors” were seen. Individual colonies were trypsinized and transferred to multi-well plates for further propagation in the presence of selective medium.

2.2.9 Plasmid preparation

- **Transformation**

Bacterial transformations were performed by electroporation using a BTX electroporator (Genetronics) according to the manufacturer's instructions.

- **Nucleic acid isolation** (Nucleobond Maxi protocol for genomic DNA isolation)

Plasmid DNA was prepared according to the following protocol (Clontech). We inoculated a 3–5 mL starter culture of LB medium containing the appropriate selective antibiotic (ampicillin) with a single colony that was picked from a freshly streaked agar plate. Two ml of bacterial suspension was added to 200 ml LB medium containing the appropriate selective antibiotic (ampicillin). The cells were incubated (overnight) on a 37°C shaker at 300 r.p.m until early log phase (2 x 10^7 org/ml), before harvesting by centrifugation (4,500–6,000 rpm for 10min at 4 °C.) Cells were resuspended using 12 ml lysis buffer plus RNAase A by pipetting cells up and down. We gently added 12 ml of lysing solution and then incubated at room temperature for 5 minutes. A NucleoBond Xtra Column was equilibrated together with the inserted column filter with Equilibration Buffer EQU (25mL). Next, we added 12 ml neutralization buffer and mixed the lysate gently. A short centrifugation step in a blue rotator ca. 3-5 minutes at 4000 rpm at 20°C was performed. The lysate was simultaneously cleared and loaded on to the column. The column filter was washed with Column (Buffer EQU: 15 mL EQU was applied to the filter of the NucleoBond Xtra Column and the column was washed with 25 ml WASH buffer. 15 ml ELU buffer was added to the wall of the column (very slowly). Then, 10.5 ml isopropanol was added to precipitate the eluted plasmid DNA under the laminar flow hood and vortexed for 5 minutes. The eluent was centrifuged at 15000 g for 30 minutes at 4°C. Five mL 70% ethanol was added to wash and dry the pellet before centrifugation at 15000 g for 10 minutes at room temperature. We carefully removed the ethanol completely from the tube with a pipette tip and allowed the pellet to dry at room temperature (for a maximum of one hour or until it was clear). The DNA pellet was dissolved in 200 µl or 300 µl of RNAase and DNAase free water (dissolved under gentle pipetting up and down), respectively. The plasmid concentration was measured using a spectrophotometer. This protocol was found to yield high-molecular-weight DNA.

2.2.10 Irradiation

Irradiation was performed at RT using the X-ray generator (Gulmay) with 200 keV, 15 mA, and an additional Cu-filter at a dose rate of 0.8 Gy/min.

2.2.11 Graphics and statistics

All experiments were at least two times repeated. Error bars represent the mean (± SEM) of all individual experiments. Statistical analysis, data fitting and graphic production were performed with the Graph Pad Prism program, version 5.

3 RESULTS

With the intention of achieving robust radiosensitization in tumor cells, the aim of this study was to target ATM, which is the key regulator of DNA damage response after ionizing irradiation. In order to realize this aim, several strategies were used (**Figure 10**). Such an approach may even permit specific radiosensitization of tumor cells, which is the most important condition for efficient tumor treatment. Consequently, special attention was given to approaches allowing for endogenous down-regulation of ATM using miRNAs that could be achieved by stable integration of specific vectors.

As a first approach, ATM kinase activity was inhibited using a specific inhibitor (KU55933). This technique was used to demonstrate the mechanisms by which inhibition of ATM may result in augmented radiosensitization.

In the second approach, ATM expression was downregulated using small interfering RNAs (siRNAs), while in a third approach ATM was deleted via short hairpin RNAs (shRNAs). The latter two strategies were used to test whether an efficient downregulation of ATM can be achieved by specifically targeting the transcription of ATM. For the second approach, cells were transiently transfected with specific siRNAs, whereas for the third approach tumor cells were stably integrated using a lentiviral vector expressing specific shRNAs to generate stable ATM-depleted clones.

Finally, in a fourth approach, endogenous micro RNAs (emiRNAs) were applied to downregulate ATM. This approach was conducted because previous data from our laboratory demonstrated that in tumor cells, ATM is also regulated by the expression of specific emiRNA (Mansour et al. 2013). Furthermore, artificial micro RNAs (amiRNAs) were used for downregulation of ATM. Both strategies were tested using stable ATM-depleted clones with stably integrated vectors. Earlier *in vivo* data did not demonstrate an inverse relationship between a single miRNA and its target (Hanna et al. 2012) which raises the possibility that several miRNAs are required to decrease target ATM protein expression. Hence, we examined the possible synergistic effects of combinatorial endogenous and exogenous co-expressed miRNAs on the regulation of ATM gene expression.

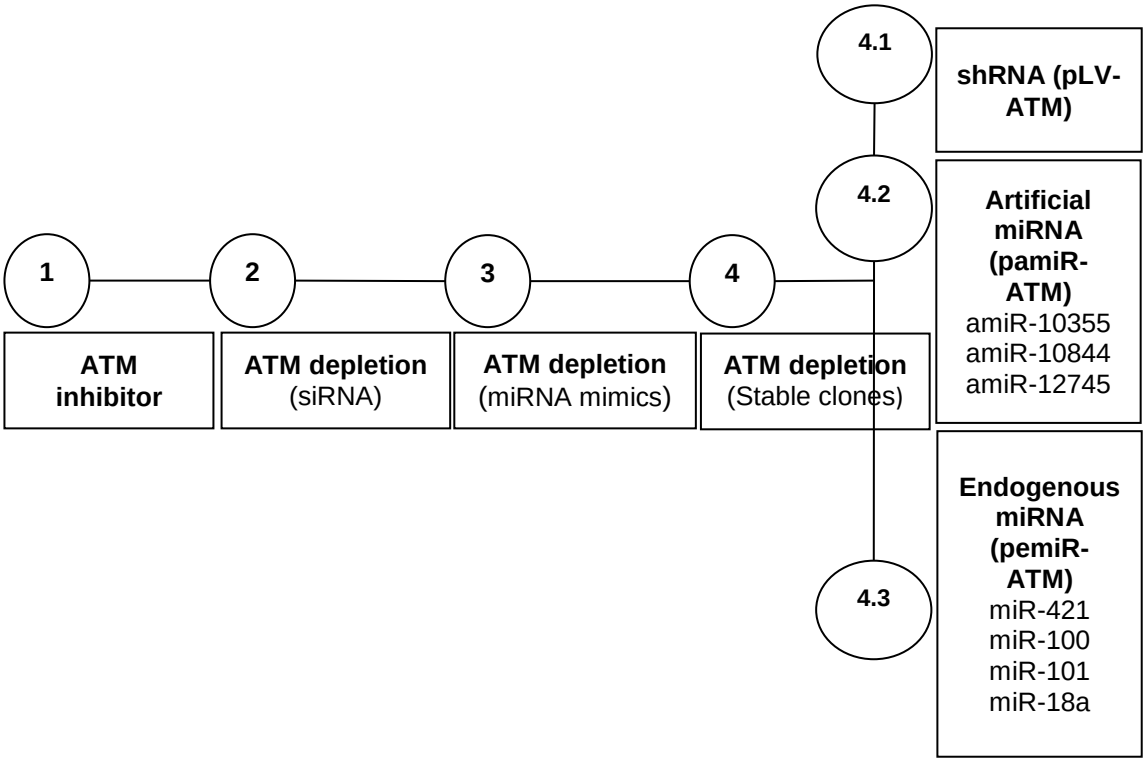

Figure 10. Diagram illustrates thesis milestones and aim. ATM was targeted in different tumor cell lines using different methods in order to enhance radiosensitivity. 1. ATM inhibitor (KU55933). 2. ATM depletion using small interference RNAs (siRNAs). 3. ATM depletion using micro RNAs mimics (miRNAs mimics). 4. ATM depletion using vectors expressing short RNAs (shRNAs) [4.1], plasmids expressing artificial miRNAs (amiRNAs) [4.2] and endogenous miRNAs (emiRNAs) [4.3].

3.1 Targeting ATM using the ATM inhibitor KU55933

In the first experiment, it is important to demonstrate the mechanisms leading to ATM inhibition, which may result in an augmented increase in radiosensitivity. To this end, the specific chemical inhibitor KU55933 was applied to three different breast cancer cell lines MCF7, MDA-231 and MDA-468.

3.1.1 Inhibition of ATM activity

Figure 11 shows the effect of the inhibitor KU55933 on the autophosphorylation of ATM at residue Ser-1981, which is the first important biochemical pathway in mammalian cells after irradiation. Experiments were performed using three different breast cancer cell lines MCF7, MDA-231 and MDA-468. Cells were treated with/without KU55933 (10 µM) for one hour before X-irradiation (10Gy) and phosphorylation of ATM on residue Ser-1981 was monitored after 20 minutes by Western blot analysis using specific monoclonal antibody. In all three cell lines, KU55933 strongly reduces the pATM signal normally observed after irradiation (**Figure 11A**).

The effect of the inhibitor was also tested for its impact on the phosphorylation of Chk2, which is a downstream signal of ATM (Rotman and Shiloh 1998; Matsuoka et al. 2000). Here, only a moderate reduction was observed for all three cell lines (**Figure 11A**), probably because of the redundant activation pathway through ATR and DNA-PKcs (Li and Stern 2005; Wang et al. 2006).

The effect of KU55933 on pATM at residue Ser-1981 was also determined via immunohistochemistry (**Figures 11B and C**). Cells were again treated with/without KU55933 (10 µM) for one hour before X-irradiation with 2 Gy. One hour after irradiation cells were fixed and stained for pATM on residue Ser-1981. **Figure 11B** demonstrates that for the MCF7 cell line KU55933 is able to abolish almost all autophosphorylation of ATM that would normally be observed after exposure to 2 Gy. Without treatment using KU55933 almost all irradiated cells were positive for pATM when assessed 1 hour after irradiation (**Figure 11C**). This percentage was strongly reduced to less than 20% when cells were pre-treated with KU55933. The effect was the strongest for the breast cancer cell line MDA-468 with the percentage of pATM-positive cells reduced to 10% (**Figure 11C**). Overall, these data clearly demonstrate that the inhibitor KU55933 can be used for efficient blockage of ATM autophosphorylation that normally occurs after irradiation.

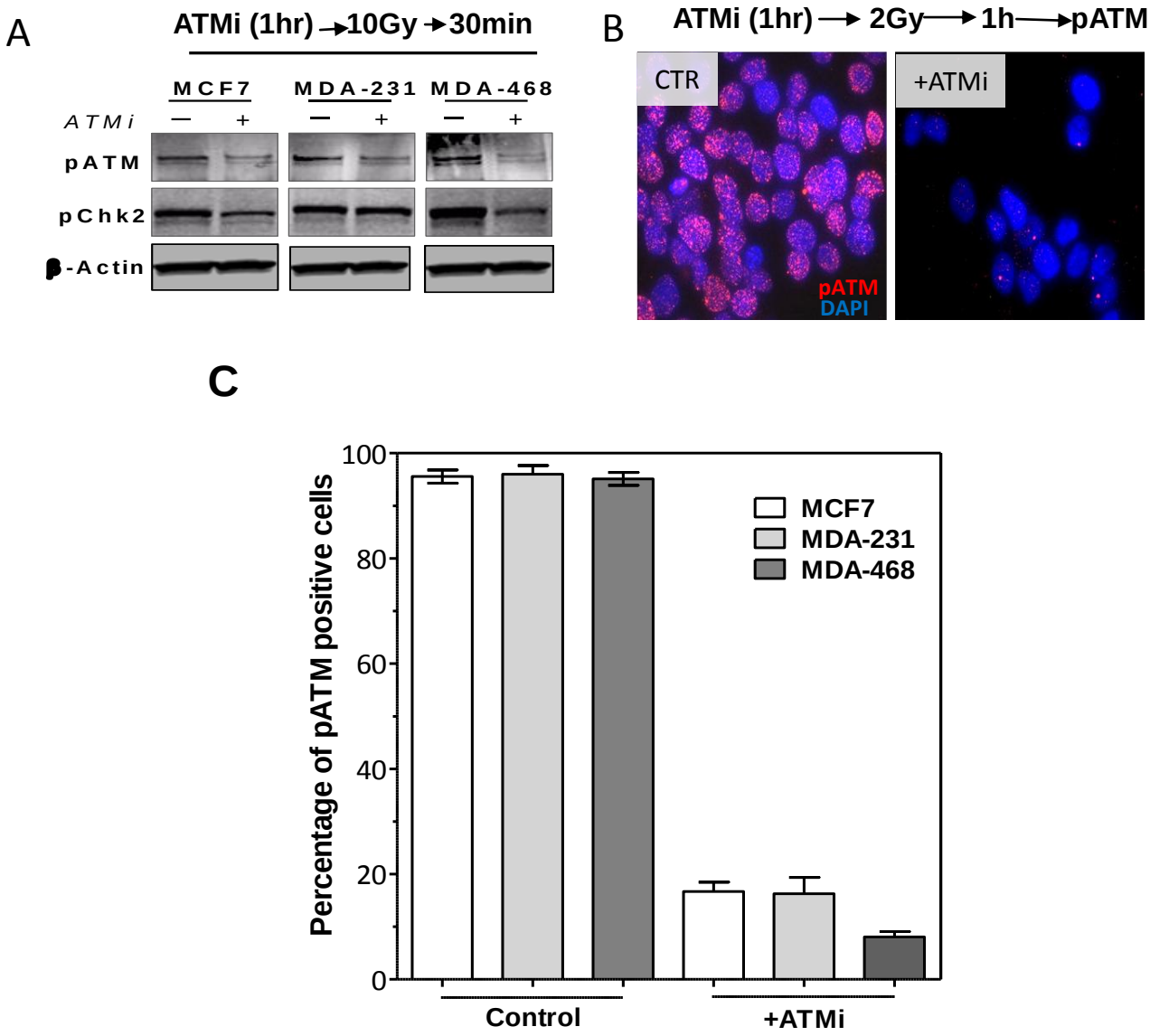

Figure 11. ATM inhibition with KU55933 disrupts the DNA damage response. A) Western blot analysis of p-ATM and pChk2 signal in different breast cancer cell lines (MCF7, MDA-231 and MDA-468) pretreated with (+) and wihout (-) 10µM KU55933 and then irradiated with 10 Gy. 30 min after irradiation cell lysate were analyzed. pATM Ser-1981 (upper panel) pChk2 Thr-68 (middle panel). ß-actin (lower panel) served as a loading control. B) Representative micrographs of p-ATM foci (red color) in irradiated cells (2Gy) treated with (+ATMi) and without (CTR) inhibitor, DAPI (Blue color). CTR indicate control irradiated cells. C) Quantification of percentage of p-ATM positive cells after KU55933. Indicated cells were treated for one hour with KU55933 prior to irradiation. One hour after irradiation (2 Gy) cells were fixed and stained. Note that more than ten p-ATM foci/ nuclei were considered positive. Error bars represent the SEM of three independent experiments.

3.1.2 ATM inhibition impairs double-strand breaks repair efficiency

Upon irradiation, the autophosphorylation of ATM at residue Ser-1981 is known to be especially important for the initiation and organization of DNA double-strand break (DSB) repair (Saha et al. 2013). Activated ATM is recruited to DSBs via the MRN complex formed by the proteins MRE11, RAD50 and NBS1. There, ATM is needed for the phosphorylation of the histone variant H2AX on residue Ser-139 along both sides of the DSB for up to several MBp (Rogakou et al. 1999). This phosphorylated H2AX, also denoted as γH2AX, can be visualized via immunohistochemistry as discrete foci in the cell nucleus and therefore are potential optimal surrogates for the detection of DSBs (Taneja et al. 2004).

Figure 12A shows the presence of γH2AX foci in MCF7 cells 1 or 24 hours after exposure to 2Gy using specific phosphor-monoclonal antibodies against γH2AX. Cells were also stained with DAPI to identify the nuclei. For each cell, discrete foci can be observed allowing the determination of the mean number of γH2AX foci present per cell. This technique was used to monitor the formation of γH2AX foci as a marker of double-strand breaks (DSBs).

In non-irradiated cells no γH2AX foci are generally seen (**Figure 12A**, upper lane, left). However, 1h after exposure to 2 Gy, numerous foci can be detected in the MCF7 cells (**Figure 12A**, upper lane, in the middle). No significant change in this number is seen, when cells were pre-treated with KU55933 for one hour (**Figure 12A**, upper lane, right). When irradiated MCF7 cells were allowed to undergo repair for 24 h, the number of foci was drastically reduced with only a few foci remaining (**Figure 12A**, lower lane, left). However, when these cells were pre-treated with KU55933 for 1 h, the number of residual foci was clearly higher indicating an efficient inhibition of DSB repair (**Figure 12A**, lower lane, right).

Detailed quantification of DSBs was performed for the two tumor cell lines (MCF7 and MDA-MB-468) pre-treated with/without the ATM inhibitor KU55933. There was no significant difference in the initial number of γH2AX foci measured one hour after irradiation when MCF7 and MDA-468 cells were treated with KU55933 compared with DMSO-treated control cells (**Figures 12B & C**).

However, when cell lines were allowed to undergo repair for 24 hours, a large reduction in the number of γH2AX foci were seen for both cell lines from about 28 to 30 foci per cell, respectively, down to approximately 4 to 5 foci per cell. These data indicate a very efficient (at least 80%) DSB repair within this time interval (**Figures 12 B and C**).

The repair of DSB was clearly affected when cells were perturbed using the ATM inhibitor. In MCF7 cells, the number of residual γH2AX foci was approximately 13

foci per cell, which is a repair efficiency of approximately 53%. For MDA-468 inhibition of DSB repair by KU55933, the effect was even stronger with a decline in the number of γH2AX foci to only 16 foci per cell, an approximate repair efficiency of only 48%. This difference is in line with the stronger reduction in pATM described above for this cell line (**Figure 11C**).

Together, these data clearly show that the inhibition of the radiation-induced ATM autophosphorylation on residue Ser-1981 caused by the inhibitor KU55933 results in a large reduction in DSB repair capabilities.

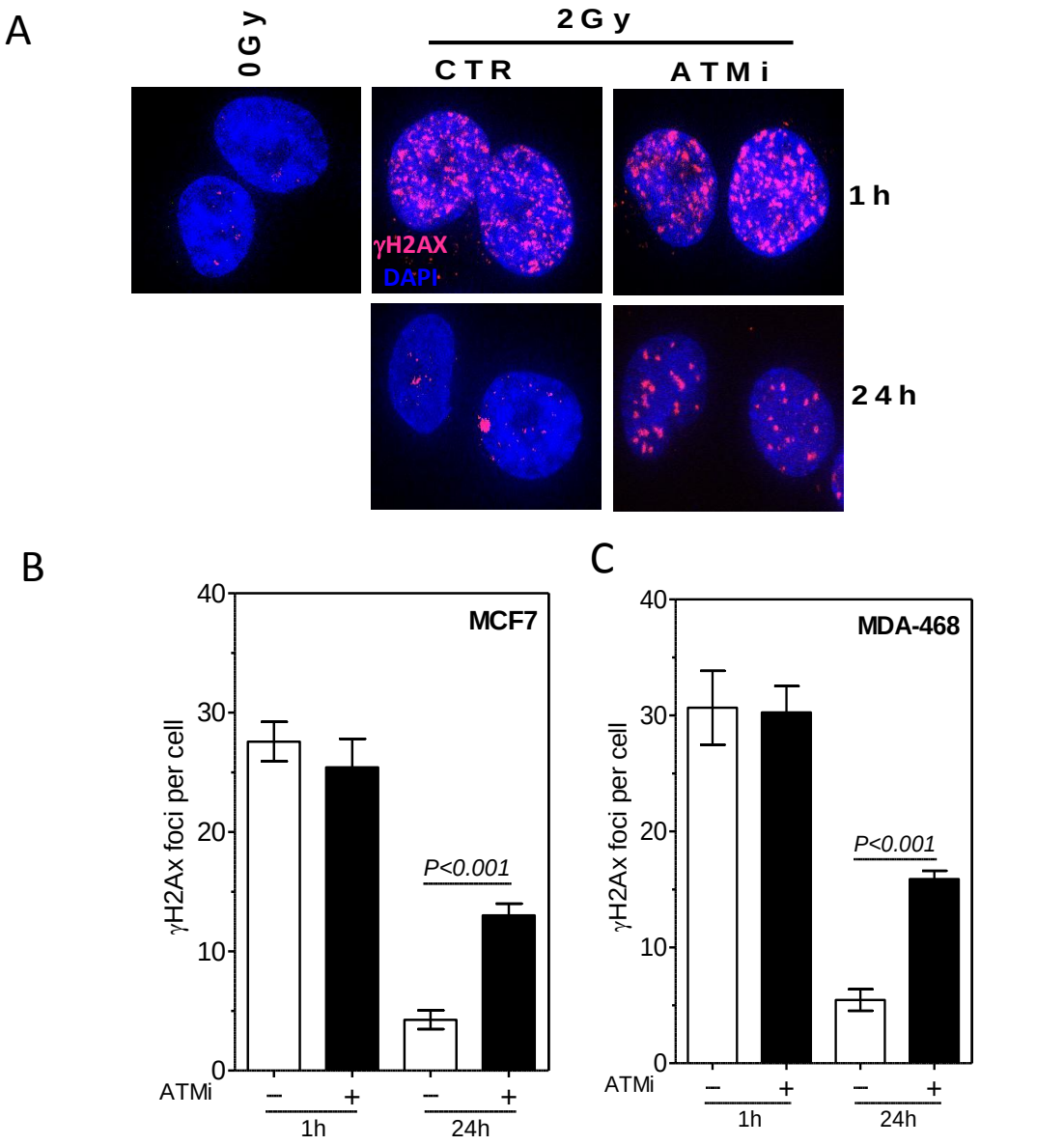

Figure 12. ATM inhibition using KU55933 impaired DSB repair efficiency. A) Representative IF photos for γH2AX foci (red color) in tumor cells treated with (ATMi) and without inhibitor (CTR), 1 and 24 hours after irradiation with 2Gy. 0Gy refer to non-irradiated cells. DAPI (Blue color). B, C) Quantification of γH2AX foci after ATM inhibition in MCF7 and MDA-468 cells, respectively. The number of foci counted in non-irradiated cells was subtracted from that counted in irradiated cells. Error bars represent the SEM of three independent experiments.

3.1.3 ATM inhibition enhanced radiosensitivity in tumor cells

Upon irradiation, cell survival as measured by colony forming assay is primarily determined by the DSB repair efficiency. In contrast, cell killing caused by X-irradiation primarily depends on the amount of non- and miss-repaired DSBs (Taneja et al. 2004) remaining per cell. As a consequence, a decrease in DSB repair efficiency as

demonstrated above by the ATM inhibitor KU55933 is considered to result in a substantial increase in cellular radiosensitivity.

The effect of KU55933 on the radiosensitivity of three breast cancer cell lines is shown in **figure 13**. As before, cells were initially treated with the ATM inhibitor for one hour and then irradiated with X-irradiation at doses up to 4Gy. After irradiation, cells were kept in the incubator for up to 15 days to allow colony formation of surviving cells. The survival of non-irradiated cells treated with or without KU55933 was normalized to 1 (100% survival). For all three breast cancer cell lines, KU55933 was found to result in clearly enhanced radiosensitivity (**Figure 13**). For the two cell lines MCF7 and MDA-231, radiosensitivity was enhanced approximately two-fold. This was indicated by a similar survival fraction (SF) of about 15% after being exposed to 4Gy X-irradiation alone, in comparison to an X-ray dose of only 2Gy when cells were pre-treated with KU55933. For MDA-468 cells, radiosensitivity was enhanced 4-fold, as evidenced by a similar SF measured after 4Gy compared with 1Gy when cells were pre-treated with the inhibitor. The higher radiosensitization seen here for the MDA-468 corroborates the stronger reduction in DSB repair efficiency demonstrated in **figure 12C**.

In conclusion, these findings revealed that the efficient targeting of ATM using the inhibitor KU55933 strongly impaired DSB repair, resulting in a pronounced increase in cell killing. In addition, these data also demonstrate that even a small difference in reduced ATM activity can have a clear effect on DSB repair efficiency as demonstrated for the cell line, MDA-468, which showed the strongest reduction in ATM auto-phosphorylation correlating with the strongest increase in cell killing.

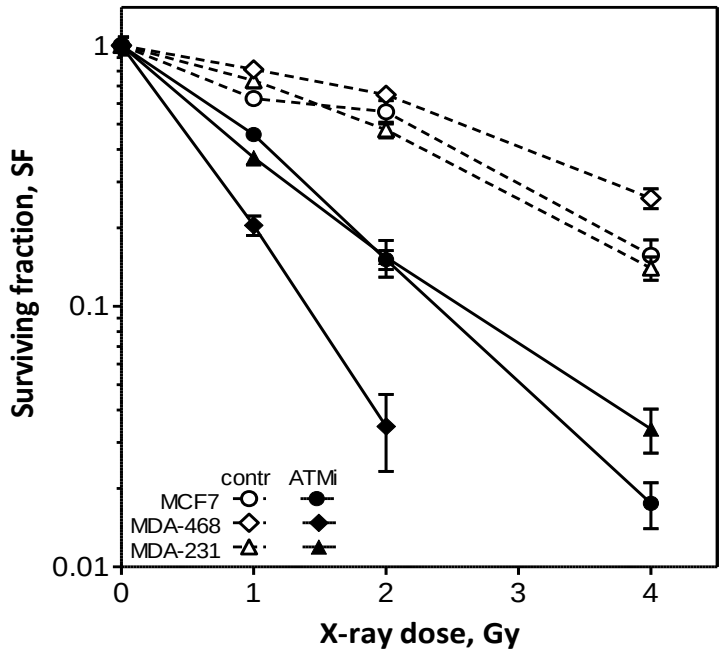

Figure 13. ATM inhibition using KU55933 enhanced radiosensitivity. Clonogenic survival assay to assess the effect of KU55933 on cellular radiosensitivity. Cells were treated with KU55933 one hour before irradiation. Fifteen days later, the colonies were stained and counted, and the survival curves were constructed with normalized values. Values shown are the means ± SEM from three different experiments.

3.2 Targeting ATM using small interfering RNAs (siRNAs)

In the second approach, the technique of small interfering RNA (siRNA) was used to downregulate ATM. The siRNA are double-stranded RNA molecules with a length of 20-25 base pairs, which interfere with and activates the RNA-induced silencing complex (RISC). This results in the degradation of mRNA from the targeted gene leading to inhibition of its translation into a functional protein (Agrawal et al. 2003).

3.2.1 ATM depletion using small interference RNAs

For depletion of ATM by siRNA, a pool of four different oligonucleotides were used to ATM mRNA, thus enhancing the knockdown effect (Koecher et al. 2012). The sequences of these siRNAs with diagrammatic presentation of targeted sites in the ATM mRNA are depicted in **figure 14**.

For the experiments, cells were transiently transfected with 50 nM scrambled or control siRNA/ATM siRNAs for up to 72 hours using RNAiMax transfection agent

(Invitrogen) according to the manufacturer's protocol. **Figure 15A** shows the impact of this treatment on the expression of ATM as determined for MCF7 cells collected after 24, 48 and 72 hours, after treatment with siRNA. Cell lysate was analyzed using Western blot and ATM expression was detected using specific antibody with ß-actin as a loading control. After incubation for 24 h, ATM expression was downregulated to 50%, followed by a further reduction to approximately 25% when incubated for a period of 48 h. After incubation for 72 hours, the level of ATM was reduced to approximately 5% of the control, when treated by scrambled RNA (**Figure 15A**). Overall, these data show that siRNA can be used as a very efficient strategy to silence ATM expression and that the specific sequences used for siRNAs were able to abrogate ATM expression almost completely.

3.2.2 Impact of ATM depletion by siRNA on double-strand breaks repair

Figure 15B shows the impact of ATM of siRNA on the formation of γH2AX foci in MCF7 cells exposed to 2 Gy. For these experiments, MCF7 cells were transiently transfected with scrambled/ATM siRNAs for 48 hours before being X-irradiated with 2 Gy. This was followed by a repair incubation of one hour to measure the initial γH2AX foci formation or after 24 hours to measure the residual number of γH2AX foci. In non-irradiated cells, no γH2AX foci are seen (**Figure 15B, upper left lane**). In control irradiated cells treated with scRNA, a massive formation of γH2AX foci are seen one hour after irradiation (**Figure 15B, upper lane, in the middle**). No differences in the initial formation of these foci were observed when MCF7 cells were treated with siRNA targeting ATM (**Figure 15B, upper lane, right**). When MCF7 cells were incubated for 24 h, it is clear that less foci are observed indicating a very efficient repair (**Figure 15B, lower lane, left**).

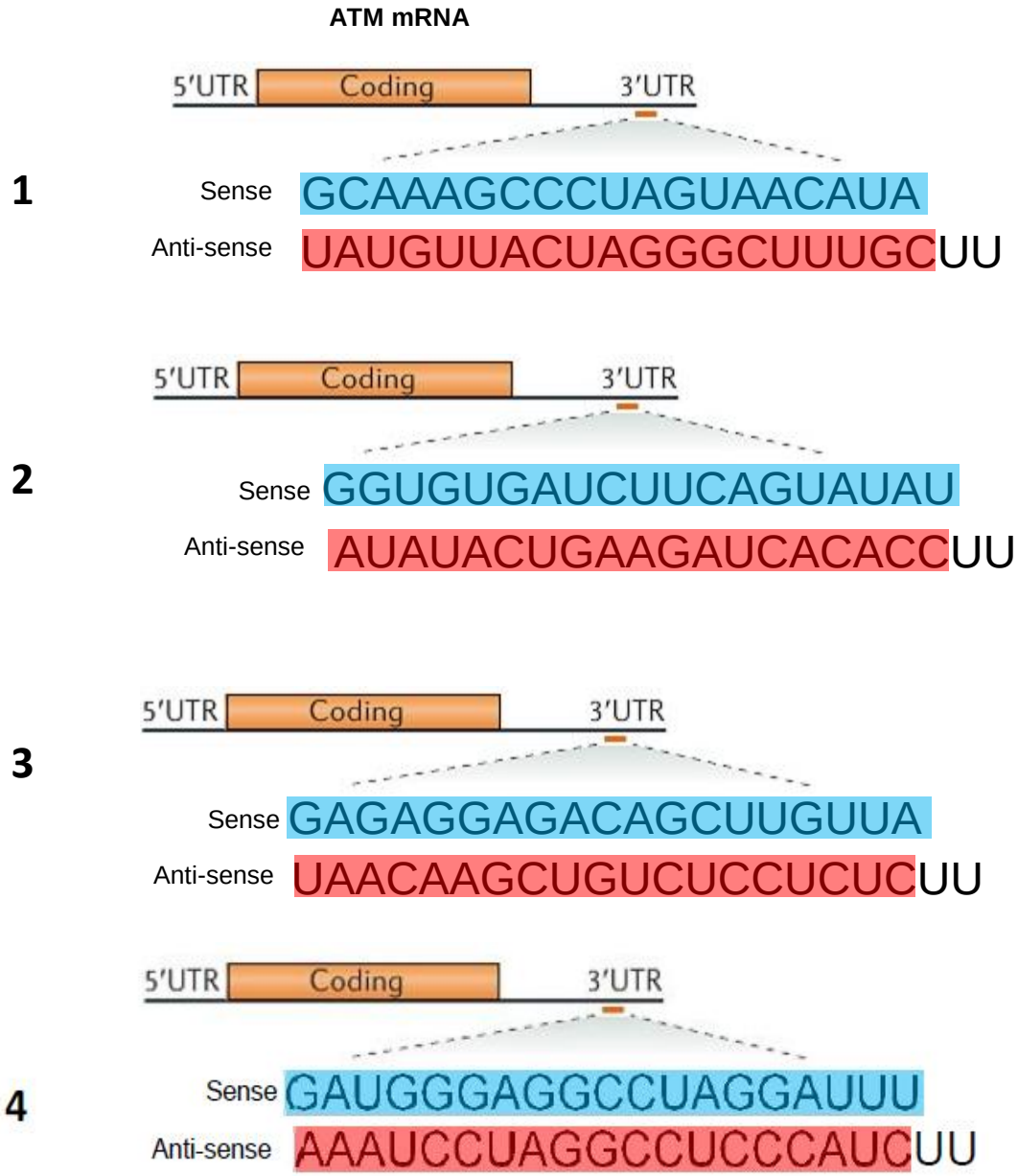

Figure 14. Simplified diagram showing the sense (Blue color) and antisense (Red color) sequences of ATM siRNAs with diagrammatic presentation of binding sites in the ATM messenger RNA (mRNA). ORF, open reading frame; 5'UTR, 5'untranslated regions. 3'UTR, 3-untranslated region.

It is clear that more foci are present when MCF7 cells were pre-treated with siRNA (**Figure 15B, lower lane, right**). The detailed analyses of these data are depicted in **figure 15C**. As described above, there is no significant difference in the initial number of γH2AX foci measured 1 h after exposure to 2 Gy with 28±2 and 25±2 foci, respectively, for MCF7 cells treated either with scRNA or siATM. After incubation

for 24 h, the number of γH2AX foci had decreased to approximately 5 foci per cell indicating an efficient DSB repair of more than 80% (**Figure 15C**).

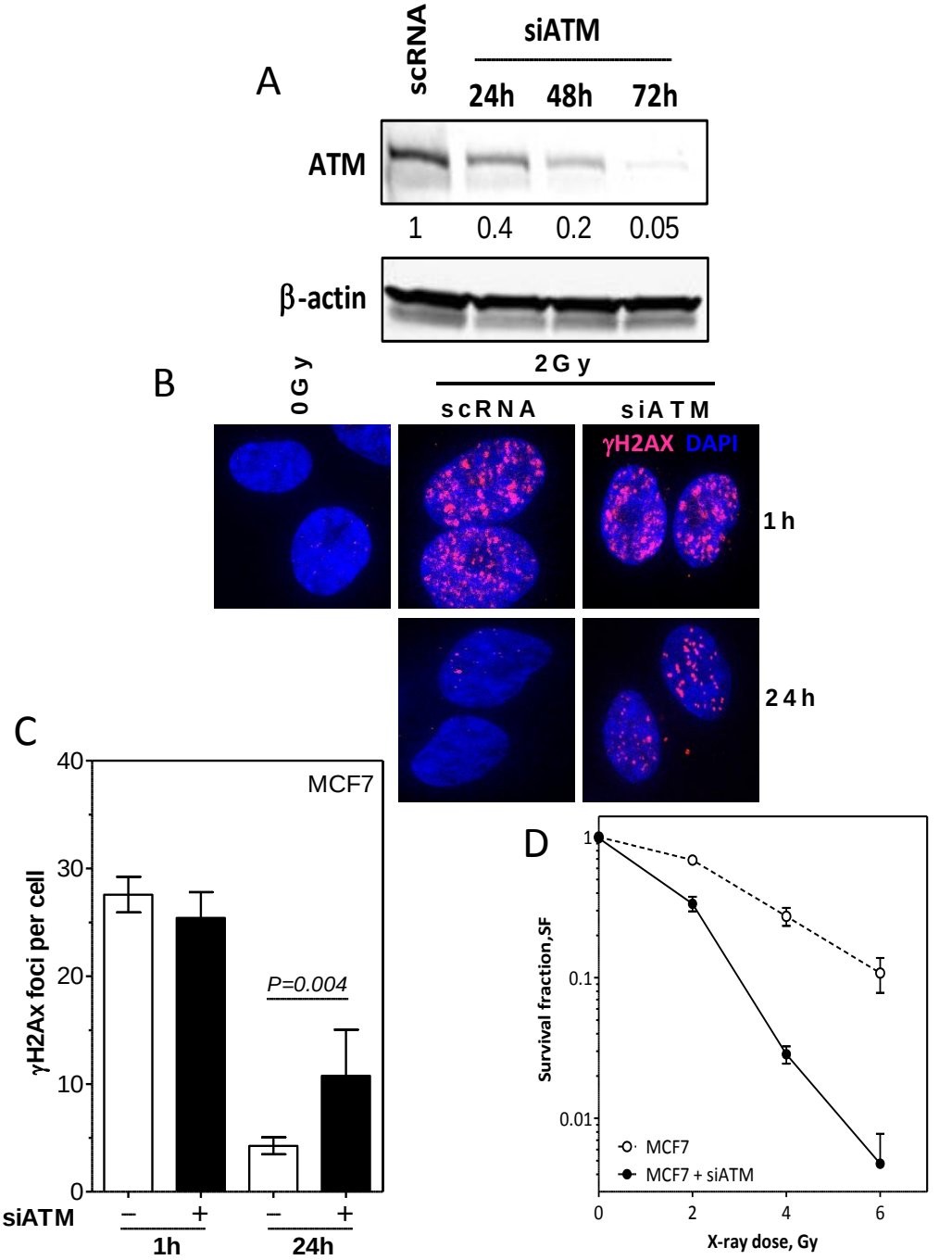

Figure 15. ATM depletion *via* small interfering RNAs (siRNA) impaired DSB repair efficiency and enhanced radiosensitivity. A) Western blot analysis of ATM expression in MCF7 cells treated with either scrambled control RNA (scRNA) or siRNAs ATM (siATM) for up to 72 hours. ATM expression [upper panel] and ß-actin (loading control) [lower panel]. B) Representative IF photos for ɣH2AX foci (red color) in tumor cells after ATM depletion, One and 24 hours after irradiation with 2Gy. C) Quantification of ɣH2AX foci after ATM depletion. One & 24 h after irradiation, cells are fixed and stained. The number of foci observed in non-irradiated cells was subtracted from that counted in irradiated cells. Error bars represent the SEM of three independent experiments. D) Colony formation assay after ATM depletion using siATM. Cells were irradiated with different X-rays doses up to 4 Gy. Survival curves were constructed with normalized values. Values shown are the means ± SEM from three different experiments.

In contrast, when cells were pre-treated with siATM for 48 h, the number of residual γH2AX foci was found to decline to only 11 foci per cell which is equivalent to a repair efficiency of only 41%. This result corroborates the strong reduction of ATM expression achieved by siRNA (**figure 15A**). These data demonstrated that knockdown of ATM using siRNAs clearly impaired DSB repair efficiency.

3.2.3 Impact of ATM depletion by siRNAs on cellular radiosensitivity

Figure 15D shows the effect of ATM depletion by siRNA on the cellular radiosensitivity of MCF7 cells using the colony forming assay. Cells incubated in 6-well plates were transiently transfected with 50nM scrambled/ATM siRNAs for 48 hours and then exposed to X-ray doses up to 6 Gy. The number of colonies measured for non-irradiated cells treated by ATM siRNA was normalized to 1. Down-regulation of ATM by siRNAs was demonstrated to clearly enhance radiosensitivity of MCF7 cells (**Figure 15D**). Quantitative analysis suggested that cellular radiosensitivity was enhanced approximately 2-fold as indicated by a similar survival fraction (SF) of about 30% after 4 Gy alone, and also after irradiation with 2Gy when pre-treated with siATM (**Figure 15D**). This enhanced radiosensitivity correlates with the reduction in DSB repair efficiency shown above (**Figure 15C**).

In summary, the data showed that effective targeting of ATM using siRNAs will lead to impairment of DSBs repair efficiency, which consequently will lead to enhanced radiosensitivity. Importantly, depletion of the ATM protein using siRNAs pool leads to enhanced radiosensitivity as in the case of treatment using the ATM inhibitor. These data revealed that at least for MCF7 cells, these two strategies can be regarded as being effective.

3.3 Targeting of ATM by short hairpin RNAs (shRNAs)

In the third approach, the efficiency of short hairpin (shRNAs) was tested for downregulation of ATM. This approach was performed using a lentiviral vector expressing shRNA, which was stably integrated into the genome of the targeted cells. This strategy was also chosen to determine the effect of persistent downregulation of ATM. ShRNA sequences are transcribed and subsequently integrated into the cell chromosome, which can then be replicated through cellular divisions (Manjunath et al. 2009). Once shRNA molecules are transcribed, they are exported to the cytoplasm where they can be processed by Dicer to generate short siRNAs duplexes loaded into RISC. This leads to more potent inhibition of target-gene expression (Perwitasari et al. 2013).

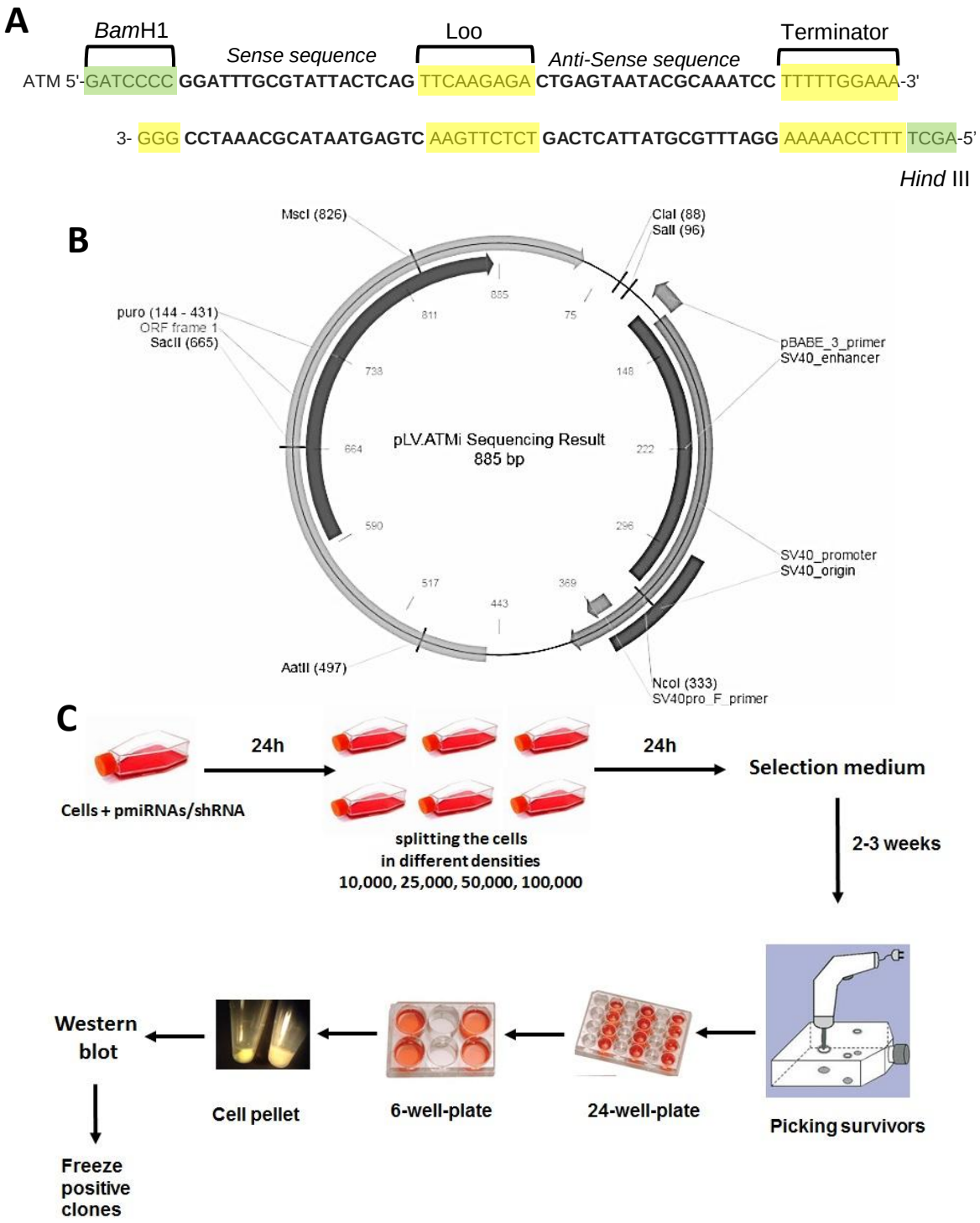

Figure 16. Stable integration of the pLV-ATMi vector. (A) Annealed shRNA oligonucleotides form dsDNA fragment that show the sense and antisense sequences targeting ATM mRNA, *Bam*HI/*Hind* III sites (shown by green) at the ends, where loop and terminator sequence shown in yellow. B) Map of a typical lentiviral expression vector. The vector contains the promoter for expression of short hairpin RNA (shRNA), a prokaryotic resistance gene against ampicillin and a eukaryotic resistance gene against puromycin (Puro). Simian virus 40 (SV40) promoter controls the expression of puromycin. shRNA constructs have to be cloned into the *Bam*HI and *Hin*dIII sites. C) Procedure of stable integration using selection medium containing appropriate antibiotic.

3.3.1 Stable shRNAs-mediated ATM knockdown

Figure 16A shows the sequences used for the shATM, which is part of a lentiviral vector (pLV-ATMi) (**Figure 16B**). These shRNA sequences were previously described (Ariumi et al. 2005). For this experiment, 2 µg of the shATM expressing vector were transfected into either the breast cancer cell line, MCF7 or the prostate cancer cell line, PC3 using Fugene HD (Promega) according to the manufacturer's instructions. The cells which harbor the shATM expressing vector were selected by growth in medium containing 3µg/ml and 1µg/ml puromycin, respectively according to the graph shown in **Figure 16C**. For each cell line, resistant clones were selected by micro-trypsinization and expanded for further analysis.

Figures 17A & B show the ATM expression in MCF7 and PC3 clones. Whole-cell lysate proteins from all picked clones were prepared and ATM expression was detected using Western blot with ß-actin as a loading control. For MCF7, several clones (M9 and M21) showed no or only slight ATM downregulation, while others (M7, 16, 20 and 23) were found with moderate ATM downregulation by about 70-80% in comparison to control empty vector (EV). However, there were also several clones (M8, 11, 15, 17, 18, 19, 24 and 25) which showed a strong downregulation of ATM by up to 95% (**Figure 17A**).

A similar result was obtained for the clones selected by PC3 (**Figure 17B**). No reduction in ATM expression was observed for some clones (P6 and P13), while for others, there was a clear reduction by approximately 80% (P11, 15, 16, 17 and 19) when compared to control EV. Again, several clones (P1, 3, 4, 18, 28 and 30) showed a strong ATM downregulation by up to 95%. Similar results were obtained when clones were grown for several days, suggesting that ATM knockdown achieved was stable over time.

3.3.2 Impact of ATM-knockdown by shRNAs on cellular radiosensitivity

Next, the effect of persistent ATM silencing using a shRNAs expressing vector was determined for cellular radiosensitivity in MCF7 clone 8 and for PC3 clone 3, which both showed strong ATM downregulation abilities (**Figures 17A and B**). Cells were seeded and irradiated with X-ray doses up to 4Gy. After irradiation, cells were kept in the incubator for up to 15 days to allow colony formation. The number of colonies measured for non-irradiated cells was normalized to 1. **Figures 17 C & D** shows that the radiation dose response curve measured for these clones are clearly different from the respective parental cell lines. For MCF7, cellular radiosensitivity was enhanced 3-fold as indicated by a similar survival fraction (SF) of approximately 20% after 4Gy

irradiation for the parental clone and between 1 and 2 Gy for the MCF7 clone 8 (**Figure 17C**).

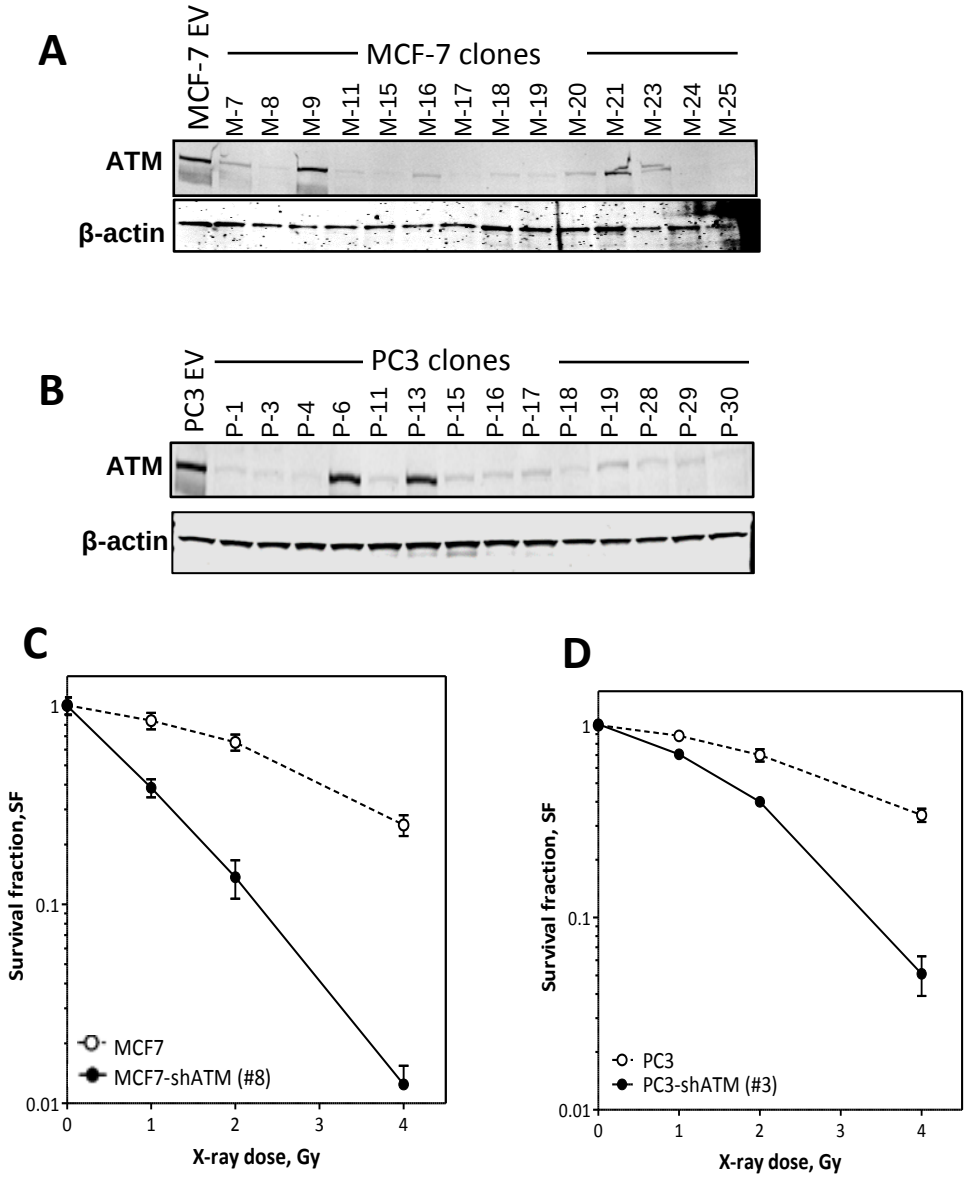

Figure 17. ATM depletion by short hairpin RNAs (shRNAs) enhanced radiosensitivity. A, B) Western blot analysis of different MCF7 and PC3 clones harboring plasmid lentiviral vector expressing ATM shRNAs (pLV-ATMi), respectively. ATM expression [upper panel] and ß-actin (loading control) [lower panel]. EV indicate control empty vector. C, D) Clonogenic survival assay for the stable ATM-depleted clones, MCF7#8 and PC3#3 respectively. Cells were irradiated with different X-rays doses up to 4Gy. The survival curves were constructed with normalized values. Values shown are the means ± SEM from two different experiments.

For PC3, the cellular radiosensitivity was enhanced 2-fold as indicated by a similar survival fraction of about 15% after 4Gy and 2Gy for clone PC3#3 (**Figure 17D**).

In summary, these data demonstrated that the efficient targeting of ATM achieved using a shRNA expressing lentiviral vector (pLV-ATMi) leads to clearly enhanced radiosensitivity in both cell lines tested. For MCF7 this result can be compared with the effect obtained when ATM was downregulated by siRNA (**Figure 15**). For this approach, downregulation of ATM was found to enhance the cellular radiosensitivity by a factor of 2 (**Figure 15D**). This further enhancement observed for MCF7 when ATM was downregulated by shRNA may arise for two reasons: i) transient vs continuous knockdown; transiently introduced siRNAs lack the ability to self-replicate resulting in transient knockdown of ATM, which lasts for a couple of days and eventually is lost due to a dilution effect through subsequent cellular division. Meanwhile, the shRNA expressing vector is integrated into the cell chromosome producing continuous siRNAs. ii) transfection vs selected clones; the transfection efficiency of a chemically introduced method depends on the amount of siRNAs used and can vary from cell line to other cell lines, while virus-mediated ATM knockdowns are integrated into the cell chromosome and replicates contemporaneously with the genome. Consequently, it segregates into daughter cells, which enables sustainable ATM knockdown.

3.4 Targeting of ATM by micro RNA

It is well known that in human cells, gene expression is also regulated by micro RNAs (miRNAs). Such miRNAs are non-coding single-stranded RNAs (ssRNAs) that are generated from endogenous hairpin transcripts. They negatively regulate gene expression by binding to the target messenger RNAs (mRNAs), usually in the 3‘untranslated region (UTR) (Kim 2005). There are several reports showing that such regulation of gene expression by miRNA is observed particularly for tumor cells (Ng et al. 2010; Yan et al. 2010; Song et al. 2011; Mansour et al. 2013).

3.4.1 ATM knockdown by miRNA

Previously in our laboratory, it has been demonstrated that a specific miRNA may also affect the expression of ATM (Mansour et al. 2013). It was shown that in the squamous cell carcinoma cell line, SKX, ATM was downregulated due to overexpression of miRNA-421. The sequence of this specific miRNA is listed in **Table 1**.

Table 1. miRNA used for ATM down-regulation

Name	Sequence
hsa-miR-421	5' AUCAACAGACAUUAAUUGGGCGC 3'
hsa-miR-100-5p	5' AACCCGUAGAUCCGAACUUGUG 3'
hsa-miR-101-3p	5' UACAGUACUGUGAUAACUGAA 3'
hsa-miR-18a-5p	5' UAAGGUGCAUCUAGUGCAGAUAG 3'

Figure 18 shows the effect of miRNA-421, 100-5p, 101-3p and 18a-5p on the expression of ATM in PC3 cells. Western blot assay was used to analyze ATM expression with ß-actin as loading control. Cells were transiently transfected in a "reverse" format with 25nM miRNA mimics using RNAiMax (Invitrogen) transfection reagent according to the manufacturer's protocol.

The aforementioned data demonstrate that the downregulation of ATM strongly depends on the final level achieved and that even small differences will have a significant impact on DSB repair as well as cellular radiosensitivity (**see Figures 12, 13 and 15**). Therefore, down-regulation of ATM was also tested for other miRNA (miR-421, miR-100-5p, miR-101-3p, miR-18a-5p) previously reported to affect ATM (Mansour et al. 2013; Ng et al. 2010; Yan et al. 2010; Song et al. 2011) as well as the combination of all four miRNAs (**Figure 18**). The sequences of these specific miRNAs are listed in **Table 1**. Strikingly, transfection with miR-100 and miR-101 was found to have only a moderate effect on ATM expression. Meanwhile, Transfection with miRNA-421 was found to reduce the cellular level of ATM in PC3 cells to about 20% of control levels. Also, a remarkable effect was measured for miR-18a with a reduction down to 40% of control levels. However, it was also observed that the combination of all four miRNA showed the strongest effect with a reduction in ATM of levels down to 10% of control. These data showed that miRNAs can be used to downregulate ATM and that the most efficient downregulation is best achieved when using a combination of 4 miRNAs (miR-421, miR-100-5p, miR-101-3p, and miR-18a-5p).

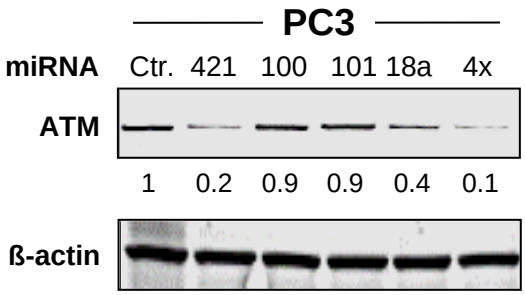

Figure 18. Endogenous miRNA (miR-100, 101, 421, 18a) mimics downregulate ATM expression. Western blot analysis of ATM expression in PC3 cells after miRNAs overexpression using miRNA mimics. Cells were transfected in "reverse" with 25nM control or miRNA mimics (miR-100, 101, 421, 18a**)** singly or in combination (4x). ATM expression [upper panel] and ß-actin (loading control) [lower panel].

3.4.2 ATM knockdown by stable expression of miRNA

The next step was to test the effect of miRNA on ATM expression, when stably expressed in PC3 cells. To this end, the pcDNA6.2-GW/emGFP-miRNA expression system (Life Technologies) was used. DNA oligonucleotides encoding hsa-miR-421, hsa-miR-18a-5p, has-miR-100-5p and has-miR-101-3p were designed as shown in **Table 3**. The four sequences of the miRNAs (in tandem) were embedded into a natural miR backbone to form pre-miRNA hairpin structure, and then impeded into pcDNA^{TM}6.2- GW/EmGFP-miR expression vector (Invitrogen), which was denoted pemiR-4X (**Figure 19A).**

To stably integrate this plasmid (pemiR-4X,) PC3 cells were seeded in 6-well plates and transfected with plasmid DNA (2 µg/well) using Fugene HD (Promega) according to the manufacturer's instructions. The cells which assimilated the pemiR-4X were then selected by growing in medium containing 15µg/ml blasticidin antibiotic. Several resistant clones were selected by micro-trypsinization and expanded for further analysis.

In order to analyze ATM knockdown efficiency, whole-lysate proteins from all clones were analyzed by Western blot analysis and ATM expression was detected using specific antibody with ß-actin as loading control. **Figure 19B** shows the ATM expression in two resistant clones (#23 and #24). Only a moderate reduction in ATM expression was measured for clone #23 and only a reduction of down to 50% was determined for clone #24, compared with control. For comparison, clone #3 was used as previously established by stable integration of shRNA (**Fig. 17B**) showing a strong reduction of ATM. After several passages, clone #24 re-expressed ATM. Identical analysis was performed for the other PC3 clones with stable integration of pemiR-4X.

For most clones, no significant or more pronounced reduction in ATM was observed (data not shown).

3.4.3 Impact of ATM knockdown by stable integration miRNA on radiosensitivity

Figure 19C shows the effect of ATM knockdown on cellular radiosensitivity once stable integration of miRNA using the expressing vector (pemiR-4X) was achieved.

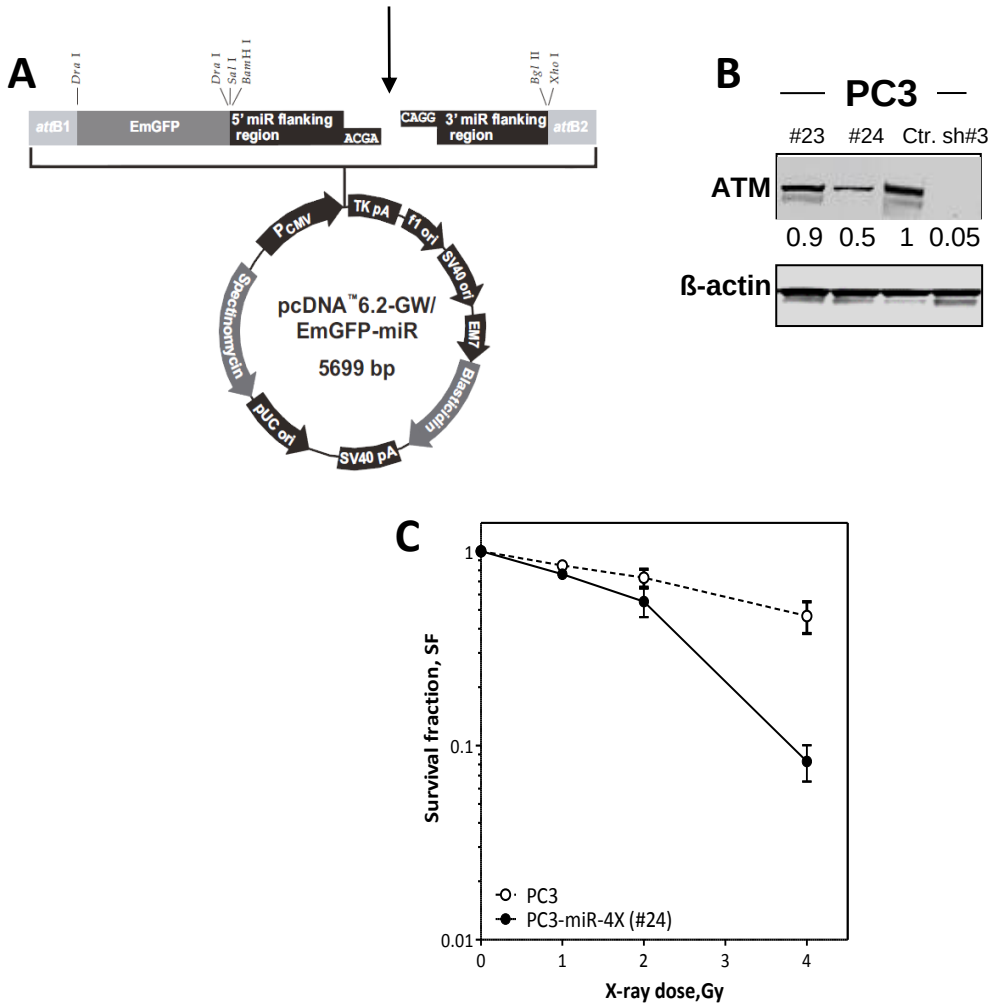

Figure 19. Combined miRNAs downregulate ATM and enhance radiosensitivity.
(A) A map of pcDNA6.2-GW/EmGFP-miR plasmid. B) Western blot showing ATM expression in stably integrated PC3 (#23 and #24) clones harboring pemiR-4x vector expressing the four endogenous miRNAs (miR-18a, 100, 101, 421). ATM expression [upper panel] and ß-actin (loading control) [lower panel]. Ctr, refer to normal cells which used as negative control. Sh, ATM-depleted clone by shRNAs used as a positive control. C) Clonogenic survival experiments for stable ATM-depleted clone (PC3#24). Cells were irradiated with different X-rays doses up to 4 Gy. The survival curves were constructed with normalized values. Values shown are the means ± SEM from two different experiments.

Parental cell line PC3 and the ATM-depleted clone #24 (PC3#24) were both seeded and then irradiated with X-ray doses up to 4Gy. The number of colonies measured for non-irradiated cells was normalized to 1. When compared to the parental cell line, clone #24 had a much higher radiosensitivity. The radiosensitivity was enhanced by a factor of approximately 2 as indicated by a similar survival fraction of 15% for the parental cell line after 4Gy, and after 2Gy for clone #24. Surprisingly, this increase in radiosensitivity precipitated by stable ATM downregulation using miRNA was similar to the level observed, when ATM was downregulated by shRNA although in the latter instance, the downregulation of ATM to 10% was much stronger (**figure 17B**). This observed radiosensitivity was completely diminished after several culture passages (data not shown).

3.4.4 Targeting ATM using artificial micro RNAs (amiRNAs)

Since the downregulation of ATM by stably integrated miRNA was not as effective as expected, the technology of artificial miRNA was tested. For this technology, artificial miRNA sequences embedded into a natural miRNA backbone are used (Chung et al. 2006).

DNA oligonucleotides against ATM were designed using software available at http://rnaidesigner.lifetechnologies.com/rnaiexpress leading to three different constructs termed: amiR-10355, amiR-10844 and amiR-12745 (**Table 2**). Either the individual or three artificial miRNAs (in tandem) were embedded into the natural miRNA backbone to form a pre-miRNA hairpin structure, and then constructed into a pcDNA6.2- GW/EmGFP-miR vector named pamiR-3X, which was identical to the vector used for miRNA (**Figure 19A**).

Table 2. Artificial miRNA designed for ATM downregulation

Name	Sequence
hsa-amiR-ATM-10355	5’ GAAAGAAGAAGCCCAATGGAT 3’
hsa-amiR-ATM-10844	5’ ATAAAGGTGGGACACATGGAA 3’
hsa-amiR-ATM-12745	5’ TTAATCTGGACACAACTGTTC 3’

Figure 20 shows the effect of artificial miRNAs singly or in combination with respect to effect on the ATM expression in MCF-7 cells. Cells were transiently transfected in a “Forward” mechanism with artificial miRNAs constructs (amiR-10355,

amiR-10844 and amiR-12745 or combined) using Fugene HD (Promega) for up to 72 hours, according to the manufacturer's instructions. ATM expression was detected using Western blot analysis with ß-actin as loading control. No significant or only a marginal reduction in ATM expression was observed for the single amiRNA, with a maximum reduction in expression of 85% after amiR-12745 was employed for incubation during a 72 h period. However, when cells incubated with all three amiRNA (pamiR-mix) for 72 h, expression of ATM was found to be reduced down to 45% of control levels (**Figure 20**).

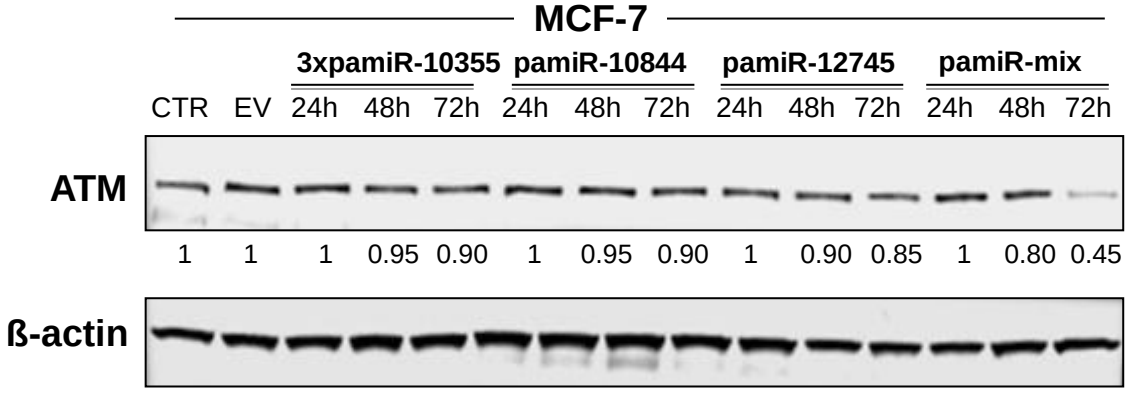

Figure 20. Artificial miRNAs (pamiR-10355, 10844, 12745 and a combination of these) downregulate ATM expression. ATM expression in MCF-7 cells transfected with previous plasmids. Cells were seeded and transiently transfected in a "Forward" direction with plasmid artificial miRNAs singly or in combination (-mix). ATM expression [upper panel] and ß-actin (loading control) [lower panel]. EV indicate control empty vector.

3.4.5 Downregulation of ATM by stably integrated artificial miRNA

The combination of the three amiRNA was used to study the effect of stably integrated amiRNA on ATM expression in both MDA-MB-468 and PC3 cells. The plasmid expressing the artificial miRNA (pamiR-3X) was introduced in both cell lines. To this end, 2 µg of the pamiR-3X was introduced using Fugene HD transfection reagent (Promega). Cell lines which harbored the pamiR-3X plasmid were selected by growth in medium containing 15µg/ml and 5µg/ml blasticidin antibiotic, respectively. For each cell line, several resistant clones could be selected by micro-trypsinization and expanded for further analysis.

Up to 10% of the selected clones demonstrated ATM knockdown to a level of 10% of control but there were also clones, which had no effect whatsoever (data not shown). **Figures 21A and B** show the ATM expression in two respective clones for MDA-MB-468 (#90 and #91) or PC3 (#39 and #40). For both parental as well as

selected clones, whole-lysate proteins were prepared and ATM expression was detected using Western blot with ß-actin as loading control. No significant reduction was detected for clones MDA-MB-468#90 and PC3#39. In contrast, a strong reduction in ATM was detected for clone MDA-MB-468#91 and PC3#40 with a reduction down to 15% and 10% of control, respectively. Identical results were obtained from the same clones several days later indicating that ATM knockdown was stable over time. This reduction in ATM was similar to the strong reduction obtained for respective clones with stably integrated shRNA (PC3 sh#3) as plotted in **Figure 21A and B**.

These data show that stably integrated amiRNA can be used to precipitate efficient down-regulation of ATM down to levels of 10-15% of control expression.

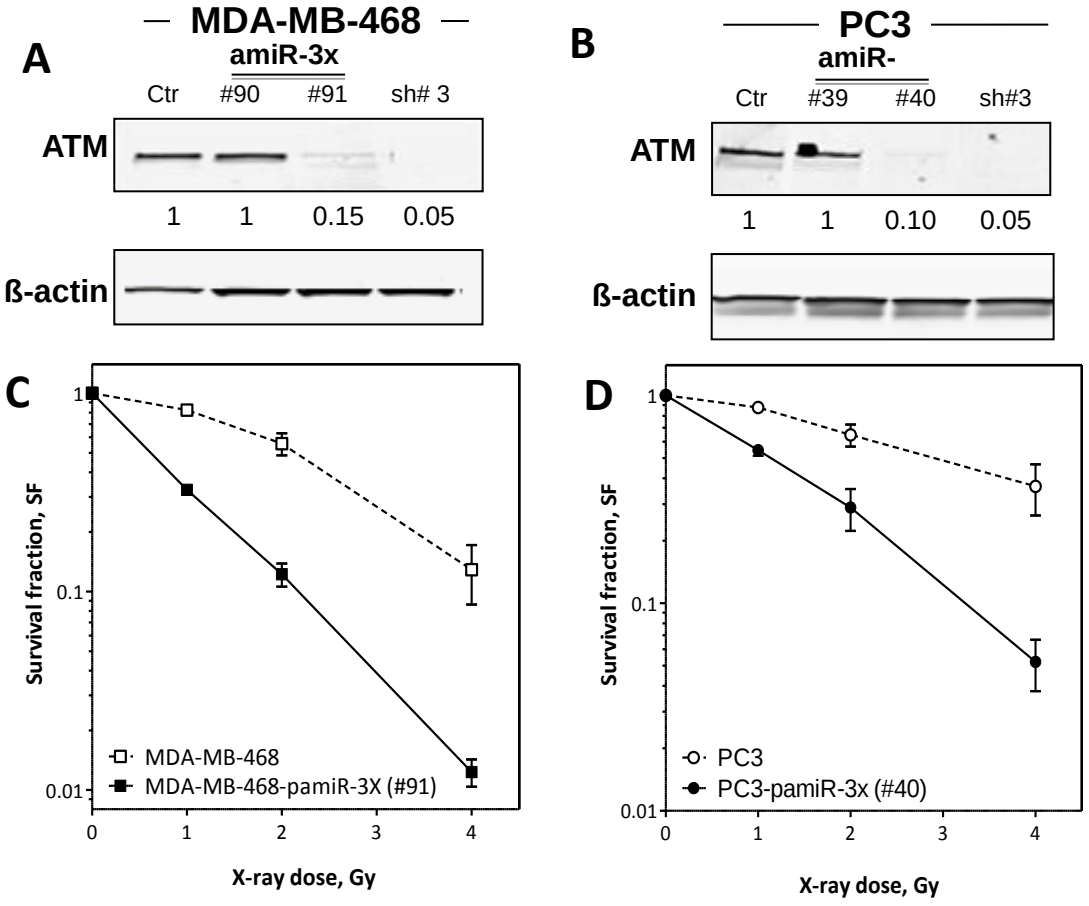

Figure. 21 ATM depletion by Artificial miRNAs enhance radiosensitivity.
A, B) Western blot of ATM expression in stably integrated MDA-MB-468 clones (#90 and #91) and PC3 (#39 and #40) clones, respectively, harboring pamiR-3x vector expressing the three artificial miRNAs. Ctr indicate control cells which used as negative control. shRNAs (sh) was used as a positive control. ATM expression [upper panel] and ß-actin (loading control) [lower panel]. C, D) colony formation assay for the stable ATM-depleted clones (MDA-MB-468#91 and PC3#40). Cells were irradiated with different X-rays doses up to 4Gy. The survival curves were constructed with normalized values. Values shown are the means ± SEM from at least two different experiments.

3.4.6 Impact of ATM knockdown by stably integrated amiRNA on radiosensitivity

Figures 21C and D demonstrate the effect of ATM knockdown through stably integrating plasmids expressing amiRNA for both MDA-MB-468 and PC3 cells. Together with the respective clones (MDA-MB-468#91, PC3#40), the parental cells were seeded and irradiated with X-ray doses up to 4Gy. After irradiation, cells were kept in the incubator for up to 15 days to allow colony formation of surviving cells. Survival of non-irradiated cells was normalized to 1. For both cell lines, a clear increase in radiosensitivity was observed when compared to the clones with integrated plasmids. For MDA-MB-468#91, cellular radiosensitivity was enhanced by approximately 2-fold as indicated by a similar survival fraction of about 15% after 4Gy irradiation of the parental cell line and after 2Gy for clone#91 (**Figure 21C**). For PC3 cells, cellular radiosensitivity was enhanced by a factor of approximately 3 as indicated by a similar survival fraction of about 40% after 4Gy for the parental cell line and an irradiation dose of between 1 to 2 Gy for clone#40 (**Figure 21D**).

Overall, these data demonstrate that the stably integrated combination of three amiRNA can be used to achieve an efficient downregulation of ATM resulting in pronounced radiosensitization for both MDA-MB-468 and PC3 cells.

3.5 Comparative analysis

Several techniques were used to target ATM with the final aim of achieving a pronounced increase in cellular radiosensitivity. For all techniques, there was always a substantial increase in radiosensitivity obtained that were at least 2-fold or even higher (**Table 3**).

Table 3. Fold-increase in cellular radiosensitivity* achieved by different techniques in ATM downregulation

	Cell lines			
Technique	*MCF7*	*MDA-231*	*MD-468*	*PC3*
ATMi KU55933	~ 2	~ 2	~ 4	-
siRNA	~ 2			
shRNA stably integrated	~ 3			~ 2
miRNA stably integrated				~ 2
amiRNA stably integrated			~ 2	~ 3

* Increase in radiosensitivity was always estimated for the survival level obtained after a dose of 4Gy delivered to the control cells.

However, for the effect of stably integrated plasmids, which was the central aspect of this study, clear differences can be observed. All three different techniques (shRNA, miRNA, and amiRNA) were tested on PC3 cells. A fairly similar effect was obtained for both shRNA and miRNA with an enhancement factor of about 2. However, for a permanent downregulation of ATM using stably integrated amiRNA, a higher factor of about 3 was recorded. These data indicate that downregulation of ATM by stably integrated plasmids appears to result in the strongest enhancement of cellular radiosensitivity when using amiRNAs in combination.

4 DISCUSSION

Breast cancer is the most common cancer of women worldwide and is largely a hormone-driven disease. It has been estimated that approximately 1.7 million cases of breast cancer were diagnosed in 2012 globally, which approximate a quarter of all cancers diagnosed in women (Ferlay et al. 2014). The age-standardized rate (ASR) per 100,000 is considerably higher in European women compared with their North American counterparts (e.g., 112 per 100,000 in Belgium compared with 93 per 100,000 in the United States) (Ferlay et al. 2014). In Germany, a strong tradition of cancer registration exists; therefore, the diagnosis of breast cancer and other cancers are accurately recorded, which should permit prompt treatment of these patients. However, although survival after breast cancer diagnosis results in a relative survival rate of 81% after five years, approximately 18,000 women in Germany succumb to breast cancer on an annual basis (Katalinic et al. 2009).

Improved health promotions, more prompt diagnoses and treatment of the disease, and an increased awareness of the benefits of a balanced diet have all contributed to the decreased prevalence of older populations in the developed world. Nevertheless, the incidence of cancer overall has increased in recent years. In German men, prostate cancer is the most common but while the relative five-year survival rate approximates 93%, recurrent disease is common; it is the third most lethal cancer in men (Robert Koch Institute 2014). As with breast cancer, prostate cancer has a genetic component, which predisposes individuals to the disease and two genes (BRCA1 and BRCA2) confer an increased risk of breast cancer in families (Gayther et al. 2000).

Although cancer prevention and treatment has been the focus of significant fiscal investment in the developed world, certain cancers are incredibly resistant to modern-day treatment methods, resulting in premature morbidity and mortality. Consequently, a need to reevaluate treatment strategies exists, and the increase in ‘biologicals’ suggests that cancer treatment in the years ahead may be much more person-specific (Schrem et al. 2016). Identification of a particular gene *loci* in ethnic groups may permit a more tailored approach to the treatment of certain types of cancers (Struewing et al. 1997).

4.1 Radiotherapy treatment of cancers

Historically, the management of solid cancers has relied on systemic treatment, often provided for palliative purposes. Surgery, chemotherapy, and radiation are the cornerstones for treating early cancers. However, in recent years, new medical

technologies have emerged, such as monoclonal antibody therapies and stereotactic body radiotherapy (SBRT) (Tree et al. 2014). Indeed, adjuvant radiotherapy (RT) has been used in combination with monoclonal antibodies in the treatment of HER-2-positive breast cancer, with some degree of success (Cao et al. 2016). While RT is an important therapy in the treatment of single tumor sites, RT can become ineffective, due to development of radio-resistance.

The majority of cancer patients treated with RT tend to receive fractionated radiotherapy. Exposures are usually repeated on a daily regimen until the maximum tolerable doses are attained in normal tissues. Overall, cure of tumors with fractionated RT approximates 65% (Rao et al. 2014). Consequently, in recent years, there have been considerable efforts to tease out the mechanisms of radio-resistance to potentiate RT of cancer. As an example, Rao and colleagues (2014) employed the use of axitinib, a highly effective and selective receptor tyrosine kinase inhibitor of VEGFR1, 2 and 3, to augment radiosensitization in tumors and permit a decreasing dose to be used over time. Although this study assessed axitinib-RT combination in *in vitro* and *in vivo* pre-clinical studies, potential exists for such small-molecule drugs to affect key biochemical pathways, which translates into potentiation of fractionated RT.

The outcome after RT greatly depends on the integrity and feasibility of the DNA damage response (DDR). Shortly after ionizing radiation (IR), many DSBs are induced, which activates the DNA damage response system. The efficiency of DDR depends on the activation of different protein kinases, such as ATM, which relay a very strong signal to various downstream effectors that play a role in repair of DSB machinery and cell cycle checkpoint activation. Therefore, ATM is the first responder to potentially lethal DSBs and the main carrier of DNA damage signaling (Shiloh and Ziv 2013). Ataxia-telangiectasia patients carry a mutation in the ATM gene and have a marked defect in responding to DNA lesions, including DSBs, which is associated with clinical and cellular radiosensitivity (Lavin 2008).

4.2 Optimization of RT radiosensitization using miRNAs

Base excision repair (BER) is a critical pathway in radiosensitivity dynamics and is a response to oxidative DNA base lesions generated through DSBs. Apurinic/apyrimidinic endonuclease/redox effector factor (denoted as APE1) is an essential enzyme involved in the BER response and is integrally involved in the radio-resistance of cancers (Dai et al. 2016). Dai and colleagues utilized an approach involving microRNAs (miRNAs) to target APE1 and downregulate the expression of this key biochemical modulator. As a consequence, they were able to increase radio-

sensitivity to osteosarcoma and suggest that this is a viable approach to augmenting therapeutic efficacy of RT. MiRNAs regulate gene expression at the post-transcriptional level through cleavage of mRNA or inhibition of translation process. MiRNAs can fine tune the expression of many proteins involved in DDR, such as ATM and H2AX (Lal et al. 2009; Hu et al. 2010). ATM can be targeted by miRNA-421, miRNA-18a, miRNA-101 and miRNA-100 (Ng et al. 2010; Wang et al. 2012; Mansour et al. 2013; Wu et al. 2013). The ability of miRNAs to modulate several proteins involved in the DDR pathway creates new possibilities for targeting ATM. Instead of employing ATM inhibitors or small interference RNAs (siRNAs), miRNAs can be used to silence ATM and inhibit DDR machinery in tumor cells. Although it has been demonstrated that different miRNAs downregulate ATM expression, examining the combinatorial effect of these miRNAs at the level of ATM expression and the concomitant impact on the radiation response is unclear. Given that the regulation elicited by miRNAs is highly complex, it is no surprise that a single miRNA can influence the expression of many mRNAs, while it is also possible for a single mRNA to be influenced by multiple miRNAs. This study demonstrates a new miRNA-based strategy by which co-expression of three synthetic miRNAs results in the potent knockdown of ATM, further enhancing radiosensitivity in different tumor cell lines from breast and prostate cancer.

4.3 Targeting ATM activity by KU55933

Stable expression and efficient activation of DDR proteins is considered one of the main determinants of ionizing radiation response (Goldstein and Kastan 2015). ATM was identified as a major player in the DNA damage response, which is activated after DSBs induction (Shiloh 2006). In response to IR, ATM activates several downstream targets, including p53, Chk1 and Chk2, which are involved in various DNA repair processes (Shiloh 2003). In cancer therapy, inhibition of the DDR is considered an attractive therapeutic prospect for several reasons, which include resistance to genotoxic therapies associated with an increase in DDR signaling. Furthermore, a number of cancers have defects in certain aspects of the DDR, which makes them very dependent on other DDR pathways for cellular survival (Weber and Ryan, 2015).

The DDR has been conserved through eukaryotic cells from yeast to humans and is divided into two discrete pathways that respond to different types of DNA damage, although the consensus is that an element of overlap exists. The ATM responds to DSBs induced by IR and results in activation of a number of targets, including the Chk2 checkpoint kinase and H2AX. The second pathway involves ATR

(ATM- and Rad3-related), another member for the PI3 kinase family, which senses excess replication protein A-coated single stranded DNA that originates during S phase because of stalled replication forks (Smith–Roe et al. 2015). A number of environmental and genotoxic factors precipitate this pathway, including ultraviolet light.

This study shows that KU55933 rapidly inhibited ATM activity after IR; consequently, the phosphorylation of its downstream targets was impaired. This was demonstrated by a moderate reduction of pChk2. This moderate reduction is most likely due to a redundant activation pathway through ATR and DNA-PKcs (Li and Stern 2005; Wang et al. 2006). Chk2 is targeted by ATM on residue Thr-68, and ATM activation triggers the phosphorylation and full activation of Chk2. Consequently, this activates the Cdc25 family of protein phosphatases, which are essential for G2/M phase cell cycle transitions (Shiloh 2003).

In addition, ATM phosphorylates H2AX on Serine 139 (ɣH2AX), an early marker of DSBs. This preserves the landing sites for many other proteins involved in initiation of DNA repair and activates the cell cycle checkpoints (Carney et al. 1998). ATM inhibition impaired the efficiency of DSBs repair, as indicated by a high number of unresolved DSBs. ATM inhibition by KU55933 resulted in enhanced sensitivity to IR at low doses (4Gy). Therefore, after IR, ATM appears to play a key role in correcting DNA lesions and promoting cellular survival. These results corroborate previously published data where it was possible to enhance tumor radiosensitivity through ATM inhibition using small molecule inhibitors (Rainey et al. 2008).

Although the ATM inhibitor KU55933 has been shown to be effective, evidence for off-target effects has also been provided. KU55933 has been identified through screening for compounds and may efficiently inhibit autophagy by targeting Vps34 independently of ATM kinase activity (Farkas et al. 2011). Furthermore, there is significant concern relating to enzymatic inactivation of ATM in normal cells. This may significantly enhance genomic instability thereby generating a reverse effect that would promote the development of secondary tumor growth after radiotherapy, an undesirable side-effect of therapy (Stagni et al. 2014). In conclusion, the ability of this inhibitor to target other pathways makes it potentially impractical for use in clinics. That said, a recent study demonstrated that KU55933 was successful in reducing radio-resistance of bladder cancer tumors in patients with a DAB2IP gene defect (Zhang et al. 2015). For the purposes of this study, an alternative means of regulating ATM expression by post-transcription regulators was sought.

4.4 ATM gene expression silencing by RNA interference (RNAi)

RNA interference (RNAi) is considered an efficient tool for disruption of gene functionality. In this approach, the gene is post-transcriptionally regulated via specific double-stranded RNA molecules (siRNAs) (Meister and Tuschl 2004; Zamore and Haley 2005). The protein depletion effect is due to higher complementary associations between the sequence of siRNAs and the 3'UTR (untranslated region) of mRNA. Consequently, the generated mRNAs are cleaved by different exonucleases (Lam et al. 2015).

Furthermore, short hairpin RNAs (shRNAs) can induce degradation of target mRNAs similar to siRNAs, leading to specific gene silencing and mediation of persistent gene silencing. In this study, cancer cell lines were transfected with either the siRNAs pool (MCF7) or shRNAs expressing vector (PC3 and MCF7), and in both cases, it was demonstrated that ATM was efficiently inhibited. The ATM expression depleted cells using siRNAs were unable to repair DSBs, as proven by an increased prevalence of the residual DSBs marker, ɣH2AX. ATM protein knockdown in tumor cells lead to inefficient DSBs repair thus culminating in enhanced radiosensitivity observed after low doses of IR (4Gy). Importantly, by treating tumor cells with siRNAs or a shRNAs-based siRNA vector, this resulted in enhanced cytotoxic effects of IR and produced a level of radiosensitivity similar to that observed in cells treated with KU55933. One possible explanation for this higher radiosensitivity is that ATM knockdown cells are unable to detect levels of DNA damage that would otherwise lead to initiation of the DNA repair machinery, leading to catastrophic genomic damage. Furthermore, ATM knockdown cells cannot induce checkpoint arrest following DNA damage, resulting in replication of damaged DNA and propagation of errors to a high extent. As a consequence, the cell is directed to a process of apoptosis by an alternative P53- independent mechanism (Foray N 1997).

Efficient ATM knockdown using shRNAs is hampered by a number of different problems, which frequently arise from shRNA overexpression. First, overexpression of shRNAs can cause toxicity due to endogenous miRNA pathway oversaturation (Grimm et al. 2010; Kanasty et al. 2012). Second, shRNA sequences are usually designed with a perfectly matched guide, and passenger strands may increase off-target effects. Finally, shRNAs often induce an immune response, which may compound or mask RNAi-specific effects (Judge et al. 2005, 2006). Hence, shRNAs can affect significantly more than the target of interest, which may result in non-beneficial effects. The ability to manipulate shRNA expression levels is important to maximizing efficient use of shRNA, since levels that are too low may not be effective,

while levels that are too high can cause toxicity. Furthermore, the ability to determine siRNA expression levels is critically important for cell survival genes, where identification of inducible shRNA promoters is essential.

As a consequence of these limitations of shRNAs, a number of authors have suggested that endogenous miRNAs could be employed as a very powerful tool to negatively regulate target gene expression (Kim 2005).

4.5 ATM gene expression regulation by miRNAs

The regulation of gene expression can be achieved through two different mechanisms: 1) mRNA degradation or 2) transcription inhibition. These two mechanisms can occur by participation of miRNAs in post-transcriptional regulation (Mukherji et al. 2011).

Unlike siRNAs, miRNAs are coded on the genome and can either be transcribed individually, in clusters, or within an intron of a protein-coding gene (Carthew and Sontheimer 2009). MiRNAs are single-stranded RNAs (ssRNAs), approximately 19–25 nucleotides in length, which are generated from endogenous hairpin transcripts. They play an important role in the negative regulation of gene expression by base-pairing to the target messenger RNAs (mRNAs), usually in the 3‘untranslated region (UTR) (Kim 2005). MiRNAs have only partial complementarity to their corresponding targets (Bagga et al. 2005). However, recent evidence suggests that in addition to 3'UTRs, miRNAs can bind to other regions of target mRNAs, including the 5'UTRs and promoter and open reading frames, all leading to translation activation (Lee 2013).

The use of exogenous miRNAs may prevent the competition that exists between endogenous miRNAs and siRNAs thereby eliminating toxicity. Thus, maximal gene silencing can be achieved using a miRNA-based strategy, without the accumulation of precursor and non-processed products that may disrupt endogenous miRNA biogenesis, which leads to toxicity. Using chained artificial miRNAs (amiRNAs) for multiple gene knockdowns, Fowler and colleagues (2015) were able to demonstrate that the concatenation of several miRNAs targeting different genes is an effective modality for augmented knockdown efficacy. Such an approach has direct transferability to what was performed in this study, since a multi-gene knockdown approach also yielded a significant reduction in frequency of radio-resistance.

Bioinformatics tools predict hundreds of targets for each single miRNA but few of these miRNA have been experimentally tested (Lee and Dutta 2009). This study tested the repression effect of four endogenous miRNAs (miR-421, 100, 101 and 18a)

(Table 1) and three artificial miRNAs (amiR-10355, amiR-10844 and amiR-12745) (Table 2).

In this study, several techniques were used to target ATM with the ultimate aim of achieving a pronounced increase in cellular radiosensitivity. For the techniques used, a large (at least two-fold) increase in radiosensitivity was obtained (Table 3). The three different techniques (shRNA, miRNA, and amiRNA) were performed using the PC3 cell line. A relatively similar effect was obtained for both shRNA and miRNA with an enhancement factor of approximately 2. However, for a permanent downregulation of ATM using stably integrated amiRNA in combination, an almost 3-fold downregulation of ATM was observed.

Guo and colleagues (2014) demonstrated the ability to augment radiosensitivity in a radiation-resistant glioblastoma multiforme (GBM) cell line by overexpressing miR-26a, an endogenous gene modulator of the ATM protein. This resulted in an inhibition of the HR repair pathway and suggested that this miRNA could be an important radiosensitizing target. In the current study, we went a step further and utilized three artificial miRNAs in combination, which resulted in a synergistic downregulation of the ATM gene, with concomitant increase in radiosensitivity in a prostate cancer cell line. Our approach is similar to a recent study, which showed that the targeting of many oncogenic miRNAs in diffuse large B-cell lymphoma cell lines resulted in cell cycle arrest and apoptosis through upregulation of p38/MAPK pathway (Su et al. 2016).

In eukaryotic cells, miRNAs are transcribed individually or in clusters and often share similar target genes (Bartel 2009; Carthew and Sontheimer 2009). However, it remains unclear as to whether a combination of different miRNAs efficiently represses ATM gene expression compared with single miRNAs. It was demonstrated that using four endogenous miRNAs in combination moderately repressed ATM expression. This could be explained by the idea that each endogenous miRNA has numerous putative targets (Lewis et al. 2005). A similar methodology by Choi and colleagues (2014) employed the use of three endogenous miRNAs to downregulate expression of BRCA1, BRCA2, and Rad51 and influence downstream DSB repair in an ovarian tumor cell line. The observed effects were more profound when the miRNAs were used in combination, compared with a single miRNA. The explanation for this is most likely due to the multiple transcript targets that these individual miRNAs appear to have.

When the three artificial miRNAs were used in combination, this also led to a more pronounced reduction in ATM expression. These results were similar to a previous study that employed a siRNA pool (Hannus et al. 2014). This is also supported by the idea that each mRNA can be targeted by several miRNAs and lead to more and persistent gene silencing (Choi et al. 2014). Artificial miRNAs (amiRNAs) embedded into a natural miRNA backbone have shown to be a useful strategy for silencing gene expression and reducing off-target effects that arise from using shRNA and siRNA (Fowler et al. 2015). Furthermore, the integration of different miRNAs into prostate (PC3) and breast (MDA-MB-468) cells strongly enhanced radiosensitivity in these cell types. This study provides encouraging data that may translate into clinical benefit.

The higher number of miRNAs hairpin structures may lead to decreased integration efficiency of the expressing vector (Wang et al. 2015). This study identified few stably integrated clones with pamiR-3X showing reduced ATM expression when the number of miRNAs precursor was 3. Furthermore, the study failed to find stably integrated clones with pemiR-4X showing loss of ATM expression when the number of miRNAs precursors was increased to 4 using plasmid circular DNA vector 6.2. Xu and colleagues (2010) were able to overexpress miRNA-122 in a liver development model and used lentiviral vectors to do so. Furthermore, the authors generated stable cells possessing eight copies of the miR-122 precursor, which clearly shows a disparity between our findings, explained partly by the methodological differences.

It is important to note that miRNA must be cleaved into precursor microRNA (pre-miRNA) by Drosha (Wang et al. 2010). Subsequently, pre-miRNA is actively transported from the nucleus to the cytoplasm by the nuclear protein–guanosine triphosphate and an export receptor, exportin 5. Clearly, the processes of enzyme digestion and transport depend on the transcript sequences and their space structures. It is possible that the processing or nuclear export of pre-miRNA was influenced by conformational construct changes in the pre-miRNA or the primary construct. It seems that the optimal copy number of the miRNA in the vector used remains to be elucidated and further work should be done to explore this finding.

4.6 Translation of the research into clinical application

In summary, this study was able to inhibit or deplete ATM expression and began to uncover the mechanisms by which ATM inhibition leads to pronounced radiosensitivity. It has been shown that inhibition of ATM leads to disruption of the DNA damage response signal by reducing p-ATM and p-Chk2. As a consequence,

this impaired the repair efficiency of the DSBs repair, as indicated by an increased number of residual γH2AX foci. This reduced efficiency in repair of DSBs led to augmented radiosensitivity. By employing a number of cell lines in this study, it is postulated that an inverse relationship between miRNAs and ATM expression exists. Targeting the ATM gene was attempted by overexpressing individual miRNAs and a combination of these. This showed that transient transfection of single miRNAs had very little (<50%) or no effect on the downregulation of ATM expression. Given that a mRNA can be targeted by many miRNAs and miRNAs can target hundreds of mRNAs, the aim was to pursue a combination approach. Indeed, when miRNAs in combination were used, ATM expression was downregulated to a level of 10% of control expression, an impressive reduction.

In this study, the data are compelling and provides good evidence that artificial microRNA (amiRNA) sequences embedded in microRNA (miRNA) backbones (pcDNA6.2) are a powerful tool that could be used to suppress ATM expression by up to 90%, which mirrors the efficiency of shRNAs. Additionally, the data indicate that ATM expression could be suppressed (by up to 50%) using endogenous miRNAs. All stable ATM-depleted clones generated by these strategies show radiosensitivity correlated positively with the ATM protein level. Consequently, this study proves that to significantly suppress ATM protein expression, multiple miRNAs are simultaneously required. Therefore, the suggestion is that the regulation of ATM expression may be complicated by numerous additional regulators at the pre- and post-translational stages, such that a single miRNA cannot be used to suppress ATM expression, except in the artificial context of a luciferase assay.

The practical importance of the study findings is related to the possibility of using these combinatorial miRNAs as biological modifiers to silence DNA damage response (DDR) proteins, such as ATM, and to sensitize cancer tissues to ionizing radiation. By doing so, not only would treatment outcomes improve but this could be achieved through dose de-escalation. The combination of several miRNAs to target ATM offers a tantalizing insight into such a strategy for cancer treatment. However, further studies are required to examine the effect of this combination treatment on other genes before it can be used in the clinical *in vivo* setting.

A number of other groups have successfully used siRNA knockdown technology to abrogate ATM expression in tumor cell lines, increasing radiosensitivity both *in vitro* and *in vivo*. Li and colleagues (2016) very recently transfected a glioma cell line with a siRNA-ATMpuro (group A) lentivirus or a siRNA-HKpuro (group N, negative control) lentivirus prior to irradiation. ATM gene and protein expression were

significantly downregulated after transfection, compared with control samples. Furthermore, the expression of the p53, PCNA and surviving genes was also considerably reduced. However, while these approaches and those of this study are a promising strategy, the translation of these studies into actual clinical application is likely to be several years from now.

Optimizing radiosensitivity remains a key component of RT cancer treatment strategies, and a study by Ashton and colleagues (2016) demonstrates the potential influence of the anti-malarial drug, atovaquone, on enhanced radiosensitivity of hypoxic tumor cells in patients. The clinical studies being conducted to assess whether this drug can deliver clinical benefits to cancer patients highlight why robust, empirical research studies are important and may well translate into effective cancer treatment strategies in the near future.

4.7 Strengths and limitations of the study

This study had laudable strengths in its methodology and execution. The employment of miRNA technology could be deemed to be at the forefront of scientific research, which hopefully translates into medical benefits. Second, several different tumor cell lines were used and showed a consistent effect of ATM abrogation in breast and prostate cancer, at least *in vitro*. In addition, a number of different cell lines within the breast cancer spectra were used. Whether such an observation is reflected in the *in vivo* setting remains to be seen but should be considered in any future research studies associated with this project.

A number of different strategies to further optimize RT radiosensitivity were used through an inhibitor and a combination of siRNA strategies. This demonstrated a consistent effect, which elucidates the biochemical mechanisms behind ATM-driven RT radio-resistance. This research thus provides a solid foundation for further studies.

This study also had some limitations associated with the methods and the findings. Although different doses of RT were utilized, empirical reasoning behind the choice of doses was not demonstrated (1Gy vs 2Gy vs 4Gy). In retrospect, the research should have employed a more extended gradient of radiation dosages to truly ascertain the impact of ATM downregulation on radio-resistance. It is possible that the optimal dosing strategy was used for measurement of ATM downregulation and expression.

In addition, for the purposes of completeness, this study should have proven without a doubt that the stable transformed vectors were genomically integrated. The downstream data strongly suggest that this was the case but this has not been

definitively illustrated. A zinc finger recombinase (ZFR) approach could have been used to confirm genomic integration of the stably transformed vectors as has been done in other studies (Gersbach et al. 2011).

Finally, this study has an obvious limitation in that the experiments were performed only on *in vitro* cell lines and were not performed *in vivo*, even in an animal model. Thus, the implications of this study's findings cannot be directly extrapolated to the clinical setting at this point in time.

4.8 Future research considerations

This study provides a solid foundation for further research into the utilization of miRNA in abrogating ATM and/or ATR for the purposes of increased radiosensitivity in tumor cells. In the first instance, at the *in vitro* level, it should be possible to ascertain whether the ATM-downregulation effects observed in the breast and prostate cancer lines are mirrored in other cancer cell lines. Recent evidence suggests that ATM can also be targeted in non-small cell lung cancer and potentiate cisplatin-induced radiosensitization (Toulany et al. 2014). A combined miRNA-targeted approach of ATM in combination with cisplatin may yield impressive results with respect to augmented radiosensitization.

With respect to this type of research direction, other inhibitors that target ATM and/or ATR are being used to augment radiosensitization and support the concept of developing combination cancer therapies; this would incorporate ionizing RT and Torin2 or similar compounds (Udayakumar et al. 2016). Other biochemical targets of interest include the use of rapamycin-induced autophagy to sensitize lung cancer cells to radiation treatment.

4.9 Conclusion

Utilizing a single and combined miRNA approach for targeting ATM in cancer cells, a significant reduction in radio-resistance is shown in both breast and prostate cancer cell lines. Additionally, key biochemical pathways have been further elucidated, which could be targeted to improve cancer treatment strategies in the twenty-first century.

5 REFERENCES

Agrawal, N., Dasaradhi, P. V. N., Mohmmed, A., Malhotra, P., Bhatnagar, R. K. and Mukherjee, S. K. 2003. RNA interference: biology, mechanism, and applications. *Microbiology and Molecular Biology Reviews: MMBR* 67 (4): 657–685.

Ali, A., Zhang, J., Bao, S., Liu, I., Otterness, D., Dean, N. M., Abraham, R. T. and Wang, X.-F. 2004. Requirement of protein phosphatase 5 in DNA-damage-induced ATM activation. *Genes & Development* 18 (3): 249–254.

Aravin, A. A., Hannon, G. J. and Brennecke, J. 2007. The Piwi-piRNA pathway provides an adaptive defense in the transposon arms race. *Science* 318 (5851): 761–764.

Ariumi, Y., Turelli, P., Masutani, M. and Trono, D. 2005. DNA damage sensors ATM, ATR, DNA-PKcs, and PARP-1 are dispensable for human immunodeficiency virus type 1 integration. *Journal of Virology* 79 (5): 2973–2978.

Ashton, T.M., Fokas, E., Kunz-Schughart, L.A., Folkes, L.K., Anbalagan, S., Huether, M., Kelly, .C.J., Pirovano, G., Buffa, F.M., Hammond, E.M., Stratford, M., Muschel, R.J., Higgins, G.S. and McKenna, W.G. 2016. The anti-malarial atovaquone increases radiosensitivity by alleviating tumour hypoxia. *Nature Communications* 25; 7: 12308.

Bagga, S., Bracht, J., Hunter, S., Massirer, K., Holtz, J., Eachus, R. and Pasquinelli, A. E. 2005. Regulation by let-7 and lin-4 miRNAs results in target mRNA degradation. *Cell* 122 (4): 553–563.

Bakkenist, C. J. and Kastan, M. B. 2003. DNA damage activates ATM through intermolecular autophosphorylation and dimer dissociation. *Nature* 421 (6922): 499–506.

Bartel, D. P. 2009. MicroRNAs: target recognition and regulatory functions. *Cell* 136 (2): 215–233.

Bassing, C. H. and Alt, F. W. 2004. The cellular response to general and programmed DNA double strand breaks. *DNA Repair* 3 (8): 781–796.

Begg, A. C., Stewart, F. A. and Vens, C. 2011. Strategies to improve radiotherapy with targeted drugs. *Nature Reviews Cancer* 11 (4): 239–253.

Bensimon, A., Aebersold, R. and Shiloh, Y. 2011. Beyond ATM: the protein kinase landscape of the DNA damage response. *FEBS Letters* 585 (11): 1625–1639.

Betel, D., Wilson, M., Gabow, A., Marks, D. S. and Sander, C. 2008. The microRNA.org resource: targets and expression. *Nucleic Acids Research* 36 (Database issue): D149–53.

Bhayani, M. K., Calin, G. A. and Lai, S. Y. 2012. Functional relevance of miRNA sequences in human disease. *Mutation Research* 731 (1-2): 14–19.

Biddlestone-Thorpe, L., Sajjad, M., Rosenberg, E., Beckta, J. M., Valerie, N. C. K., Tokarz, M., Adams, B. R., Wagner, A. F., Khalil, A., Gilfor, D., Golding, S. E., Deb, S., Temesi, D. G., Lau, A., O'Connor, M. J., Choe, K. S., Parada, L. F., Lim, S. K., Mukhopadhyay, N. D. and Valerie, K. 2013. ATM kinase inhibition preferentially

sensitizes p53-mutant glioma to ionizing radiation. *Clinical cancer research: an official journal of the American Association for Cancer Research* 19 (12): 3189–3200.

Bishop, D. K., Ear, U., Bhattacharyya, A., Calderone, C., Beckett, M., Weichselbaum, R. R. and Shinohara, A. 1998. Xrcc3 is required for assembly of Rad51 complexes in vivo. *The Journal of Biological Chemistry* 273 (34): 21482–21488.

Brown, E. J. and Baltimore, D. 2000. ATR disruption leads to chromosomal fragmentation and early embryonic lethality. *Genes & Development* 14 (4): 397–402.

Brown, E. J. and Baltimore, D. 2003. Essential and dispensable roles of ATR in cell cycle arrest and genome maintenance. *Genes & Development* 17 (5): 615–628.

Cao, L., Cai, G., Xu, F., Yang, Z.Z., Yu, X.L., Ma, J.L., Zhang, Q., Wu, J., Guo, X.M. and Chen, J.Y. 2016. Trastuzumab improves locoregional control in HER2-positive breast cancer patients following adjuvant radiotherapy. *Medicine (Baltimore)*. 95 (32): e4230.

Carney, J. P., Maser, R. S., Olivares, H., Davis, E. M., Le Beau, M., Yates, J. R., Hays, L., Morgan, W. F. and Petrini, J. H. 1998. The hMre11/hRad50 protein complex and Nijmegen breakage syndrome: linkage of double-strand break repair to the cellular DNA damage response. *Cell* 93 (3): 477–486.

Carthew, R. W. and Sontheimer, E. J. 2009. Origins and mechanisms of miRNAs and siRNAs. *Cell* 136 (4): 642–655.

Catto, J. W. F., Alcaraz, A., Bjartell, A. S., De Vere White, R., Evans, C. P., Fussel, S., Hamdy, F. C., Kallioniemi, O., Mengual, L., Schlomm, T. and Visakorpi, T. 2011. MicroRNA in prostate, bladder, and kidney cancer: a systematic review. *European Urology* 59 (5): 671–681.

Chen, S., Paul, P. and Price, B. D. 2003. ATM's leucine-rich domain and adjacent sequences are essential for ATM to regulate the DNA damage response. *Oncogene* 22 (41): 6332–6339.

Choi, Y. E., Pan, Y., Park, E., Konstantinopoulos, P., De, S., D'Andrea, A. and Chowdhury, D. 2014. MicroRNAs down-regulate homologous recombination in the G1 phase of cycling cells to maintain genomic stability. *Elife* 3: e02445.

Chowdhury, D., Choi, Y. E. and Brault, M. E. 2013. Charity begins at home: non-coding RNA functions in DNA repair. *Nature Reviews. Molecular cell biology* 14 (3): 181–189.

Chun, H. H. and Gatti, R. A. 2004. Ataxia-telangiectasia, an evolving phenotype. *DNA Repair* 3 (8): 1187–1196.

Chung, K.-H., Hart, C. C., Al-Bassam, S., Avery, A., Taylor, J., Patel, P. D., Vojtek, A. B. and Turner, D. L. 2006. Polycistronic RNA polymerase II expression vectors for RNA interference based on BIC/miR-155. *Nucleic Acids Research* 34 (7): e53–e53.

Dai, N., Qing, Y., Cun, Y., Zhong, Z. Li, C., Zhang, S., Shan, J., Yang, X., Dai, X., Cheng, Y., Xiao, H., Xu, C., Li, M. and Wang, D. 2016. miR-513a-5p regulates radiosensitivity of osteosarcoma by targeting human apurinic/apyrimidinic

endonuclease. *Oncotarget* Aug 2. doi: 10.18632/oncotarget.11003. [Epub ahead of print]

De Jager, M., van Noort, J., van Gent, D. C., Dekker, C., Kanaar, R. and Wyman, C. 2001. Human Rad50/Mre11 is a flexible complex that can tether DNA ends. *Molecular cell* 8 (5): 1129–1135.

Ernestos, B., Nikolaos, P., Koulis, G., Eleni, R., Konstantinos, B., Alexandra, G. and Michael, K. 2010. Increased chromosomal radiosensitivity in women carrying BRCA1/BRCA2 mutations assessed with the G2 assay. *International Journal of Radiation Oncology, Biology, Physics* 76 (4): 1199–1205.

Esteller, M., Silva, J. M., Dominguez, G., Bonilla, F., Matias-Guiu, X., Lerma, E., Bussaglia, E., Prat, J., Harkes, I. C., Repasky, E. A., Gabrielson, E., Schutte, M., Baylin, S. B. and Herman, J. G. 2000. Promoter hypermethylation and BRCA1 inactivation in sporadic breast and ovarian tumors. *Journal of the National Cancer Institute* 92 (7): 564–569.

Farkas, T., Daugaard, M. and Jäättelä, M. 2011. Identification of small molecule inhibitors of phosphatidylinositol 3-kinase and autophagy. *Journal of Biological Chemistry* 286 (45): 38904–38912.

Ferlay J, Soerjomataram I, Ervik M, Dikshit R, Eser S, Mathers C, Rebelo M, Parkin DM, Forman D, Bray, F. GLOBOCAN 2012 v1.1, Cancer Incidence and Mortality Worldwide: IARC CancerBase No. 11 [Internet]. Lyon, France: International Agency for Research on Cancer; 2014. Available from: http://globocan.iarc.fr [accessed 17/08/16]

Foray N, P. A. A. G. B. C. C. E. A. C. 1997. Hypersensitivity of ataxia telangiectasia fibroblasts to ionizing radiation is associated with a repair deficiency of DNA double-strand breaks. *International Journal of Radiation Biology* 72 (3): 271–283.

Fourquet, A., Stoppa-Lyonnet, D., Kirova, Y. M., Sigal-Zafrani, B., Asselain, B., Group, I. C. B. C. S. and others. 2009. Familial breast cancer: clinical response to induction chemotherapy or radiotherapy related to BRCA1/2 mutations status. *American Journal of Clinical Oncology* 32 (2): 127–131.

Fowler, D. K., Williams, C., Gerritsen, A. T. and Washbourne, P. 2015. Improved knockdown from artificial microRNAs in an enhanced miR-155 backbone: a designer's guide to potent multi-target RNAi. *Nucleic Acids Research* 44 (5): e48.

Francia, S., Michelini, F., Saxena, A., Tang, D., de Hoon, M., Anelli, V., Mione, M., Carninci, P. and d' Adda di Fagagna, F. 2012. Site-specific DICER and DROSHA RNA products control the DNA-damage response. *Nature* 488 (7410): 231–235.

Gandellini, P., Rancati, T., Valdagni, R. and Zaffaroni, N. 2014. miRNAs in tumor radiation response: bystanders or participants? *Trends in molecular medicine* 20 (9): 529–539.

Garzon, R., Marcucci, G. and Croce, C. M. 2010. Targeting microRNAs in cancer: rationale, strategies and challenges. *Nature reviews Drug discovery* 9 (10): 775–789.

Gatti, R. A., Berkel, I., Boder, E., Braedt, G., Charmley, P., Concannon, P., Ersoy, F., Foroud, T., Jaspers, N. G., Lange, K. and others. 1988. Localization of an ataxia-telangiectasia gene to chromosome 11q22-23.

Gayther, S.A., de Foy, K.A., Harrington, P., Pharoah, P., Dunsmuir, W.D., Edwards, S.M., Gillett, C., Ardern-Jones, A., Dearnale,y D.P., Easton, D.F., Ford, D., Shearer, R.J., Kirby, R.S., Dowe, A.L., Kelly, J., Stratton, M.R., Ponder, B.A., Barnes, D. and Eeles, R.A. 2000. The frequency of germ-line mutations in the breast cancer predisposition genes BRCA1 and BRCA2 in familial prostate cancer. The Cancer Research Campaign/British Prostate Group United Kingdom Familial Prostate Cancer Study Collaborators. *Cancer Res*earch 60 (16): 4513-8.

Gersbach, C.A., Gaj, T., Gordley, R.M., Mercer, A.C., and Barbas III, C.F. 2011. Targeted plasmid integration into the human genome by an engineered zinc-finger recombinase. *Nucleic Acids Research* 39 (17): 7868–7878. Goldberg, A. D., Allis, C. D. and Bernstein, E. 2007. Epigenetics: a landscape takes shape. *Cell* 128 (4): 635–638.

Goldstein, M. and Kastan, M. B. 2015. The DNA damage response: implications for tumor responses to radiation and chemotherapy. *Annual Review of Medicine* 66: 129–143.

Goodarzi, A. A., Jonnalagadda, J. C., Douglas, P., Young, D., Ye, R., Moorhead, G. B. G., Lees-Miller, S. P. and Khanna, K. K. 2004. Autophosphorylation of ataxia-telangiectasia mutated is regulated by protein phosphatase 2A. *The EMBO Journal* 23 (22): 4451–4461.

Griffiths-Jones, S. 2004. The microRNA registry. *Nucleic Acids Research* 32 (suppl 1): D109–D111.

Grimm, D., Wang, L., Lee, J. S., Schürmann, N., Gu, S., Börner, K., Storm, T. A. and Kay, M. A. 2010. Argonaute proteins are key determinants of RNAi efficacy, toxicity, and persistence in the adult mouse liver. *The Journal of Clinical Investigation* 120 (9): 3106–3119.

Guo, P., Lan J,, Ge J., Nie, Q., Guo, L., Qiu, Y. and Mao, Q. 2014. MiR-26a enhances the radiosensitivity of glioblastoma multiforme cells through targeting of ataxia-telangiectasia mutated. *Experimental Cell Research* 320 (2): 200-208.

Hanna, J. A., Wimberly, H., Kumar, S., Slack, F., Agarwal, S. and Rimm, D. L. 2012. Quantitative analysis of microRNAs in tissue microarrays by in situ hybridization. *Biotechniques* 52 (4): 235.

Hannus, M., Beitzinger, M., Engelmann, J. C., Weickert, M.-T., Spang, R., Hannus, S. and Meister, G. 2014. siPools: highly complex but accurately defined siRNA pools eliminate off-target effects. *Nucleic Acids Research* 42 (12): 8049–8061.

Harper, J. W. and Elledge, S. J. 2007. The DNA damage response: ten years after. *Molecular Cell* 28 (5): 739–745.

Hickson, I., Zhao, Y., Richardson, C. J., Green, S. J., Martin, N. M. B., Orr, A. I., Reaper, P. M., Jackson, S. P., Curtin, N. J. and Smith, G. C. M. 2004. Identification and characterization of a novel and specific inhibitor of the ataxia-telangiectasia mutated kinase ATM. *Cancer Research* 64 (24): 9152–9159.

Hu, H., Du, L., Nagabayashi, G., Seeger, R. C. and Gatti, R. A. 2010. ATM is down-regulated by N-Myc-regulated microRNA-421. *Proceedings of the National Academy of Sciences* 107 (4): 1506–1511.

Huen, M. S. Y., Sy, S. M. H. and Chen, J. 2010. BRCA1 and its toolbox for the maintenance of genome integrity. *Nature Reviews. Molecular cell biology* 11 (2): 138–148.

Iorio, M. V. and Croce, C. M. 2012. microRNA involvement in human cancer. *Carcinogenesis*: bgs140.

Jackson, S. and Bartek, J. 2009. The DNA-damage response in human biology and disease. *Nature* 461 (7267): 1071–1078.

Jazayeri, A., Falck, J., Lukas, C., Bartek, J., Smith, G. C. M., Lukas, J. and Jackson, S. P. 2006. ATM- and cell cycle-dependent regulation of ATR in response to DNA double-strand breaks. *Nature Cell Biology* 8 (1): 37–45.

Judge, A. D., Bola, G., Lee, A. C. H. and MacLachlan, I. 2006. Design of noninflammatory synthetic siRNA mediating potent gene silencing in vivo. *Molecular therapy : the journal of the American Society of Gene Therapy* 13 (3): 494–505.

Judge, A. D., Sood, V., Shaw, J. R., Fang, D., McClintock, K. and MacLachlan, I. 2005. Sequence-dependent stimulation of the mammalian innate immune response by synthetic siRNA. *Nature Biotechnology* 23 (4): 457–462.

Kanasty, R. L., Whitehead, K. A., Vegas, A. J. and Anderson, D. G. 2012. Action and reaction: the biological response to siRNA and its delivery vehicles. *Molecular therapy : the journal of the American Society of Gene Therapy* 20 (3): 513–524.

Katalinic, A., Pritzkuleit, R. and Waldmann, A. 2009. Recent Trends in Breast Cancer Incidence and Mortality in Germany. *Breast Care (Basel)* 4 (2): 75-80.

Khalil, H., Tummala, H. and Zhelev, N. 2012. ATM in focus: A damage sensor and cancer target. *Biodiscovery* 5.

Khanna, K. K. and Jackson, S. P. 2001. DNA double-strand breaks: signaling, repair and the cancer connection. *Nature Genetics* 27 (3): 247–254.

Kim, J. and Wong, P. K. Y. 2009. Loss of ATM impairs proliferation of neural stem cells through oxidative stress-mediated p38 MAPK signaling. *Stem Cells (Dayton, Ohio)* 27 (8): 1987–1998.

Kim, V. N. 2005. MicroRNA biogenesis: coordinated cropping and dicing. *Nature Reviews Molecular Cell Biology* 6 (5): 376–385.

Koecher, S., Rieckmann, T., Rohaly, G., Mansour, W. Y., Dikomey, E., Dornreiter, I. and Dahm-Daphi, J. 2012. Radiation-induced double-strand breaks require ATM but not Artemis for homologous recombination during S-phase. *Nucleic Acids Research*: gks604.

Konstantinidou, G., Bey, E. A., Rabellino, A., Schuster, K., Maira, M. S., Gazdar, A. F., Amici, A., Boothman, D. A. and Scaglioni, P. P. 2009. Dual phosphoinositide 3-kinase/mammalian target of rapamycin blockade is an effective radiosensitizing strategy for the treatment of non-small cell lung cancer harboring K-RAS mutations.

Cancer Research 69 (19): 7644–7652.

Kozlov, S. V., Graham, M. E., Jakob, B., Tobias, F., Kijas, A. W., Tanuji, M., Chen, P., Robinson, P. J., Taucher-Scholz, G., Suzuki, K. and others. 2011. Autophosphorylation and atm activation additional sites add to the complexity. *Journal of Biological Chemistry* 286 (11): 9107–9119.

Lal, A., Pan, Y., Navarro, F., Dykxhoorn, D. M., Moreau, L., Meire, E., Bentwich, Z., Lieberman, J. and Chowdhury, D. 2009. miR-24-mediated downregulation of H2AX suppresses DNA repair in terminally differentiated blood cells. *Nature Structural & Molecular Biology* 16 (5): 492–498.

Lam, J. K., Chow, M. Y., Zhang, Y. and Leung, S. W. 2015. siRNA Versus miRNA as Therapeutics for Gene Silencing. *Molecular Therapy—Nucleic Acids* 4 (9): e252.

Lau, N. C., Lim, L. P., Weinstein, E. G. and Bartel, D. P. 2001. An abundant class of tiny RNAs with probable regulatory roles in Caenorhabditis elegans. *Science* 294 (5543): 858–862.

Lavin, M. F. 2008. Ataxia-telangiectasia: from a rare disorder to a paradigm for cell signalling and cancer. *Nature Reviews Molecular Cell Biology* 9 (10): 759–769.

Lee, H.-J. 2013. Exceptional stories of microRNAs. *Experimental Biology and Medicine (Maywood, N.J.)* 238 (4): 339–343.

Lee, J.-H., Goodarzi, A. A., Jeggo, P. A. and Paull, T. T. 2010. 53BP1 promotes ATM activity through direct interactions with the MRN complex. *The EMBO Journal* 29 (3): 574–585.

Lee, M.-N., Tseng, R.-C., Hsu, H.-S., Chen, J.-Y., Tzao, C., Ho, W. L. and Wang, Y.-C. 2007. Epigenetic inactivation of the chromosomal stability control genes BRCA1, BRCA2, and XRCC5 in non-small cell lung cancer. *Clinical cancer research : an official journal of the American Association for Cancer Research* 13 (3): 832–838.

Lee, Y. S. and Dutta, A. 2009. MicroRNAs in cancer. *Annual Review of Pathology* 4: 199.

Lewis, B. P., Burge, C. B. and Bartel, D. P. 2005. Conserved seed pairing, often flanked by adenosines, indicates that thousands of human genes are microRNA targets. *Cell* 120 (1): 15–20.

Li, J. and Stern, D. F. 2005. Regulation of CHK2 by DNA-dependent protein kinase. *Journal of Biological Chemistry* 280 (12): 12041–12050.

Li ,Y., Li, L., Li, B., Wu, Z., Wu, Y., Wang, Y., Jin, F., Li, D., Ma, H. and Wang, D. 2016. Silencing of ataxia-telangiectasia mutated by siRNA enhances the in vitro and in vivo radiosensitivity of glioma. *Oncology Reports* 35 (6): 3303-12.

Lips, J. and Kaina, B. 2001. DNA double-strand breaks trigger apoptosis in p53-deficient fibroblasts. *Carcinogenesis* 22 (4): 579–585.

Löbrich, M., Shibata, A., Beucher, A., Fisher, A., Ensminger, M., Goodarzi, A. A., Barton, O. and Jeggo, P. A. 2010. gammaH2AX foci analysis for monitoring DNA double-strand break repair: strengths, limitations and optimization. *Cell cycle (Georgetown, Tex.)* 9 (4): 662–669.

Lord, C. J. and Ashworth, A. 2012. The DNA damage response and cancer therapy. *Nature* 481 (7381): 287–294.

Luch, A. 2005. Nature and nurture-lessons from chemical carcinogenesis. *Nature Reviews Cancer* 5 (3): 113–125.

Lytle, J. R., Yario, T. A. and Steitz, J. A. 2007. Target mRNAs are repressed as efficiently by microRNA-binding sites in the 5' UTR as in the 3' UTR. *Proceedings of the National Academy of Sciences of the United States of America* 104 (23): 9667–9672.

Manjunath, N., Wu, H., Subramanya, S. and Shankar, P. 2009. Lentiviral delivery of short hairpin RNAs. *Advanced Drug Delivery Reviews* 61 (9): 732–745.

Mansour, W. Y., Bogdanova, N. V., Kasten-Pisula, U., Rieckmann, T., Köcher, S., Borgmann, K., Baumann, M., Krause, M., Petersen, C., Hu, H. and others. 2013. Aberrant overexpression of miR-421 downregulates ATM and leads to a pronounced DSB repair defect and clinical hypersensitivity in SKX squamous cell carcinoma. *Radiotherapy and Oncology* 106 (1): 147–154.

Matsuoka, S., Rotman, G., Ogawa, A., Shiloh, Y., Tamai, K. and Elledge, S. J. 2000. Ataxia telangiectasia-mutated phosphorylates Chk2 in vivo and in vitro. *Proceedings of the National Academy of Sciences* 97 (19): 10389–10394.

Meister, G. and Tuschl, T. 2004. Mechanisms of gene silencing by double-stranded RNA. *Nature* 431 (7006): 343–349.

Mestdagh, P., Derveaux, S. and Vandesompele, J. 2012. Whole-genome RT-qPCR microRNA expression profiling. *Methods in Molecular Biology (Clifton, N.J.)* 815: 121–130.

Miranda, K. C., Huynh, T., Tay, Y., Ang, Y.-S., Tam, W.-L., Thomson, A. M., Lim, B. and Rigoutsos, I. 2006. A pattern-based method for the identification of MicroRNA binding sites and their corresponding heteroduplexes. *Cell* 126 (6): 1203–1217.

Mohr, S. E., Smith, J. A., Shamu, C. E., Neumüller, R. A. and Perrimon, N. 2014. RNAi screening comes of age: improved techniques and complementary approaches. *Nature reviews. Molecular cell biology* 15 (9): 591–600.

Mukherjee, B., Tomimatsu, N., Amancherla, K., Camacho, C. V., Pichamoorthy, N. and Burma, S. 2012. The dual PI3K/mTOR inhibitor NVP-BEZ235 is a potent inhibitor of ATM- and DNA-PKCs-mediated DNA damage responses. *Neoplasia (New York, N.Y.)* 14 (1): 34–43.

Mukherji, S., Ebert, M. S., Zheng, G. X. Y., Tsang, J. S., Sharp, P. a and van Oudenaarden, A. 2011. MicroRNAs can generate thresholds in target gene expression. *Nature Genetics* 43 (9): 854–859.

Murga, M., Jaco, I., Fan, Y., Soria, R., Martinez-Pastor, B., Cuadrado, M., Yang, S.-M., Blasco, M. A., Skoultchi, A. I. and Fernandez-Capetillo, O. 2007. Global chromatin compaction limits the strength of the DNA damage response. *The Journal of Cell Biology* 178 (7): 1101–1108.

Ng, W. L., Yan, D., Zhang, X., Mo, Y.-Y. and Wang, Y. 2010. Over-expression of miR-100 is responsible for the low-expression of ATM in the human glioma cell line:

M059J. *DNA Repair* 9 (11): 1170–1175.

Nikjoo H, U. S. W. W. H. M. G. D. 1998. Track structure in radiation biology: theory and applications. *International journal of radiation biology* 73 (4): 355–364.

O'Connor, M. J. 2015. Targeting the DNA damage response in cancer. *Molecular Cell* 60 (4): 547–560.

Orom, U. A., Nielsen, F. C. and Lund, A. H. 2008. MicroRNA-10a binds the 5′ UTR of ribosomal protein mRNAs and enhances their translation. *Molecular Cell* 30 (4): 460–471.

Östling, P., Leivonen, S.-K., Aakula, A., Kohonen, P., Mäkelä, R., Hagman, Z., Edsjö, A., Kangaspeska, S., Edgren, H., Nicorici, D., Bjartell, A., Ceder, Y., Perälä, M. and Kallioniemi, O. 2011. Systematic analysis of microRNAs targeting the androgen receptor in prostate cancer cells. *Cancer Research* 71 (5): 1956–1967.

Perry, J. and Kleckner, N. 2003. The ATRs, ATMs, and TORs are giant HEAT repeat proteins. *Cell* 112 (2): 151–155.

Perwitasari, O., Bakre, A., Tompkins, S. M. and Tripp, R. A. 2013. siRNA Genome Screening Approaches to Therapeutic Drug Repositioning. *Pharmaceuticals (Basel, Switzerland)* 6 (2): 124–160.

Rainey, M. D., Charlton, M. E., Stanton, R. V. and Kastan, M. B. 2008b. Transient inhibition of ATM kinase is sufficient to enhance cellular sensitivity to ionizing radiation. *Cancer Research* 68 (18): 7466–7474.

Rao, S.S., Thompson, C., Cheng, J., Haimovitz-Friedman, A., Powell, S.N., Fuks, Z. and Kolesnick, R.N. 2014. Axitinib sensitization of high Single Dose Radiotherapy. *Radiotherapy Oncology* 111 (1): 88-93.

Richardson, C. and Jasin, M. 2000. Frequent chromosomal translocations induced by DNA double-strand breaks. *Nature* 405 (6787): 697–700.

Richardson, C., Horikoshi, N. and Pandita, T. K. 2004. The role of the DNA double-strand break response network in meiosis. *DNA Repair* 3 (8): 1149–1164.

Robert Koch Institute. 2014. http://www.gekid.de/Doc/kid2014_english.pdf [accessed 17/08/16]

Rogakou, E. P., Boon, C., Redon, C. and Bonner, W. M. 1999. Megabase chromatin domains involved in DNA double-strand breaks in vivo. *The Journal of Cell Biology* 146 (5): 905–916.

Rogakou, E. P., Pilch, D. R., Orr, A. H., Ivanova, V. S. and Bonner, W. M. 1998. DNA double-stranded breaks induce histone H2AX phosphorylation on serine 139. *Journal of Biological Chemistry* 273 (10): 5858–5868.

Rothkamm, K. and Löbrich, M. 2003. Evidence for a lack of DNA double-strand break repair in human cells exposed to very low x-ray doses. *Proceedings of the National Academy of Sciences* 100 (9): 5057–5062.

Rotman, G. and Shiloh, Y. 1998. ATM: from gene to function. *Human Molecular Genetics* 7 (10): 1555–1563.

Saha, J., Wang, M. and Cucinotta, F. A. 2013. Investigation of switch from ATM to ATR signaling at the sites of DNA damage induced by low and high LET radiation. *DNA Repair* 12 (12): 1143–1151.

Savitsky, K., Sfez, S., Tagle, D. A., Ziv, Y., Sartiel, A., Collins, F. S., Shiloh, Y. and Rotman, G. 1995. The complete sequence of the coding region of the ATM gene reveals similarity to cell cycle regulators in different species. *Human Molecular Genetics* 4 (11): 2025–2032.

Savitsky, K., Uziel, T., Gilad, S., Sartiel, A., Shiloh, Y., Rotman, G., Platzer, M., Rosenthal, A. and Elroy-Stein, O. 1997. Ataxia-telangiectasia: structural diversity of untranslated sequences suggests complex post-transcriptional regulation of ATM gene expression. *Nucleic Acids Research* 25 (9): 1678–1684.

Schrem, H., Schneider, V., Kurok, M., Goldis, A, Dreier, M., Kaltenborn, A., Gwinner, W., Barthold, M., Liebeneiner, J., Winny, M., Klempnauer, J. and Kleine, M. 2016. Independent Pre-Transplant Recipient Cancer Risk Factors after Kidney Transplantation and the Utility of G-Chart Analysis for Clinical Process Control. *PLoS One*.11 (7) :e0158732.

Shiloh, Y. 1997. Ataxia-telangiectasia and the Nijmegen breakage syndrome: related disorders but genes apart. *Annual Review of Genetics* 31: 635–662.

Shiloh, Y. 2003. ATM and related protein kinases: safeguarding genome integrity. *Nature Reviews Cancer* 3 (3): 155–168.

Shiloh, Y. 2006. The ATM-mediated DNA-damage response: taking shape. *Trends in Biochemical Sciences* 31 (7): 402–410.

Shiloh, Y. and Kastan, M. B. 2001. ATM: genome stability, neuronal development, and cancer cross paths. *Advances in Cancer Research* 83: 209–254.

Shiloh, Y. and Ziv, Y. 2012. The ATM protein: The importance of being active. *The Journal of Cell Biology* 198 (3): 273–275.

Shiloh, Y. and Ziv, Y. 2013. The ATM protein kinase: regulating the cellular response to genotoxic stress, and more. Nature Reviews Molecular cell biology 14 (4): 197–210.

Shreeram, S., Demidov, O. N., Hee, W. K., Yamaguchi, H., Onishi, N., Kek, C., Timofeev, O. N., Dudgeon, C., Fornace, A. J., Anderson, C. W., Minami, Y., Appella, E. and Bulavin, D. V. 2006. Wip1 phosphatase modulates ATM-dependent signaling pathways. *Molecular Cell* 23 (5): 757–764.

Smith-Roe, S.L., Nakamura, J., Holley, D., Chastain II, P.D., Rosson, G.B., Simpson, D.A., Ridpath, J.R.,Kaufman, D.G.,Kaufmann, W.K. and Bultman, S.J. 2015. SWI/SNF complexes are required for full activation of the DNA-damage response. *Oncotarget* 6 (2): 732–745.

Song, L., Lin, C., Wu, Z., Gong, H., Zeng, Y., Wu, J., Li, M. and Li, J. 2011. miR-18a impairs DNA damage response through downregulation of ataxia telangiectasia mutated (ATM) kinase. *PLoS One* 6 (9): e25454.

Srivastava, N., Manvati, S., Srivastava, A., Pal, R., Kalaiarasan, P., Chattopadhyay, S., Gochhait, S., Dua, R. and Bamezai, R. N. 2011. miR-24-2 controls H2AFX expression regardless of gene copy number alteration and induces apoptosis by targeting antiapoptotic gene BCL-2: a potential for therapeutic intervention. *Breast*

Cancer Research 13 (2): 1.

Stagni, V., Oropallo, V., Fianco, G., Antonelli, M., Cinà, I. and Barilà, D. 2014. Tug of war between survival and death: exploring ATM function in cancer. *International Journal of Molecular Sciences* 15 (4): 5388–5409.

Stiff, T., O'Driscoll, M., Rief, N., Iwabuchi, K., Löbrich, M. and Jeggo, P. A. 2004. ATM and DNA-PK function redundantly to phosphorylate H2AX after exposure to ionizing radiation. *Cancer Research* 64 (7): 2390–2396.

Stracker, T. H. and Petrini, J. H. J. 2011. The MRE11 complex: starting from the ends. *Nature Reviews. Molecular Cell Biology* 12 (2): 90–103.

Struewing, J.P. Hartge, P., Wacholder, S., Baker, S.M., Berlin, M., McAdams, M., Timmerman, M.M., Brody, L.C. and Tucker, M.A. 1997. The Risk of Cancer Associated with Specific Mutations of BRCA1 and BRCA2 among Ashkenazi Jews. N*ew England Journal of Medicine*. 336: 1401-1408

Sulli, G., Di Micco, R. and d' Adda di Fagagna, F. 2012. Crosstalk between chromatin state and DNA damage response in cellular senescence and cancer. *Nature Reviews. Cancer* 12 (10): 709–720.

Takada, S. and Asahara, H. 2012. Current strategies for microRNA research. *Modern rheumatology / the Japan Rheumatism Association* 22 (5): 645–653.

Takata, M., Sasaki, M. S., Sonoda, E., Morrison, C., Hashimoto, M., Utsumi, H., Yamaguchi-Iwai, Y., Shinohara, A. and Takeda, S. 1998. Homologous recombination and non-homologous end-joining pathways of DNA double-strand break repair have overlapping roles in the maintenance of chromosomal integrity in vertebrate cells. *The EMBO Journal* 17 (18): 5497–5508.

Taneja, N., Davis, M., Choy, J. S., Beckett, M. A., Singh, R., Kron, S. J. and Weichselbaum, R. R. 2004. Histone H2AX phosphorylation as a predictor of radiosensitivity and target for radiotherapy. *Journal of Biological Chemistry* 279 (3): 2273–2280.

Toledo, L. I., Murga, M., Zur, R., Soria, R., Rodriguez, A., Martinez, S., Oyarzabal, J., Pastor, J., Bischoff, J. R. and Fernandez-Capetillo, O. 2011. A cell-based screen identifies ATR inhibitors with synthetic lethal properties for cancer-associated mutations. *Nature Structural & Molecular Biology* 18 (6): 721–727.

Toulany, M., Mihatsch, J., Holler, M., Chaachouay, H. and Rodemann, H.P. 2014 Cisplatin-mediated radiosensitization of non-small cell lung cancer cells is stimulated by ATM inhibition. *Radiotherapy & Oncology* 111 (2): 228-236.

Tree, A.C., Khoo, V.S., Eeles, R.A., Ahmed, M., Dearnaley, D.P., Hawkins, M.A., Huddart, R.A., Nutting, C.M., Ostler, P.J. and van As N.J. 2013 Stereotactic body radiotherapy for oligometastases. *Lancet Oncol*ogy 14 (1): e28-37.

Udayakumar, D., Pandita, R.K., Horikoshi, N., Liu, Y., Liu, Q., Wong, K.K., Hunt, C.R., Gray, N.S., Minna, J.D., Pandita, T.K. and Westover, K.D. 2016 Torin2 Suppresses Ionizing Radiation-Induced DNA Damage Repair. *Radiation Research* 185 (5): 527-38.

Uziel, T., Savitsky, K., Platzer, M., Ziv, Y., Helbitz, T., Nehls, M., Boehm, T., Rosenthal, A., Shiloh, Y. and Rotman, G. 1996. Genomic Organization of the ATM gene.

Genomics 33 (2): 317–320.

Valko, M., Rhodes, C. J., Moncol, J., Izakovic, M. and Mazur, M. 2006. Free radicals, metals and antioxidants in oxidative stress-induced cancer. *Chemico-biological Interactions* 160 (1): 1–40.

Veuger, S. J., Curtin, N. J., Richardson, C. J., Smith, G. C. and Durkacz, B. W. 2003. Radiosensitization and DNA repair inhibition by the combined use of novel inhibitors of DNA-dependent protein kinase and poly (ADP-ribose) polymerase-1. *Cancer Research* 63 (18): 6008–6015.

Wang, F., Yang, F., Zhang, L. and Sun, S. 2010. Is increasing the copy number of the microRNA precursor in a vector really helpful for further improving the level of mature microRNA in stable cells? *Hepatology* 52 (4): 1517.

Wang, J., He, J., Su, F., Ding, N., Hu, W., Yao, B., Wang, W. and Zhou, G. 2013. Repression of ATR pathway by miR-185 enhances radiation-induced apoptosis and proliferation inhibition. *Cell Death & Disease* 4: e699.

Wang, R., Wang, H.-B., Hao, C. J., Cui, Y., Han, X.-C., Hu, Y., Li, F.-F., Xia, H.-F. and Ma, X. 2012. MiR-101 is involved in human breast carcinogenesis by targeting Stathmin1. *PLoS One* 7 (10): e46173.

Wang, T., Xie, Y., Tan, A., Li, S. and Xie, Z. 2015. Construction and Characterization of a Synthetic MicroRNA Cluster for Multiplex RNA Interference in Mammalian Cells. *ACS Synthetic Biology*.

Wang, W. and Lang, J. 2012. Strategies to optimize radiotherapy based on biological responses of tumor and normal tissue (Review). *Experimental and Therapeutic Medicine* 4 (2): 175–180.

Wang, X. Q., Redpath, J. L., Fan, S. T. and Stanbridge, E. J. 2006. ATR dependent activation of Chk2. *Journal of Cellular Physiology* 208 (3): 613–619.

Weber, A.M. and Ryan, A.J. 2015. ATM and ATR as therapeutic targets in cancer. *Pharmacology & Therapeutics* 149: 124-138.

Westphal, C. H., Hoyes, K. P., Canman, C. E., Huang, X., Kastan, M. B., Hendry, J. H. and Leder, P. 1998. Loss of atm radiosensitizes multiple p53 null tissues. *Cancer Research* 58 (24): 5637–5639.

Willems, P., Claes, K., Baeyens, A., Vandersickel, V., Werbrouck, J., De Ruyck, K., Poppe, B., Van den Broecke, R., Makar, A., Marras, E., Perletti, G., Thierens, H. and Vral, A. 2008. Polymorphisms in nonhomologous end-joining genes associated with breast cancer risk and chromosomal radiosensitivity. *Genes, Chromosomes & Cancer* 47 (2): 137–148.

Wu, C.-W., Dong, Y.-J., Liang, Q.-Y., He, X.-Q., Ng, S. S., Chan, F. K., Sung, J. J. and Yu, J. 2013. MicroRNA-18a attenuates DNA damage repair through suppressing the expression of ataxia telangiectasia mutated in colorectal cancer. *PLoS One* 8 (2): e57036.

Xu, H., He, J.H., Xiao, Z.D., Zhang, Q.Q., Chen, Y.Q., Zhou, H., Qu, L.H. 2010. Liver-enriched transcription factors regulate microRNA-122 that targets CUTL1 during liver

development. *Hepatology* 52 (4): 1431-42.

Yan, D., Ng, W. L., Zhang, X., Wang, P., Zhang, Z., Mo, Y.-Y., Mao, H., Hao, C., Olson, J. J., Curran, W. J. and Wang, Y. 2010. Targeting DNA-PKcs and ATM with miR-101 sensitizes tumors to radiation. *PLoS One* 5 (7): e11397.

Zamore, P. D. and Haley, B. 2005. Ribo-gnome: the big world of small RNAs. *Science (New York, N.Y.)* 309 (5740): 1519–1524.

Zhang, T., Shen, Y., Chen, Y., Hsieh, J.T. and Kong, Z. 2015. The ATM inhibitor KU55933 sensitizes radioresistant bladder cancer cells with DAB2IP gene defect. *International Journal of Radiation Biology* 91 (4): 368-78.

Zhao, L., Bode, A. M., Cao, Y. and Dong, Z. 2012. Regulatory mechanisms and clinical perspectives of miRNA in tumor radiosensitivity. *Carcinogenesis* 33 (11): 2220–2227.

ZUSAMMENFASSUNG

Die Radiotherapie ist eine effektive Behandlung maligner Tumorerkrankungen, deren Einsatz jedoch durch drei Hauptfaktoren limitiert wird zum Beispiel: Das Ansprechen eines Tumors auf die Bestrahlung ist individuell und u.a. abhängig von der DNA Reparaturkapazität eines Tumors. Durch eine gezielte Dysregulation der *DNA damage response* kann eine Radiosensibilisierung von Tumoren *in vitro* induziert werden. Dies gelingt z.B. durch Inhibition der ATM, einem Schlüsselenzym der Doppelstrangbruchreparatur. Ein *Knockdown* von Zielgenen kann *in vitro* durch microRNAs erfolgen. Die mRNA der ATM wird bekanntermaßen durch die microRNAs miR-18a, miR-100, miR-101a und miR-421 targetiert und die Translation und damit die Genexpression reduziert. In diesem Forschungsprojekt liegt das Ziel darin, die synergistische Wirkung von Targeting-ATM durch Verwendung von vier endogenen miRNAs (miR-18a, miR-100-5p, miR-101-3p und miR-421) oder drei künstlichen miRNAs auf Strahlungsempfindlichkeit in der Prostatakrebs-Zelllinie (PC3) und in Brustkrebszelllinien (MCF-7 und MDA-MB-468-Zellen) zu untersuchen. In diesem Forschunsprojekt, Targeting-ATM durch einem ATM-Inhibitor, KU55933, siRNAs resultiert in einem ATM-defizienten Phänotyp von Beeinträchtigung Doppelstrangbruch (DSB) Reparatur, die durch eine erhöhte Anzahl der γH2AX nach 2Gy, und wichtig ist eine verbesserte Strahlungsempfindlichkeit. Außerdem Targeting-ATM mit einem Vektor, der eine Kombination aus vier endogenen miRNAs (pmiRNAs-4X) oder die drei künstlichen miRNAs (pmiRNAs-3X) in den Prostata Krebs-Zelllinie oder in die Brust Krebs-Zellinien, zeigte eine effiziente Herunterregulieren der Expression von ATM und die verstärkten Strahlungsempfindlichkeiten.

Im Ergebnis zeigt die Studie, dass eine kombinierte miRNA zu effizienten Knockdown ATM führt, und außerdem die Strahlenempfindlichkeit von verschiedenen Krebszelllinien verbessert. Diese Ergebnisse haben erhebliche Auswirkungen auf die zukünftigen Behandlungsstrategien von Krebs.

ABSTRACT

Tumor cells use a different signaling pathways to repair damage and prevent the cytotoxic effects of anticancer agents. specific targeting of these signaling pathways enhance tumor radiosensitivity is of urgent need. Ionizing radiation (IR) is considered as a main anticancer therapy which induce a lot of cytotoxic events such as double-strand breaks (DSBs). the efficiency of radiotherapy is basically depending on several aspects. One of these aspects is the activation of DNA damage response (DDR). Ataxia-telangiectasia mutated (ATM) kinase is the main orchestrator of the DDR after IR. As consequence, the knockdown of ATM may confer extraordinary radiosensitization effect. In the current study, we aim to investigate the synergistic effect of using vector expressing either four endogenous (miR-18a, miR-100-5p, miR-101-3p and miR-421) or the three artificial miRNAs in combination in order to knockdown ATM expression in breast cancer cell lines (MCF7 and MDA-MB-468) and the prostate cancer cell line (PC3).

In this study, ATM was targeted using ATM inhibitor, KU55933, siRNAs which lead to increased number of DSBs as shown by higher number of DSBs and high radiosensitivity. Interestingly, Cells harboring either the three artificial miRNAs or the four endogenous miRNAs showed an efficient downregulation in the expression of ATM and enhanced radiosensitivity. In conclusion, the study showed a combined miRNA strategy to target ATM resulted in an additive effect in vitro and enhanced radiosensitivity.

Eidesstattliche Versicherung

Hiermit erkläre ich an Eides statt, dass ich die vorliegende Dissertationsschrift selbst verfasst und keine anderen als die angegebenen Quellen und Hilfsmittel benutzt habe.

Declaration on oath

I hereby declare, on oath, that I have written the present dissertation by my own and have not used other than the acknowledged resources and aids.

Hamburg, 26.9.2016 Unterschrift

Hamed Helal

Maria C. Arruda
76 Cottage Street
New Bedford, MA 02740
U.S.A.

mcarruda@hotmail.com

August 30, 2016

To whom it may concern:

This is to certify that I proofread and edited the Mr. Hamed Helal PhD thesis for grammar, spelling and other language problems.

Best regards

Maria Arruda